AD-A111 303 MARTIN MARIETTA AEROSPACE DENVER CO QUALITY ASSURANC--ETC F/G 11/4
ENHANCED X-RAY STEREOSCOPIC NDE OF COMPOSITE MATERIALS.(U)
JUN 80 W D RUMMEL, T TEDROW, H D BRINKERHOFF F33615-79-C-3220

UNCLASSIFIED AFWAL-TR-80-3053 NL

1 of 3
AD
A111303

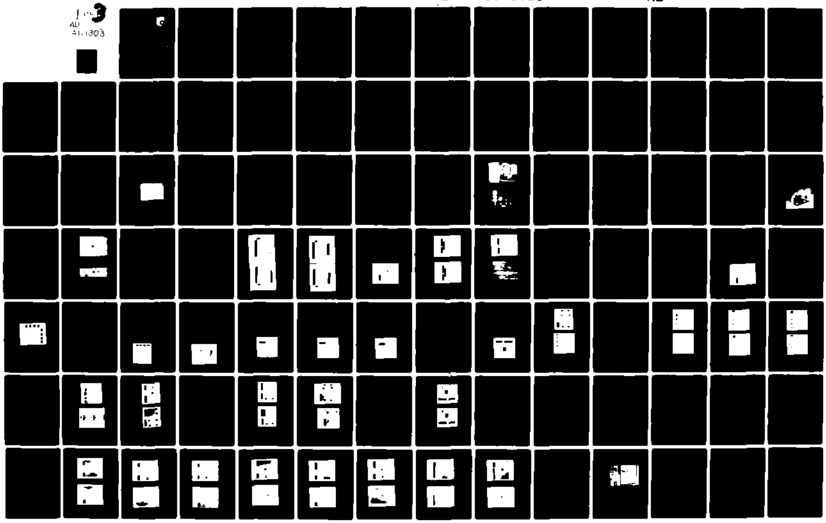

2

AFWAL-TR-80-3053

ENHANCED X-RAY STEREOSCOPIC NDE OF COMPOSITE MATERIALS

WARD D. RUMMEL
THOMAS TEDROW
H. D. BRINKERHOFF

MARTIN MARIETTA CORPORATION, DENVER AEROSPACE
QUALITY ASSURANCE, ADVANCED TECHNOLOGY DEPARTMENT
P. O. BOX 179
DENVER, CO 80201

JUNE 1980

TECHNICAL REPORT AFWAL-TR-80-3053
Final Report for Period July 1979 — May 1980

FLIGHT DYNAMICS LABORATORY
AIR FORCE WRIGHT AERONAUTICAL LABORATORIES
AIR FORCE SYSTEMS COMMAND
WRIGHT-PATTERSON AIR FORCE BASE, OHIO 45433

NOTICE

When Government drawings, specifications, or other data are used for any purpose other than in connection with a definitely related Government procurement operation, the United States Government thereby incurs no responsibility nor any obligation whatsoever, and the fact that the government may have formulated, furnished, or in any way supplied the said drawings, specifications, or other data, is not to be regarded by implication or otherwise as in any manner licensing the holder or any other person or corporation, or conveying any rights or permission to manufacture, use, or sell any patented invention that may in any way be related thereto.

This technical report has been reviewed and is approved for publication.

George P. Sendeckyj

GEORGE P. SENDECKYJ
Project Engineer

Frank D. Adams

FRANK D. ADAMS, Actg Chief
Structural Integrity Branch

FOR THE COMMANDER:

Ralph L. Kuster Jr.

RALPH L. KUSTER, JR., Colonel, USAF
Chief, Structures & Dynamics Division
Flight Dynamics Laboratory (AFWAL)

"If your address has changed, if you wish to be removed from our mailing list, or if the addressee is no longer employed by your organization, please notify AFWAL/FIBE W-P AFB, OH 45433 to help us maintain a current mailing list."

Copies of this report should not be returned unless return is required by security considerations, contractual obligations, or notice on a specific document.

AIR FORCE/56780/3 February 1982 — 440

SECURITY CLASSIFICATION OF THIS PAGE (When Data Entered)

REPORT DOCUMENTATION PAGE

READ INSTRUCTIONS BEFORE COMPLETING FORM

1. REPORT NUMBER
AFWAL-TR-80-3053

2. GOVT ACCESSION NO.
AD-A[illegible] 203

3. RECIPIENT'S CATALOG NUMBER

4. TITLE (and Subtitle)
Enhanced X-Ray Stereoscopic NDE of Composite Materials

5. TYPE OF REPORT & PERIOD COVERED
Final Report
7/9/79 thru 5/9/80

6. PERFORMING ORG. REPORT NUMBER

7. AUTHOR(s)
W. D. Rummel, Thomas Tedrow, and
H. D. Brinkerhoff

8. CONTRACT OR GRANT NUMBER(s)
F33615-7 9-C-3220

9. PERFORMING ORGANIZATION NAME AND ADDRESS
Martin Marietta Corp., Denver Aerospace
Quality Assurance, Advanced Technology Dept
P.O. Box 179, Denver, CO 80201

10. PROGRAM ELEMENT, PROJECT, TASK AREA & WORK UNIT NUMBERS
Program Element 61101F
Task 240101
Work Unit 24010133

11. CONTROLLING OFFICE NAME AND ADDRESS
FLIGHT DYNAMICS LABORATORY
AIR FORCE WRIGHT AERONAUTICAL LABS.
AIR FORCE SYSTEMS COMMAND

12. REPORT DATE
JUNE 1980

13. NUMBER OF PAGES

14. MONITORING AGENCY NAME & ADDRESS (if different from Controlling Office)

15. SECURITY CLASS. (of this report)
Unclassified

15a. DECLASSIFICATION/DOWNGRADING SCHEDULE

16. DISTRIBUTION STATEMENT (of this Report)
Distribution unlimited

DISTRIBUTION STATEMENT A
Approved for public release;
Distribution Unlimited

17. DISTRIBUTION STATEMENT (of the abstract entered in Block 20, if different from Report)

18. SUPPLEMENTARY NOTES

19. KEY WORDS (Continue on reverse side if necessary and identify by block number)
Nondestructive testing, composite materials, stereo-X-radiography, radiation opaque penetrant, composite materials fatigue damage, composite fracture, and penetrameter.

20. ABSTRACT (Continue on reverse side if necessary and identify by block number)
This report describes an evaluation study for the application of stereo-X-radiography as a tool for three dimensional visualization and quantitative assessment of mechanical damage in graphite-epoxy structural materials. Comparison of image quality produced using X-ray opaque liquid penetrant materials was made for stereo-X-radiographs of panels that contained mechanical damage. A new X-ray opaque penetrant material was formulated and used for development of a high resolution stereo-X-radiographic technique. The technique was used to document damage

DD FORM 1 JAN 73 1473 EDITION OF 1 NOV 65 IS OBSOLETE

UNCLASSIFIED

SECURITY CLASSIFICATION OF THIS PAGE (When Data Entered)

20. (Continued)

accumulation in a series of pre-damaged panels during incremental tension-tension fatigue loading.

The high resolution technique was shown to be useful in assessment of accumulated damage and in quantitative location of the damage within a panel. Features of the technique include use of a new X-ray opaque penetrant formulation, use of a unique penetrameter, "soft radiation" and a fine grained X-ray film.

PREFACE

This final technical report described the optimization of an "Enhanced X-Ray Stereoscopic NDE of Composite Materials" technique. The work was performed under Air Force Contract F33615-79-C3220, and covered a period from July 1979 to May 1980.

This work was performed under Contract Control F33615-79-C3220, Project 2401, Work Authorization Number 24010133, sponsored by the Flight Dynamics Laboratory, Wright-Patterson Air Force Base, Ohio. The Air Force project engineer for this contract was Dr. George Sendeckyj.

The program was performed in the Advance Technology Group of the Quality Assurance Department of Martin Marietta Corporation, Denver Aerospace, Denver, Colorado. The program manager was Ward D. Rummel, the key contributors to the program were:

Mr. Bernie Burke - Specimen Fabrication
Mr. Thomas Tedrow - Radiography
Mr. John Shepic - Specimen Testing

TABLE OF CONTENTS

TABLE OF CONTENTS (CONTD.)

LIST OF ILLUSTRATIONS

LIST OF ILLUSTRATIONS (CONTD.)

LIST OF ILLUSTRATIONS (CONTD.)

LIST OF ILLUSTRATIONS (CONTD.)

LIST OF ILLUSTRATIONS (CONTD.)

LIST OF ILLUSTRATIONS (CONTD.)

LIST OF ILLUSTRATIONS (CONTD.)

LIST OF ILLUSTRATIONS (CONTD.)

LIST OF ILLUSTRATIONS (CONTD.)

LIST OF TABLES

SUMMARY

This program explored the application of opaque penetrant enhanced, three dimensional, x-radiography to the characterization and documentation of impact damage in resin-matrix composite materials.

A program was conducted which demonstrated that opaque penetrant enhanced radiographs can be used to document the spatial (three dimensional) distribution of damage (consisting of delaminations, matrix cracks and fiber fractures) in graphite-epoxy composite materials. The program was divided into two tasks. In task one, a three-dimensional x-radiographic inspection method was selected and optimized for spatial resolution in graphite-epoxy composite materials. Emphasis was placed on simplicity and ease of operation, accuracy of damage definition, and ability to describe the damage details. In task two, use of the optimized technique was demonstrated during an investigation of damage accumulation processes in graphite-epoxy specimens that had been subjected to incremental fatigue loading.

The goal of demonstrating the enhancement of three-dimensional X-radiography for application to composite materials was met. Significant features of the program included formulation of a new X-ray opaque penetrant material; design, fabrication and application of a composite material penetrameter for image quality assessment; and development and application of a compact step wedge for use in three dimensional location of damage within a structure.

SECTION I

INTRODUCTION

Resin-matrix graphite composite materials have unique properties for structural applications. Application of resin-matrix graphite materials has evolved as a major technology challenge to a variety of scientific and engineering disciplines. In order to realize the full potential of composite materials, a variety of enabling technologies must be developed and systematically applied in design, analysis, production, acceptance and maintenance. A significant element of the analysis task is in understanding damage tolerance and damage propagation in composite materials. Characterization and predictive modeling of damage are primary requirements set forth in the United States Air Force structural integrity policy.

Unlike metals for which the dominant damage mechanism is initiation and growth of small cracks, resin-matrix composites have an extremely complicated damage initiation and damage accumulation process. Damage in composites generally consists of extensive matrix cracking, progressive delaminations, fiber buckling and fiber fractures. The matrix cracks and delaminations interact during fatigue loading, further complicating the damage accumulation process. The mode of failure depends on the stacking sequence of the laminate and the mode of loading. Nondestructive methods of evaluation are required to aid in understanding damage initiation and damage accumulation. Further, a material volume interrogation method is required due to the anisotropic properties of composites and to the complexity of damage initiation and accumulation. X-radiography, eddy current and ultrasonics are the primary nondestructive evaluation methods for material volume interrogation. Ultrasonic and eddy current methods are, however, dependent on bulk integration of imposed energy fields and have limited application in understanding micro changes within a material volume. A high resolution technique is required to detect small changes such as matrix cracks, delaminations and fiber fractures.

X-radiography is a well recognized and documented evaluation method that is applied in industry for assessment of the soundness of materials and components. Many variations of the method have been devised to meet special testing needs and requirements. Variations include several techniques in generation and in evaluation of three dimensional images. The optimum technique for a specific application is obtained by careful evaluation of the basic factors inherent to the X-radiographic method and by experimental evaluation of images produced under various test conditions for characterization of various test specimen conditions.

In general, X-radiography, a beam of penetrating radiation is typically directed perpendicularly toward the part under inspection (Figure 1) at a fixed-focus film distance. A portion of this energy is absorbed as it passes through the part and a portion is scattered. Absorption of energy by the test part is dependent upon the material composition, thickness and density. Energy which passes through the part is converted by an appropriate imaging media (film, fluoroscopy, etc.) to produce a "shadow image" of variable portions of the part.

The type and quality of X-radiation, the exposure geometry, the type of imaging media and the type of viewing/evaluation performed, provide variation in the results produced. Test parameters of concern for general application include subject contrast, film contrast, unsharpness, distortion and image density.

Image density is measured directly while other parameters are assessed by comparison to an "Image Indicator" (penetrameter) that is imaged along with the part during exposure.

Distortion and unsharpness are factors related to the exposure technique and to the internal scatter of the subject material.

Film contrast is a characteristic of the type of film and film processing used.

Subject contract is the primary, concern in X-radiographic examination of composite materials. Subject contrast is the result of differences in the absorption of radiation by the subject under examination. Subject contrast is therefore dependent on a change in density (such as a void) and/or on a change in the atomic composition within a test subject. Both graphite and organic resin-matrix materials consist of a high carbon content and therefore absorb X-radiation similarly; both differ only slightly in absorption properties from that of air. Subject contrast must therefore be enhanced by introduction of a contrast media.

The most successful previous work involving X-radiography of composite materials has been performed with the aid of tetrabromoethane (TBE) or diiodobutane (DIB) as contrasting fluids. These fluids were selected for their penetrating and image contrast properties. Both materials are halogenated hydrocarbons and therefore require special precautions in handling, use and storage. (Ref. 5)

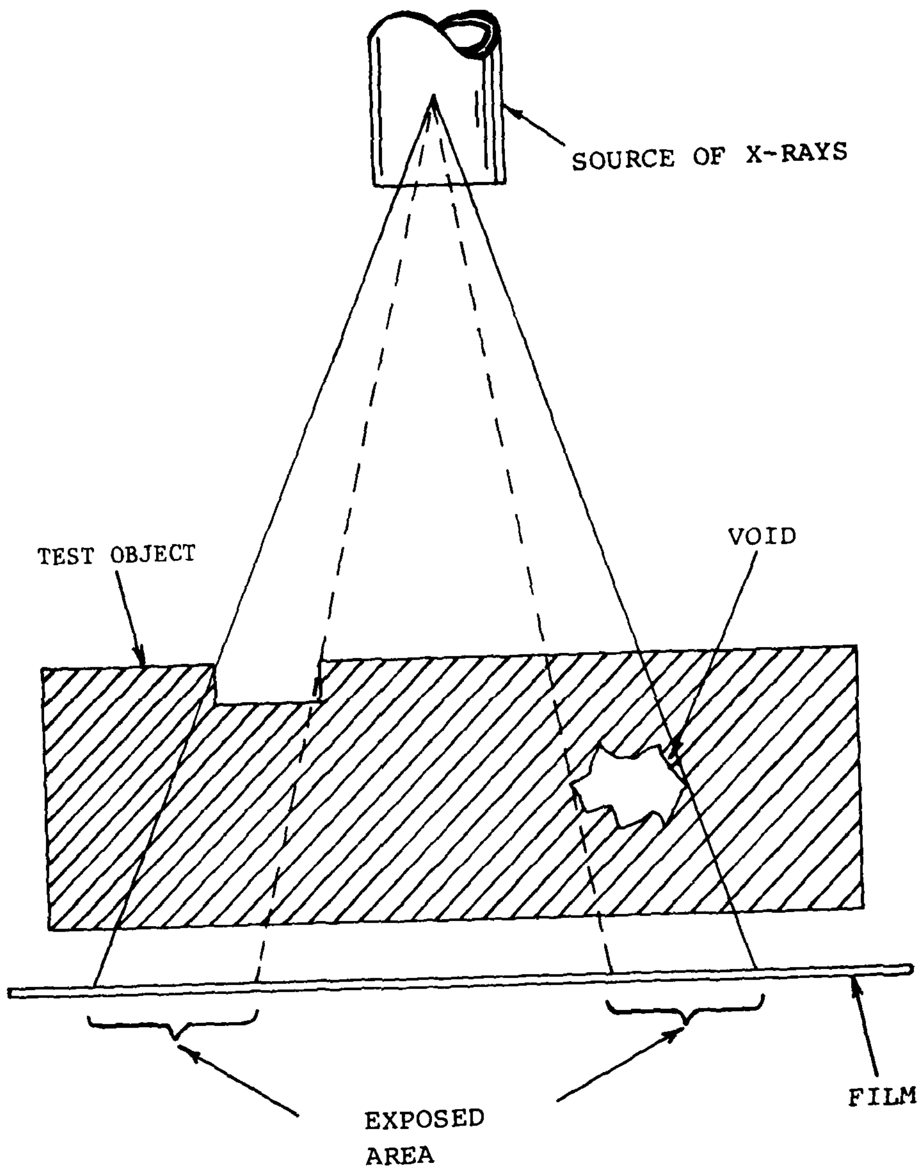

FIGURE 1 DIAGRAM OF THE RADIOGRAPHIC PROCESS

A second limitation in the use of conventional radiography is in the nature of the image produced. Such images provide detailed information on the nature and planar distribution of material damage but do not provide information on through-the-thickness distribution of damage.

The objective of the work described herein was to explore the application of opaque penetrant enhanced, three dimensional X-radiography to detect, quantify and evaluate the progress of damage in resin-matrix graphite composite materials. The work was divided into two tasks:

TASK 1 consisted of selection of an applicable three-dimensional X-radiographic method and optimization of the method for characterization of the damage detection and accumulation processes in resin matrix-composites.

TASK II consisted of a demonstration of the optimized three-dimensional X-radiographic method through its application to characterization and documentation of the damage accumulation process in resin-matrix composites as a function of fatigue loading.

SECTION II

PENETRANT SELECTION AND X-RADIOGRAPHIC TECHNIQUE OPTIMIZATION

1. Test Specimen Material Fabrication

Materials for fabrication of all test specimens were layed-out and cured in sheet form from materials on hand (i.e., T300 fiber, Fiberite 934 resin, quasi-isotropic graphite/epoxy unidirectional prepreg tape). Prior to lay-up, a test of prepreg material properties was completed with results shown below.

Test	Specification	Measured
Volatile Content	2% maximum	1.2%
Gel Time 335° to 350°F	11-30 minutes	14 Minutes
Resin Flow	13-25%	21%

Three (3) symmetrical quasi-isotropic graphite epoxy configurations were fabricated using unidirectional prepreg tape materials. One configuration was 8-plies thick. The second configuration was 16-plies thick. The third configuration was 24-plies thick. Ply configurations were as shown below:

8 ply:
Lay up 0, +45, -45, 90, 90, -45, +45, 0 degrees

16 ply:
Lay up 0, +45, -45, 90, 90, -45, +45, 0, 0, +45, -45, 90, 90, -45, +45, 0 degrees

24 ply:
Lay up 0, +45, -45, 90, 90, -45, + 45, 0, 0, + 45, -45, 90, 90, -45, +45, 0, 0, +45, -45, 90, 90, -45, +45, 0 degrees

A 177 degree C. (350 degree F.) resin was used in all sheets. Sheets were cured in a platen press using an established process consisting of the following:

a. Vacuum bag evacuation to approximately 12 pounds per square inch;

b. Heating to $250^{o}F \pm 10^{o}F$ at $3 \pm 1^{o}F$ per minute;

c. Holding at $250^{o}F$ for $15(^{+0}_{-5})$ minutes;

d. Increasing pressure 80 to 100 pounds per square inch;

e. Holding to $250^{o}F$ for $45(^{+0}_{-5})$ minutes;

f. Heating to $350^{o}F \pm 10^{o}F$ for 180 ± 80 minutes;

g. Cooling under pressure and vacuum to $175^{o}F$ before removing from the press.

Material acceptance was by visual inspection for general condition and surface anomalies, ultrasonic through-transmission inspection for cracks and delaminations, and conventional X-radiographic inspection for voids and inclusions. Ultrasonic inspection was performed using a 10 megahertz 0.375 inch diameter focused transducer in the normal through transmission reflector plate mode. X-radiographic inspection was performed at 15 kilovolts, 20 milliamperes, 48 inch target/film distance with Kodak type M film. Exposure times were 3, 6 and 10 minutes respectively for 8, 16 and 24 ply material. Sheet material was fabricated in sufficient quantity to accommodate development of impact damage techniques, radiographic techniques optimization and material/technique characterization.

2. Test Specimen Preparation

a. 8-Ply Specimens

Thirty (30) four (4) inch by four (4) inch test specimens were cut from the 8 ply sheet material. Edges were dressed and each specimen was identified using a vibro-etch marker according to their respective location within the 8-ply sheet. Specimens were identified as 8-1 through 8-30, with the identification on the botton (platen) side. Specimen thickness varied from 0.042 to 0.044 inches. 8 ply specimens were subsequently used in optimization and material compatibility studies.

b. 16-Ply Specimens

Twenty (20) three and nine tenths (3.9) inch by twelve (12) inch specimens were cut from 16-ply sheet material with the 0 degree outer plies oriented along the long (12 inch) dimension. Edges were dressed and each specimen was identified according to the material sheet number and location within the 16-ply sheets. Specimens were identified as 16A or B-1 through 10. Two additional panels were cut from a third sheet and were identified as 16B-11 and 16B-12 respectively. Specimen identification was maintained on the bottom (platen) side. Specimen thickness varied from 0.094 to 0.096 inches.

6061-T6 aluminum alloy doublers (grip end reinforcement) 3.9 inches X 3.9 inches X 0.100 inches thick were bonded to both sides of both ends of each specimen using "Hysol" EA 9030, epoxy resin (a room temperature curing adhesive). Prior to bonding, a 5 degree tapered edge was machined in the end of each doubler plate as shown in Figure 2.

The taper extended approximately 0.7 inch back from the gage section of the specimen. Sixteen ply panels were used in optimization, compatibility and fatigue test studies.

c. 24-Ply Specimens

Thirty (30), four (4) inch by four (4) inch test specimens were cut from the 24 ply sheet material. Edges were dressed and each specimen was identified using a vibro-etch marker according to their respective location within the 24-ply sheet. Specimens were identified as 24-1 through 24-30 respectively, with the identification on the bottom (platen) side. Specimen thickness varied from 0.142 to 0.144 inches. Twenty four ply panels were subsequently used for optimization and compatibility studies.

3. Single Exposure X-radiographic Technique Optimization

Optimization of X-radiographic techniques was performed by iterative exposure of graphite test samples using various, commercially available films, X-ray sources and exposure conditions. Image Quality Indicators (penetrameters) and step-wedges were used in combination with 8, 16 and 24-ply specimens to compare and optimize exposure techniques.

a. Film

Four (4) types of X-ray film were selected to evaluate relative film image contrast. These included:

- Kodak T*
- Kodak M
- Kodak DR (Double Emulsion)
- Kodak SR (Single Emulsion)

*Eastman Kodak Company, Rochester, N.Y.

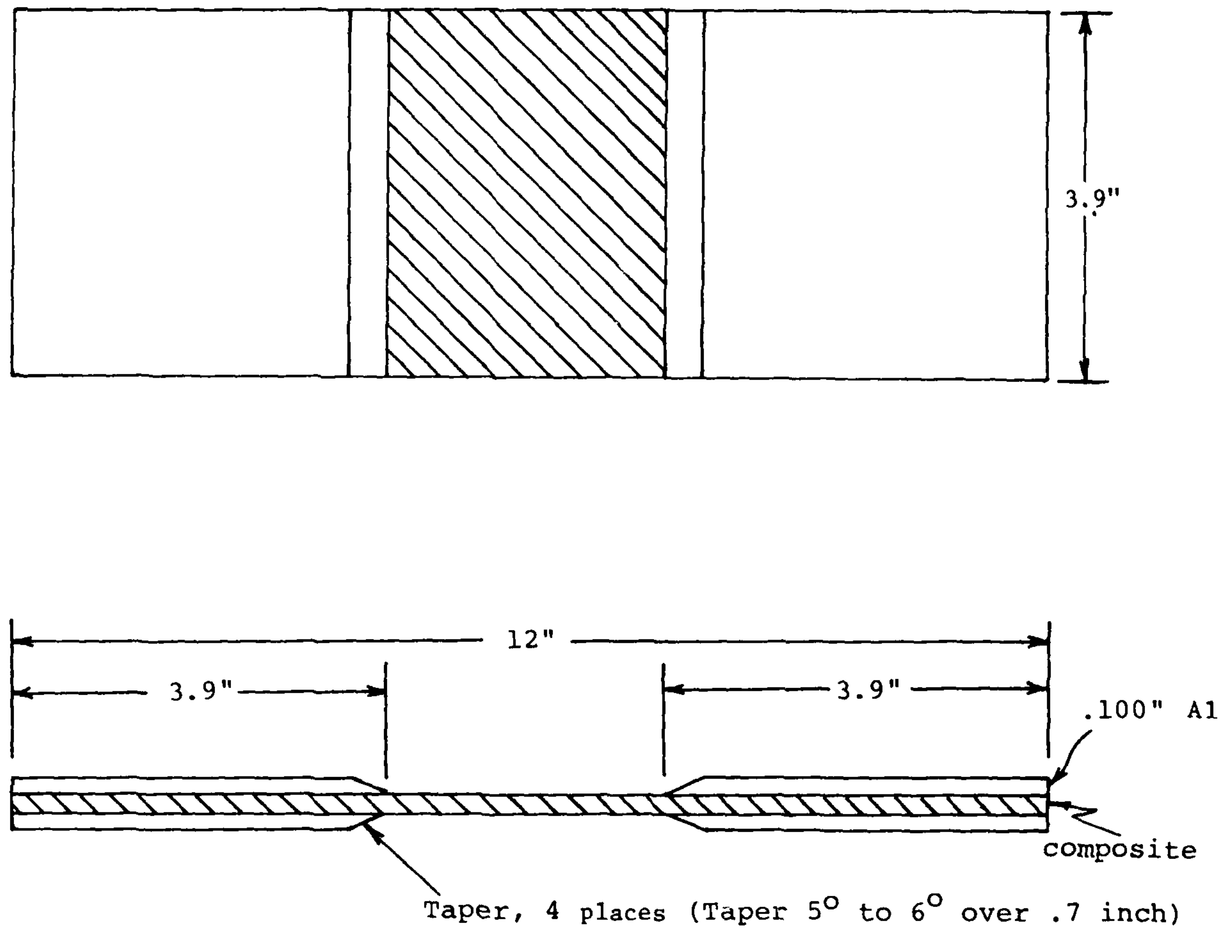

FIGURE 2 FATIGUE TEST SPECIMEN

The four Kodak films were representative of the range of industrial film types that were readily available.

b. X-Ray Sources

Four (4) X-ray systems were evaluated which provided variation in energy distribution. These consisted of:

- Norelco 150 Kilovolts, 24 milliamperes, 3 millimeter thick beryllium window, .7 and 2.5 millimeter focal-spot sizes.

- Balteau, 5-50 Kilovolts, 20 milliamperes, .25 millimeter thick beryllium window, 1.5 millimeter focal spot size.

- Magnaflux MXK-100M, microfocus X-ray unit, 0 to 100 Kilovolts, 0 to 1 milliamperes, .030 inch (.75 millimeters) thick beryllium window, variable focal spot size from 0.05 millimeters to 0.5 millimeters. Norelco-MCN-161 metal ceramic tube, 160 Kilovolts, 40 milliamperes, 1 millimeter beryllium window, .4 and 3.0 focal spot sizes.

All of the X-ray systems generally differed in the energy (Kilovoltage) range available, focal spot size, and inherent filtration (Thickness) of the beryllium window). All units have tungsten target tubes.

A large focal film distance (FFD) was selected to obtain improved geometric sharpness in all exposures.

c. Technique

The goal of the optimization was to produce an image at the lowest possible energy (Kilovoltage) TKD level and the greatest focal distance to obtain maximim radiographic contrast and sharpness.

Preliminary tests showed that the thinnest panel (8 ply - 0.042 to 0.044 inch) could not be penetrated at 10 KV with a 48 inch FFD. Further tests showed that penetration was possible at 15 KV. 15 KV was selected as lowest energy value for all trials. Various selected energy levels above this value were used for each equipment type, up to 100 KV maximum. To optimize the standard method, exposures were made using one (1) panel from each ply type with all exposure parameters and film types recorded as shown in the following:

TABLE 1	Balteau 5-50
TABLE 2	Norelco MG 150
TABLE 3	Norelco MCN 161
TABLE 4	Magnaflux MXK 100

Reduction of the focal film distance to 24 inches was required for use of the Magnaflux MXK 100 unit (Table 4) due to its low current radiation output at the small focal spot size. The small spot size option was designed to reduce geometric unsharpness thus requiring a lower current/radiation output for a given exposure. Assessment of type T film was eliminated from the Magnaflux MXK 100 unit evaluation due to practical limitations in the unit at low current settings.

d. Image Quality Indicator

Special penetrameters (image quality indicators) were fabricated from graphite/epoxy composite material for use as visual image quality indicators. Penetrameters were fabricated from single ply/procured material sheets produced with:

1) No. 181 glass bleeder cloth impression on surface 0.006 inches thick

2) No. 108 glass bleeder cloth impression on surface 0.006 inches thick

3) No. 112 glass bleeder cloth impression on surface 0.006 inches thick

Penetrameter size and hole size/configuration were kept as close as possible to that in Mil Std 00453. (See Figure 3). The No. 112 glass bleeder form was selected for application by comparison of X-ray images of the types. The No. 112 penetrameters were used as internal image quality indicators in all subsequent exposures.

e. Optimum Exposure Technique

An optimum film/exposure technique was selected for each material thickness by comparison of image quality produced by all techiques. Coincidence selection methods were used with a requirement that two independent observers select the same "best" exposure from each group. Three different observers were used in the selection of the "optimum" technique.

FIGURE 3 GRAPHITE/EPOXY PENTRAMETERS USED AS IMAGE QUALITY INDICATORS FOR X-RADIOGRAPHIC EXPOSURES

TABLE 1

BALTEAU 5-50

TYPE FILM		8-PLY						16-PLY						24-PLY					
		10 KV	15 KV	25 KV	50 KV	35 KV	100 KV	10 KV	15 KV	25 KV	50 KV	35 KV	100 KV	10 KV	15 KV	25 KV	50 KV	35 KV	100 KV
T	CURRENT	20	20	5	3.5				20	7	3				20	7	3		
	TIME	10:00	1:00	:20	:12				2:00	:20	:10				4:00	:25	:12		
	DENSITY	.035	2.08	2.2	1.9				1.9	2.1	1.9				1.8	2.0	2.0		
M	CURRENT		20	10	3.5				20	14	3				20	14	6		
	TIME		2:00	:20	:12				4:00	:20	:20				8:00	:25	:12		
	DENSITY		1.7	2:15	2.4				1.7	1.9	2.2				1.9	1.8	2.4		
DR5	CURRENT		20	20	7				20	14	3				20	14	10		
	TIME		4:00	:20	:12				8:00	:40	:35				6:00	:50	:10		
	DENSITY		1.9	1.8	1.7				1.8	1.6	1.7				1.6	1.5	1.6		
SR5	CURRENT		20	20	14				20	14	6				20	14	10		
	TIME		6:00	:30	:10				12:00	1:20	:35				30:00	1:40	:24		
	DENSITY		1.8	1.9	2.1				1.8	2.2	2.2				2.1	2.0	1.9		

RELATED FACTORS:

Current in milliamperes
Time in minutes; seconds
Density in γ units
Distance - 48 inches

Inherent filtration - .25 millimeters beryllium
Target size - 1.5 x 1.5 millimeters
Target material - Tungsten
Type of unit - Portable

TABLE 2

NORELCO MG 150

TYPE FILM		8-PLY						16-PLY						24-PLY					
		10 KV	15 IV	25 KV	50 KV	35 KV	100 KV	10 KV	15 KV	25 KV	50 KV	35 KV	100 KV	10 KV	15 KV	25 KV	50 KV	35 KV	100 KV
T	CURRENT			5	2	1.5	1			5	3	3	1			5	3	3	1
	TIME			:15	:10	2.0	:12			:20	:10	:15	:14			:20	:12	:20	:15
	DENSITY			2.0	2.1	2.0	1.9			1.8	2.5	1.8	1.9			1.9	2.3	2.3	2.0
M	CURRENT			5	3.5	3	1			5	3	3	1			5	6	6	1
	TIME			:25	:12	:25	:20			:35	:20	:30	:22			1:00	:10	:20	:24
	DENSITY			2:15	2.3	2.3	2.0			1.85	2.1	2.1	2.1			2.1	1.9	1.9	2.2
DR5	CURRENT			5	7	6	2			5	3	6	2			5	6	6	2
	TIME			1:00	:15	:30	:20			1:15	:40	:35	:20			2:00	:25	:40	:24
	DENSITY			2.1	2.0	1.9	1.6			1.55	1.9	1.7	1.4			2.1	1.8	1.6	1.6
SR5	CURRENT			5	5	6	4			5	6	6	4			5	6	6	4
	TIME			1:15	:20	:40	:20			1:40	:30	:45	:20			2:30	:27	:45	:24
	DENSITY			2.4	1.9	2.2	2.4			2.1	2.0	2.2	2.0			2.4	2.1	1.8	2.1

RELATED FACTORS:

Current in milliamperes
Time in minutes; seconds
Density in γ units
Distance - 48 inches

Inherent filtration - 3 millimeters beryllium
Target size - .7 millimeters
Target material - Tungsten
Type of unit - Fixed

TABLE 3

NORELCO MCN-161

TYPE FILM		8-PLY						16-PLY						24-PLY					
		10 KV	15 KV	25 KV	50 KV	35 KV	100 KV	10 KV	15 KV	25 KV	50 KV	35 KV	100 KV	10 KV	25 KV	50 KV	35 KV	100 KV	
T	CURRENT			5	2	3	2			5	2	3	2		5	3	3	2	
	TIME			:08	:05	:06	:02			:10	:05	:08	:02		:15	:08	:15	:02	
	DENSITY			2.0	2.1	1.7	2.6			1.6	1.7	1.8	2.0		1.7	2.1	2.3	1.8	
M	CURRENT			5	2	3	2			5	3	3	2		5	3	3	2	
	TIME			:15	:10	:10	:03			:20	:07	:15	:05		:25	:10	:20	:07	
	DENSITY			1.7	1.8	1.7	1.7			1.8	1.8	1.8	2.1		1.6	1.5	1.6	2.4	
DR5	CURRENT			5	2	3	2			5	3	3	2		5	3	3	2	
	TIME			:30	:20	:20	:07			:40	:25	:30	:10		1:00	:30	:50	:10	
	DENSITY			1.5	1.7	1.4	1.5			1.5	1.7	1.5	1.6		1.5	1.9	1.7	1.5	
SR5	CURRENT			5	2	3	2			5	3	3	2		5	3	3	2	
	TIME			1:00	:35	:40	:14			1:20	:40	1:00	:20		2:00	:45	1:20	:20	
	DENSITY			2.2	2.3	1.7	2.2			1.8	1.9	1.7	2.3		2.1	1.9	1.9	2.1	

RELATED FACTORS:

Current in milliamperes
Time in minutes; seconds
Density in γ units
Distance - 48 inches

Inherent filtration - 1 millimeters beryllium
Target size - .4 millimeters
Target material - Tungsten
Type of unit - Fixed

TABLE 4

EXPOSURE PARAMETERES USING A MAGNAFLUX MXK 100, X-RAY UNIT

TYPE FILM		8-PLY						16-PLY						24-PLY					
		10 KV	15 KV	25 KV	50 KV	35 KV	100 KV	10 KV	15 KV	25 KV	50 KV	35 KV	100 KV	10 KV	15 KV	25 KV	50 KV	35 KV	100 KV
T	CURRENT																		
	TIME																		
	DENSITY																		
M	CURRENT		.4	.5	.5		.5		.4	.5	.5		.25		.4	.5	.5		.5
	TIME		4:00	.4	.2		.1		8:00	.8	.3		.2		16.0	1.6	.4		.2
	DENSITY		1.9	1.7	1.7		1.8		2.3	1.7	1.9		1.6		2.3	2.0	2.1		2.4
DR5	CURRENT		.4	.5	.5		.5		.4	.5	.5		.5		.4	.5	.5		.5
	TIME		8:00	1.6	.4		.2		12.0	1.6	.6		.3		25.0	3.0	.8		.3
	DENSITY		2.1	2.2	1.7		1.5		2.1	1.4	1.9		2.8		2.6	1.9	2.3		1.9
SR5	CURRENT		.4	.5	.5		.5		.4	.5	.5		.5		.4	.5	.5		.5
	TIME		12:0	2.4	.6		.3		18.0	3.2	1.2		.3		30.0	4.5	1.0		.4
	DENSITY		2.4	2.4	1.9		1.7		1.7	1.8	2.4		1.4		1.8	1.8	1.7		1.6

RELATED FACTORS:

Current in Milliamperes
Time in minutes; seconds
Density in γ units
Distance - 24 inches

Inherent filtration - .0012 millimeters beryllium
Target size - 0.05 to 0.5 millimeters
Target material - Tungsten
Type of unit - Portable

The optimized technique selected and used for subsequent exposures was:

1) Equipment:

Balteau, 5-50 Kilovolts, 20 milliamperes

2) Film Type:

Eastman Kodak Industrex R Film
Double coated - code DR-5, with automatic processing (X-omat)

3) Exposure Parameters:

Ply	Kilovoltage	Milliamperes	Time	FFD
8	15	20	4 Min.	50"
16	15	20	8 Min.	50"
24	15	20	16 Min.	50"

NOTE: Focal film distance (FFD) was increased to 50 inches for convenience in calculations.

4. Introduction of Controlled Impact Damage

Methods for introducing low energy impact damage were evaluated by systematic introduction of damage by various indenter shapes and at increasing energy levels. The impact damage was intended to simulate dropping a sharp tool (such as a screwdriver) from high height. A damage level was selected to simulate a worst case condition for such an event and included broken fibers on the impacted face. A method of consistently and reproducibly introducing the required damage was established by visual comparison of the damage introduced to that produced by the dropped screwdriver samples. Test specimen size were selected to assure that damage did not extend to the specimen edge.

Controlled damage was produced by use of an 80 inch-pound Gardner variable impact tester as shown in Figure 4. The unit featured a 930 gram drop weight mounted in a guide tube. Interchangeable steel impact tools (punches) were designed and built to simulate reasonable impact damage. Four punches were built as shown in Figure 5.

No. 1 Punch - Blunt nose, 0.634 inch diameter with a large radius.

No. 2 Punch - Similar to a screwdriver tip.

No. 3 Punch - Blunt nose, 0.300 inch diameter with a small radius.

No. 4 Punch - Similar to a phillips screwdriver tip.

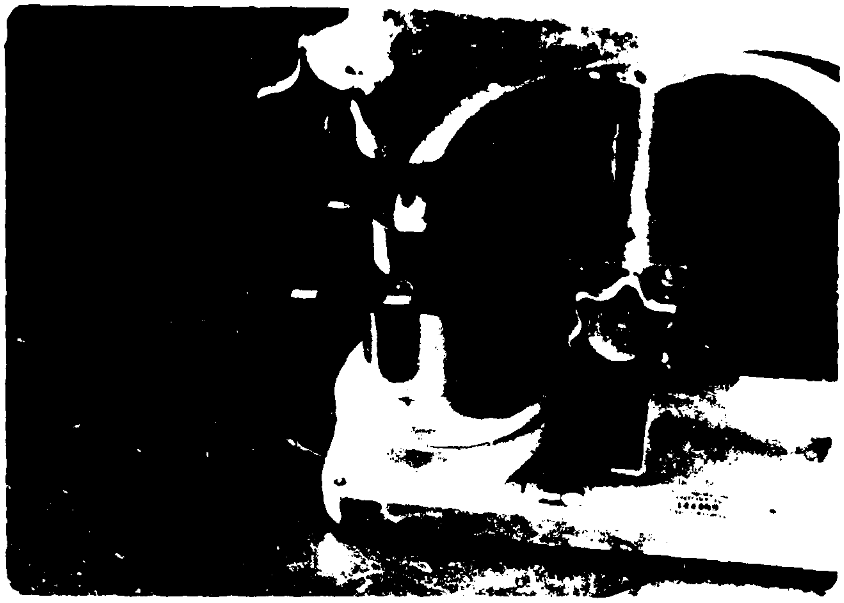

FIGURE 4 VARIABLE IMPACT TESTER

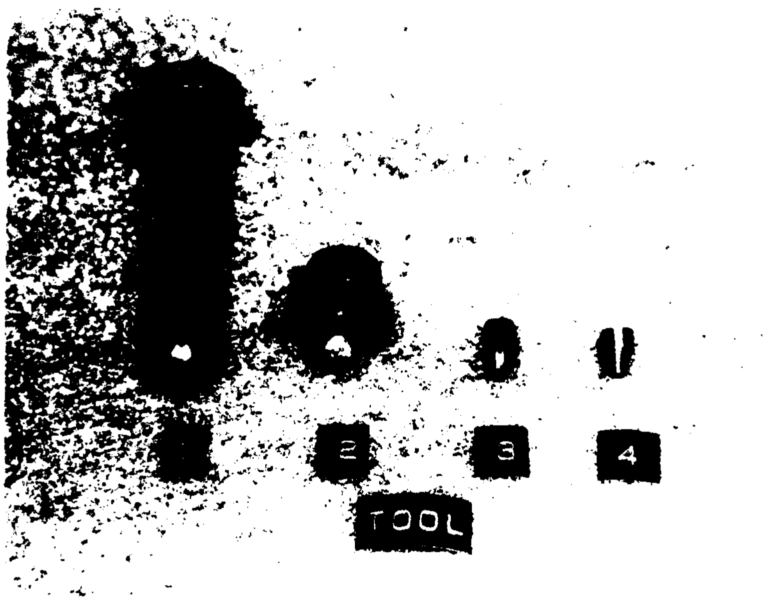

FIGURE 5 IMPACT TOOLS (PUNCHES)

Damage was produced by dropping the weight/impacter on to a panel from a prescribed height.

5. Candidate Opaque Penetrant Materials Selection

Use of X-ray opaque penetrant materials in imaging composite damage had been previously demonstrated (Ref. 5-6). Penetrants used in previous applications had been halogenated organic compounds. The toxic nature and reactivity of many of these compounds made selection of a stable form and/or an alternate material desirable.

a. Three halogenated organic compounds were selected for baseline studies to provide a basis for comparison with and a bridge to previously successful application of X-radiography to graphite-epoxy materials. These included:

- Tetrabromoethane - (TBE)
- 1, 4 Diiodobutane - (DIB)
- Diiodomethane - (CH_2I_2 - methylene iodide).

b. Two industrial X-ray opaque penetrant mixtures were selected. These included:

- ZLX-418B - Magnaflux Corporation, Chicago, Illinois (Diiodomethane base material)
- T100X - Uresco, Inc., Cerritos, California

c. Stable organic iodine compounds are used extensively in medical X-radiography and were potentially applicable to inspection of graphite/epoxy materials. One material was selected from medical sources for potential application.

Amipaque (Metrizamide) is used in medical applications as a subarachnoid contrast medium, for study of the spinal cord and adjacent structures. It is water soluble. It was mixed in proportion to 300 mg/ml for application to graphite/epoxy.

d. An X-ray opaque liquid penetrant material was developed in our laboratories as a potential low-cost, nontoxic alternative to the halogenated organic compounds. The material is based on zinc iodide (ZnI_2) as the X-ray opaque material. Both zinc and iodine (iodides) are required in the human diet; iodides in alcohol solution are used in antiseptic solutions - No special handling precautions have been identified for general use. (See Appendix B)

Zinc iodide is readily soluable in water, alcohol and alkalies and can thus be applied in relatively high concentrations. Penetrant properties of zinc iodide solution were improved by adding alcohol to give it both polar and non-polar solvent properties, and by adding a wetting agent (surfactant) such as a linear alcohol alkoxylate to reduce the surface tension of a solution. The initial formulation for the zinc iodide penetrant solution was as follows:

- Zinc iodide (ZnI_2) - 60 grams
- Water (H_2O) - 10 milliliters
- Isopropyl alcohol ($CH_3CHOHCH_3$) - 10 milliliters
- Kodak, "Photo Flo 600" - 1 milliliter (as a wetting agent)

Alternative materials considered included lead acetate, tetraethyl lead, barium halides, etc. These were right in favor of zinc iodide due to increasing complexity in handling and application.

6. Stereo-X-radiography

Stereo X-radiography is the X-radiographic equivalent of optical stereography in which two images are produced as viewed from slightly different angles and are then optically recombined to produce an apparent three dimensional image. The image emulates the two images normally viewed by the human eyes due to the spacing between the eyes. (See Figure 6).

A stereo X-radiograph film pair is produced by using an X-ray tube (source) to replace a white light source in exposing two (separate films) placed in slightly different positions with respect to the test object. Several geometries for X-ray exposure may be used to produce stereo images.

a. The source displacement method shown in Figure 7 involves holding the test object immobile while the X-ray tube is shifted in order to expose two X-radiographs from a slightly different perspective. Generally, the tube shift is one-tenth the target to film distance (1:10, ratio). At short target to film distances, the ratio may be increased to 1:13 to 1:16 to reduce eye strain. The tube is generally positioned such that the two exposures are made with the tube positioned at an equal distance on either side of the centerline of the test object.

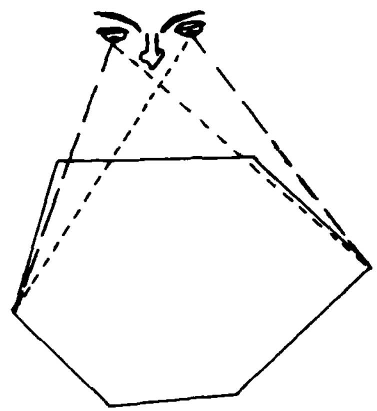

FIGURE 6 HUMAN STEREOSCOPIC VISION
The viewer is aware of the three dimensional effect caused by two slightly different images.

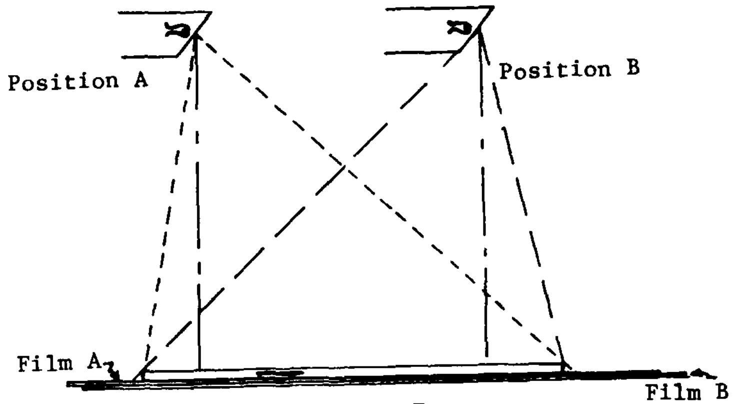

FIGURE 7

STEREORADIOGRAPHY - SOURCE DISPLACEMENT METHOD

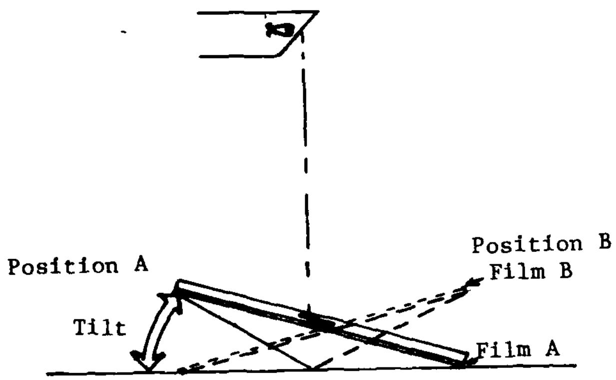

FIGURE 8

STEREORADIOGRAPHY - OBJECT TILT METHOD

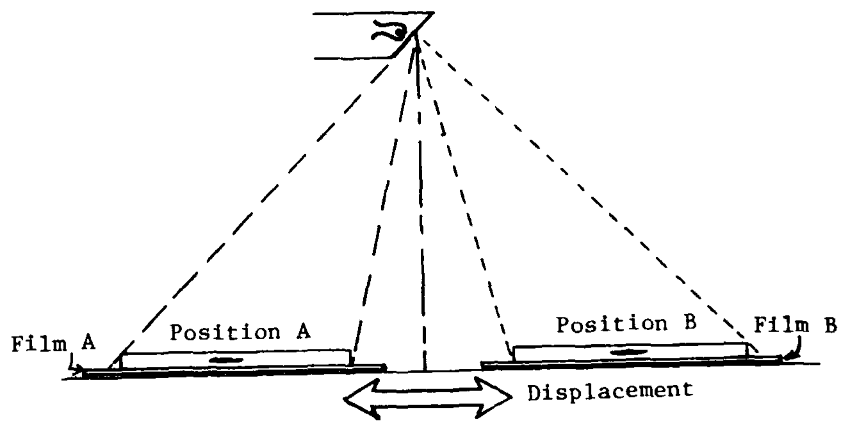

FIGURE 9

STEREORADIOGRAPHY - OBJECT DISPLACEMENT METHOD

Such techniques are used routinely in industry to locate the depth of anomolies within a weld, the depth of a component within a potted electronics module, etc.

b. The object displacement method shown in Figure 8 involves holding the X-ray source immobile while shifting (laterally displacing) the test object in order to expose a stereo X-radiograph pair. The source displacement and tube displacement methods produce identical results and may be used interchangeably for convenience in test set-up.

c. The object tilt method shown in Figure 9 involves holding the X-ray source immobile and tilting the test object with respect to the source axis to expose a stereo X-radiograph pair.

The stereo X-radiographic pairs may be viewed with the aid of a "stereo viewer" to "recombine" the images for viewing in the three dimensional mode. Figure 10.

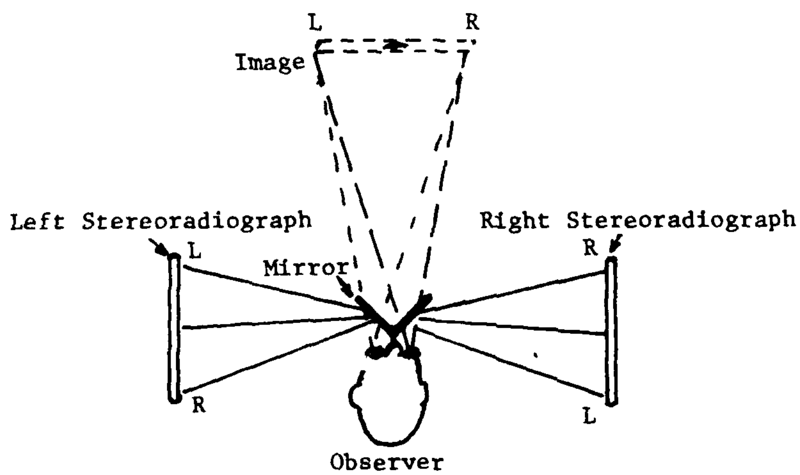

FIGURE 10 DIAGRAM SHOWING VIEWING OF A STEREO X-RADIOGRAPH PAIR

The stereo-mode provides a three dimensional view of the volume of a test object and may be used as a tool to locate an area of interest within the volume. Its capability for interrogation of a volume distinguishes it from other three dimensional interrogation techniques such as tomography (laminography, planigraphy, stratigraphy and vertigraphy) in which a selected plane through the object is imaged while structures above and below the selected plane are blurred. The stereo mode was selected as the most useful technique to monitor interaction of damage initiation sites and damage mechanisms in composites. The object displacement method was selected for its ease of application and control afford without use of special tooling.

7. *Stereo-X-Radiographic Technique Analysis Optimization*

Exposure and evaluation techniques for evaluation of the graphite epoxy panels by the stereo-x-radiographic method were optimized by successive evaluation of 16 ply and 24 ply panels. Stereo radiograph pairs were exposed using selected x-ray opaque penetrants with the optimized exposure technique previously developed. Stereo X-radiographs were viewed and analyzed with the aid of a Wild, Model ST-4 Mirror Stereoscope and a standard light box as shown in Figure 11.

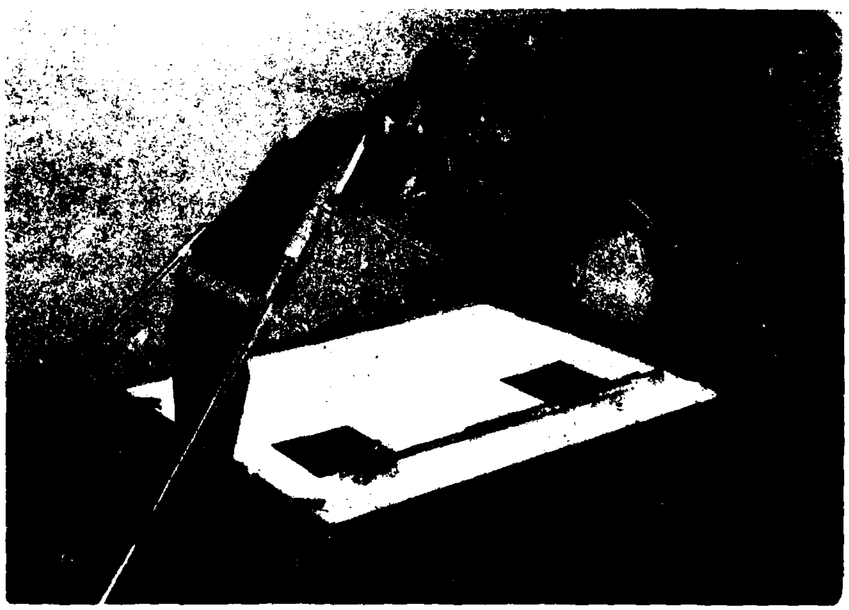

FIGURE 11 WILD ST-4, MIRROR STEREOSCOPE (VIEWER)

The conditions of viewing the radiographs should be similar to the conditions under which they were exposed: the two eyes take the place of the two positions of the focal spot of the x-ray tube, and the radiographs, as reflected in the mirrors, occupy the same position with respect to the eyes as did the films with respect to the tube during the exposures.

When each exposure is made, x-rays emerge from the focal spot of the x-ray tube and pass through the object to the film. Then, when the two radiographs are properly mounted in the stereoscope, the light rays from the illuminators pass through them and into the corresponding eyes, reproducing in reverse direction the paths followed by the x-rays in the exposure of the object. The observer sees the image of the object part just as the x-ray tube "saw" it.

In the case of radiographs exposed at long focus-film distances, a strict application of the correct conditions for viewing stereoradiographs would require that the eye-radiograph distance be equal to the focal-film distance used in making the exposures. Such long viewing distances are impractical with the usual stereoscopes, and furthermore, would make it difficult to see the finer details in the images. However, by using the appropriate stereoscopic tube-shifts at the longer focus-film distance, it is possible to view the radiographs at short distances with negligible distortion of the stereoscopic images. Suitable tube-shifts for various focus-film and eye-radiograph distances are given by the manufacturers of the equipment. A 2 9/16-inch interpupillary distance is assumed, since this has been found to be average. The viewing distance should suit the observer. (Ref. 4-5).

Variables assessed during technique optimization include:

- The angular separation between views
- Detection
- Sizing
- Depth resolution

8. Step Wedge Development

Comparison of initial exposures revealed a need to provide an internal reference for use in assessment of the depth resolution capabilities of an exposure technique. A circular step wedge was designed and fabricated for this purpose.

A circular step wedge configuration was selected to provide an internal reference of depth within the radiographic image and to cover a minimum area such that geometric unsharpness and radiation flux were essentially constant across the image.

Step wedges were fabricated to simulate individual ply steps for each of the specimen panel configurations (i.e., 8, 16, and 24 ply). A mold was machined from 6061 aluminum having a circular stair step configuration with steps equal to that of a single ply of graphite material. (See Figure 12)

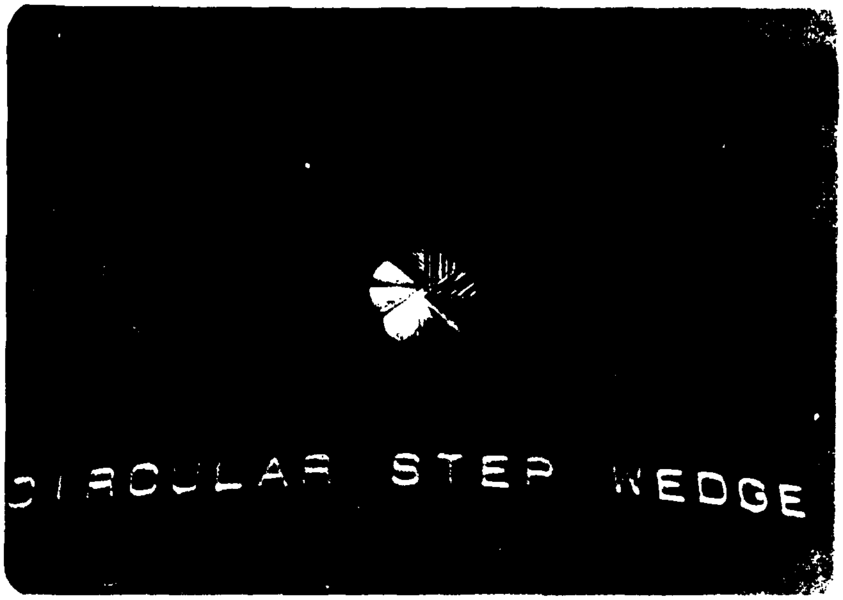

FIGURE 12 STEP WEDGE MOLD

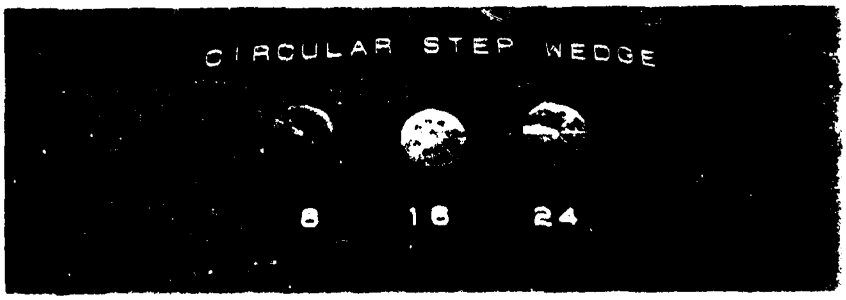

FIGURE 13 STEP WEDGE CLEAR CAST

A step wedge casting was then made from "Clear Cast" liquid casting plastic (Figure 13). Castings were machined and sanded to finished dimensions. "Clear Cast" was selected because its x-ray absorption characteristics were nearly the same as the graphite epoxy.

Lead beads were then attached to each step, and in the center at the bottom of the step wedge. These were used as an aid in the location of the various steps and depths during stereo viewing and during technique quantification.

An impact damaged, 16 ply specimen with ZLX-418B, penetrant was used to compare techniques. Exposures were made using the established exposure parameters by the object displacement method at 10:1 and 5:2 shift ratios. (See Figure 14). The 5:2 shift ratio was judged to be the maximum value obtainable within the uniform cone of radiation at a 50 inch FFD. (Focal Film Distance) Figure 15 is a stereo-x-ray image pair of an impact damaged (15 inch-pounds, no backing), area in the center of a 16 ply specimen Exposures were made at a 10:1 shift ratio. Figure 16 is a stereo x-ray image pair of the same specimen with exposures made at a 5:2 shift ratio. (See Appendix B for tips on viewing Stereo-X-Radiographs). Exposures made at the 5:2 shift ratio produced greater apparent image depth as viewed. A 5:2 shift ratio was selected for all subsequent exposures.

9. Stereo-X-Radiographic Technique Validation

Impact damage was inflicted in a 24 ply specimen (No. 24-29) using punch No. 1 at 15-inch pounds with no backing. (See Figure 17). An X-radiograph of the specimen without penetrant revealed no apparent damage. (See Figure 18). ZLX-418B penetrant was applied to the top side of the specimen (over the damaged area) and allowed to dwell for 30 minutes. An X-radiograph of the specimen showed very little capillary action or movement of penetrant into the damaged area. (See Figure 19)

ZLX-418B penetrant was applied to the bottom side of the specimen (over the damaged area) and allowed to dwell for 30 minutes. An X-radiograph of the specimen revealed good capillary action of penetrant and good imaging of the damaged area. (See Figure 20)

Stereo x-radiographs were made of the damaged specimen (with penetrant) using a 5:2 shift ratio. (Figure 21) The stereo radiographs were analyzed by three experienced radiographers and estimates of damage depth/location made. The largest delamination area was judged to be at level (step) 2 or 0.036 inch above the bottom surface of the specimen. The specimen was then microsectioned through the damaged area and the damage location was confirmed. Figure 22 shows a photomicrograph of a section of the damaged area in specimen No. 24-29. The dark line near the bottom of the photomicrograph is a delamination.

These evaluations confirmed the use of the X-ray stereo technique and highlighted the importance of getting penetrant into the damaged area(s).

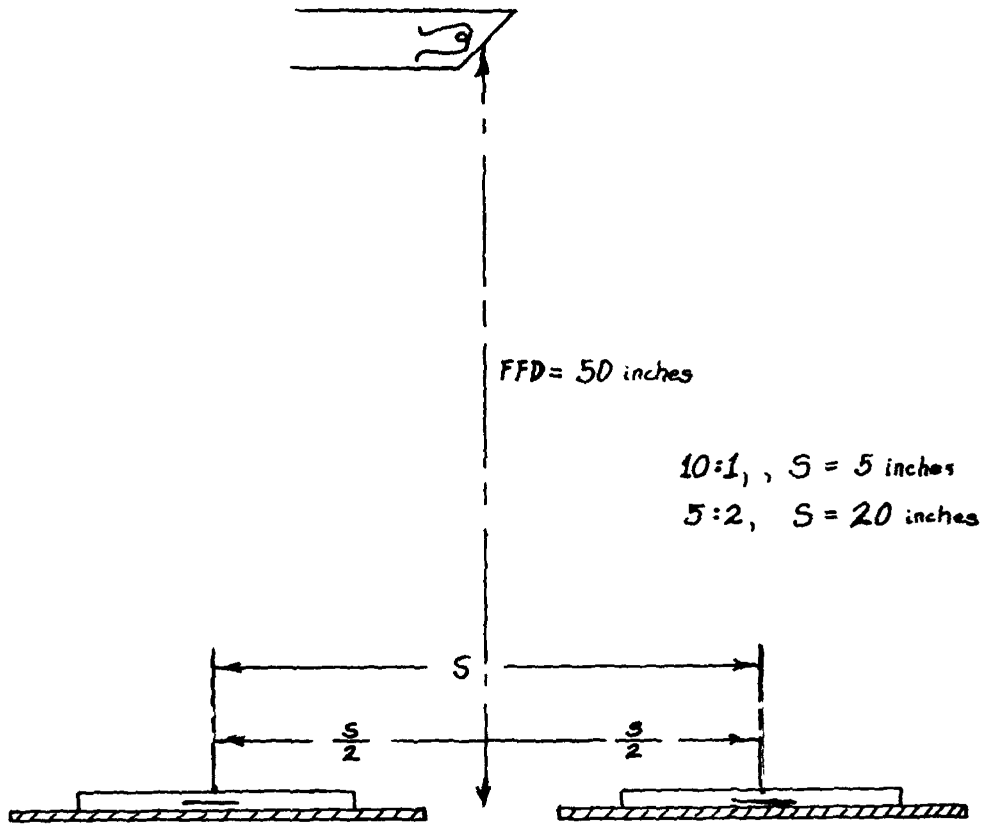

FIGURE 14 GEOMETRY OF STEREO X-RADIOGRAPH EXPOSURES AT TWO SHIFT RATIOS

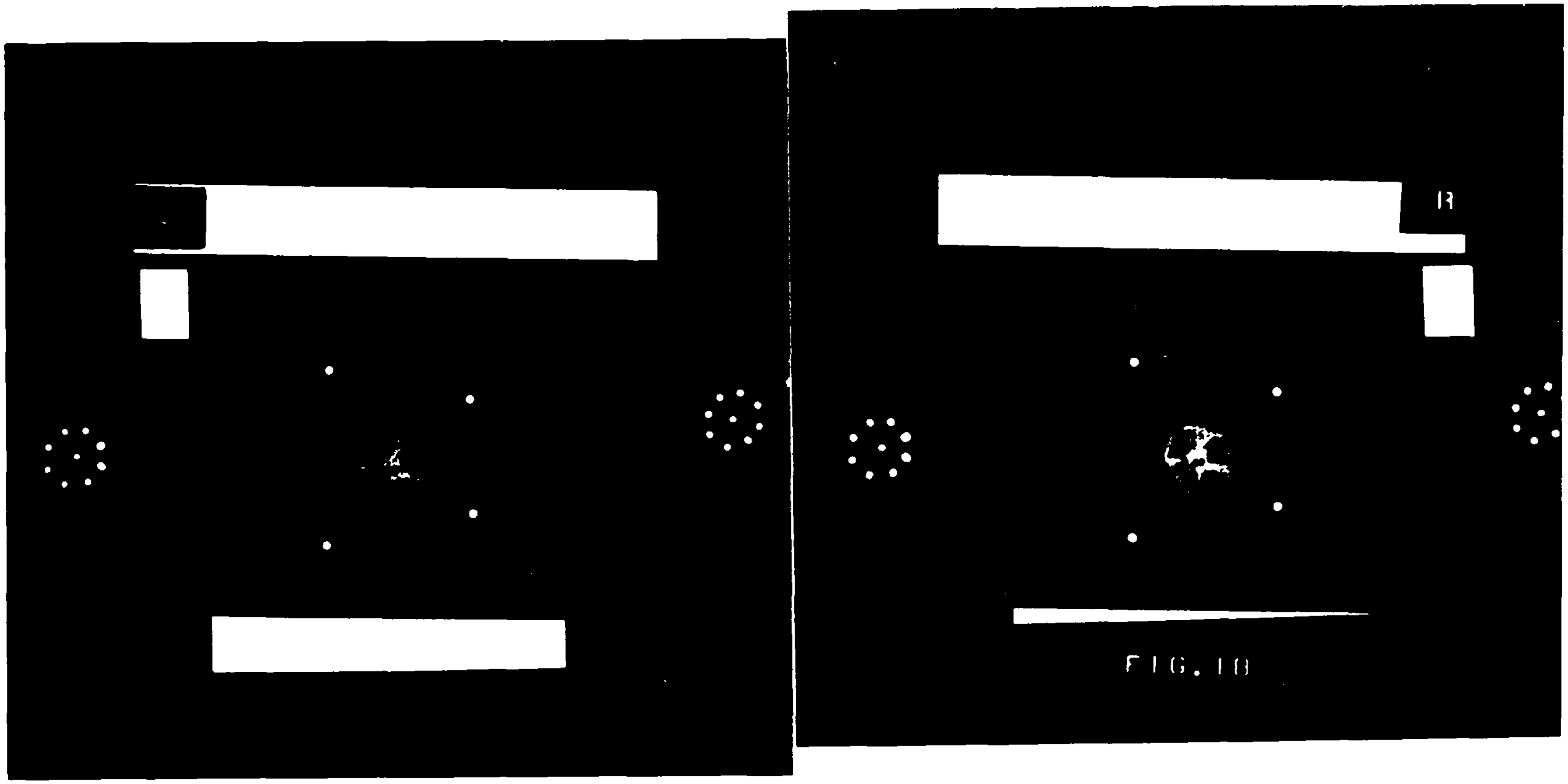

FIGURE 15 STEREO X-RAY IMAGE PAIR OF AN IMPACT DAMAGED (15 INCH POUNDS NO BACKING) AREA IN THE CENTER OF A 16 PLY SPECIMEN. EXPOSURES MADE AT A 10:1 SHIFT RATIO (PANEL NOTE NOTE STEP WEDGES)

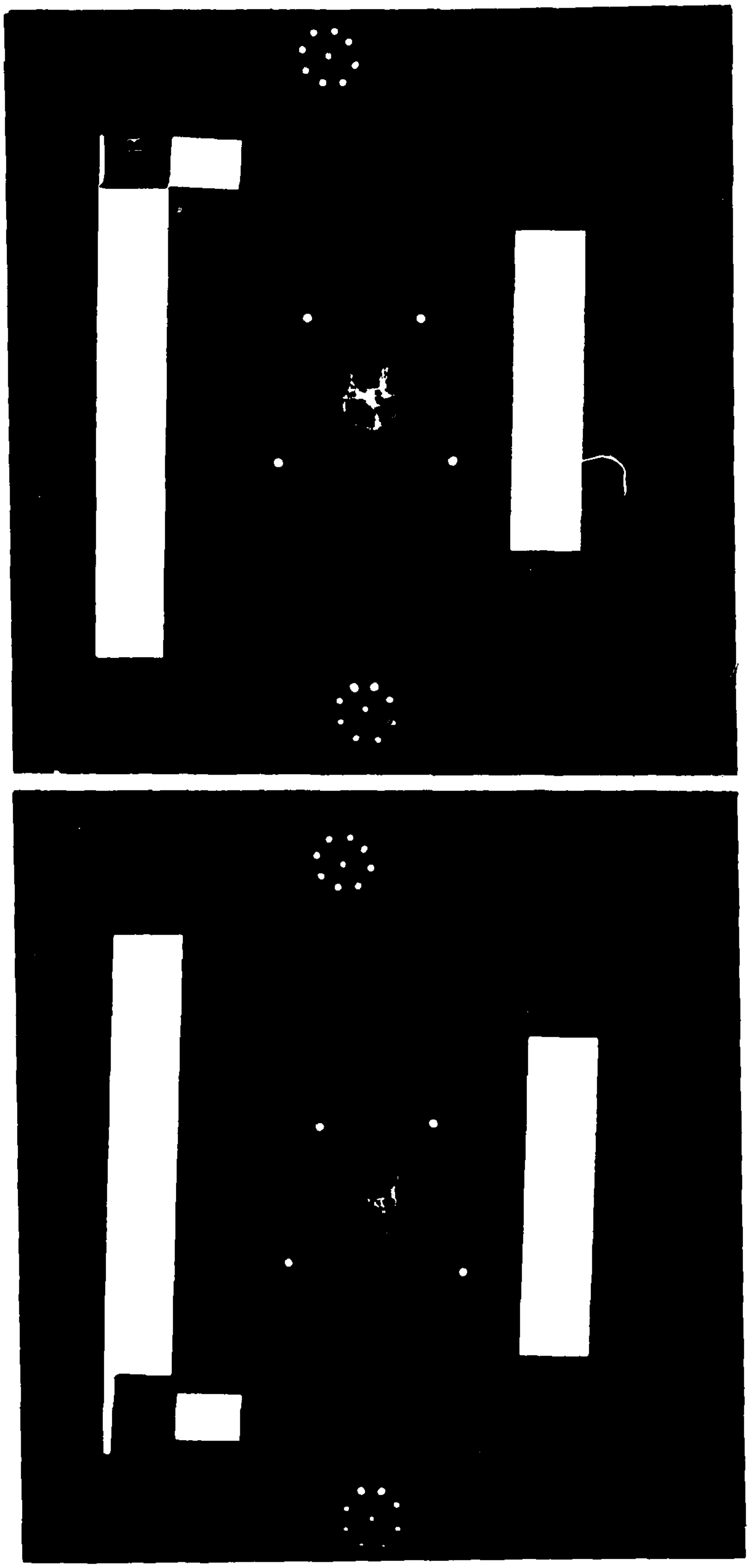

FIGURE 16 RADIOGRAPH 3D 5:2 SHIFT RATIO

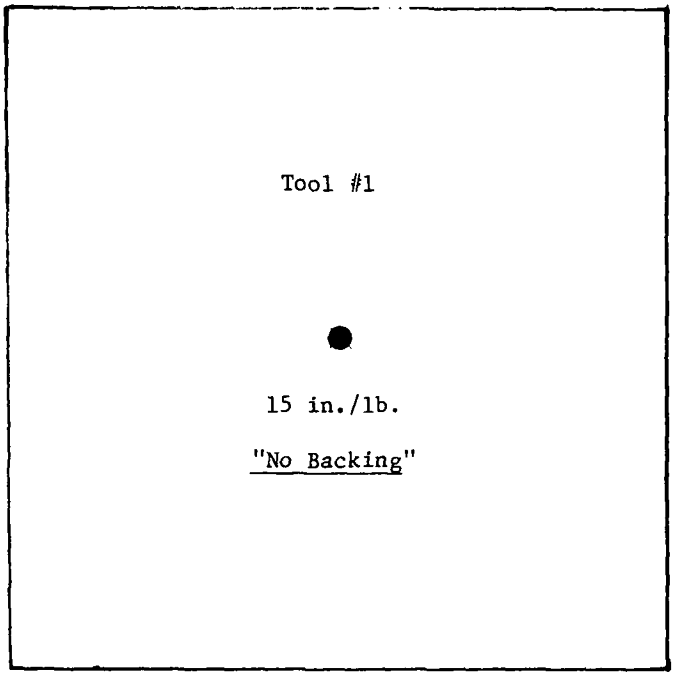

FIGURE 17 - LOCATION OF IMPACT DAMAGE IN TEST VALIDATION SPECIMEN NO. 24-29

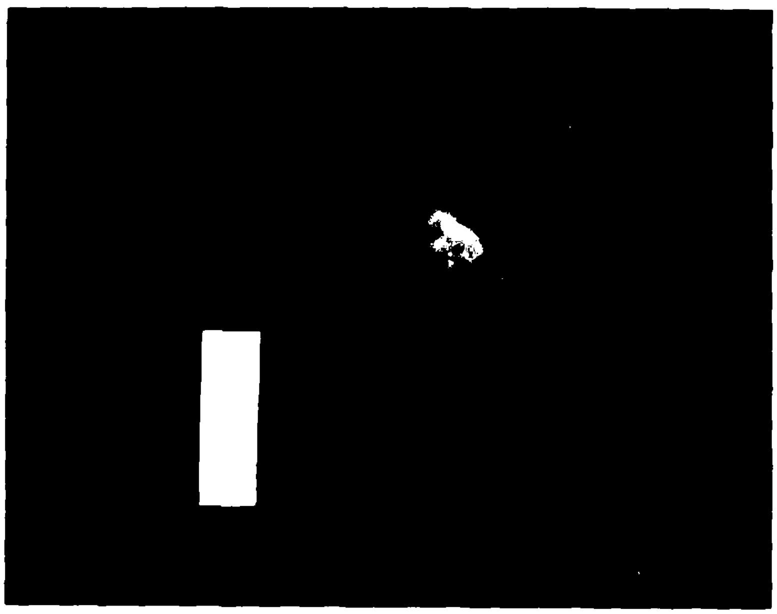

FIGURE 18 X-RADIOGRAPH OF TEST VALIDATION SPECIMEN NO. 24-29 AFTER IMPACT WITH NO PENETRANT

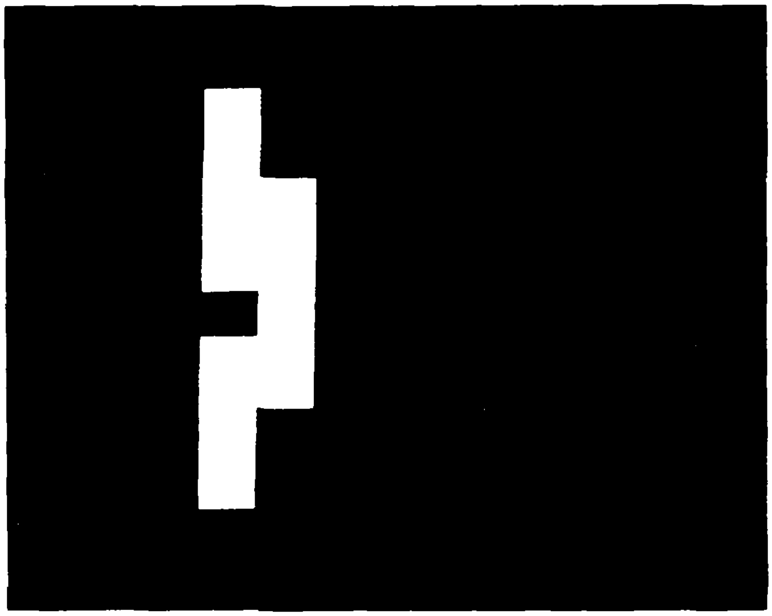

FIGURE 19 X-RADIOGRAPH OF TEST VALIDATION SPECIMEN NO. 24-29, AFTER 30 MINUTE DWELL OF ZLX-413B PENETRANT APPLIED TO THE TOP SIDE OF THE SPECIMEN

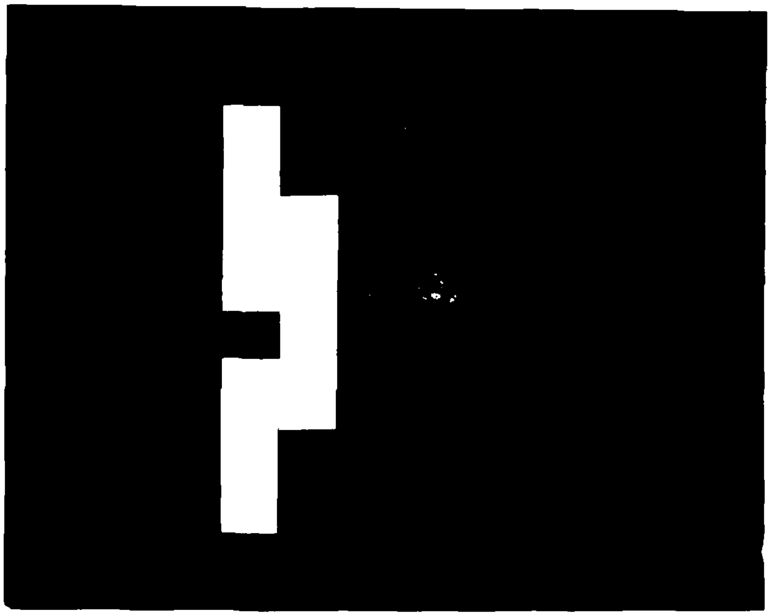

FIGURE 20 X-RADIOGRAPH OF TEST VALIDATION SPECIMEN NO. 24-29, AFTER 30 MINUTE DWELL OF ZLX-413B PENETRANT APPLIED TO THE BOTTOM SIDE OF THE SPECIMEN

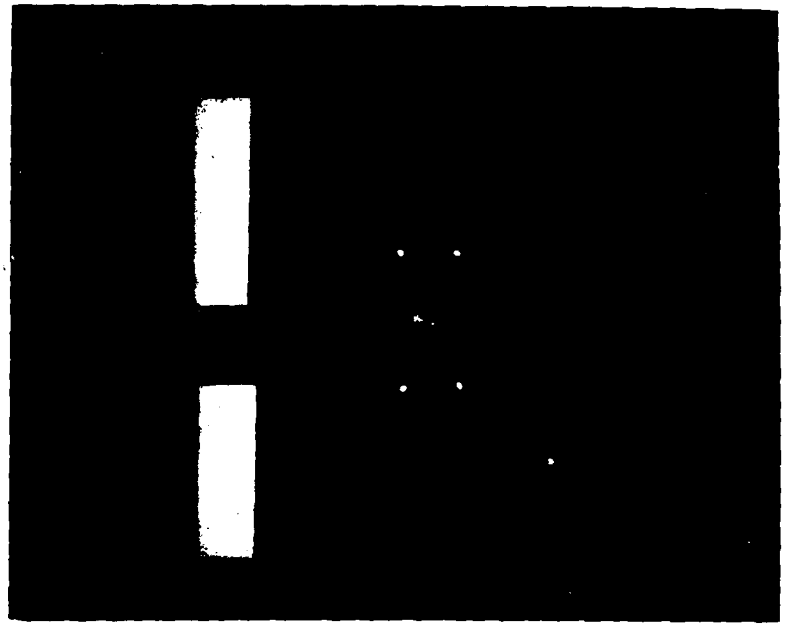

FIGURE 21 X-RAY STEREO PAIR OF TEST VALIDATION SPECIMEN NO. 24-29. AFTER PENETRANT APPLICATION

FIGURE 22 PHOTOMICROGRAPH OF A DAMAGED SECTION OF SPECIMEN OF SPECIMEN NO. 24-29

10. Conclusions:

Conclusions from the penetrant selection and X-radiographic technique optimization studies were as follows:

a. An x-ray opaque enhancement material is required for x-radiographic imaging of impact damage in resin matrix-graphite composite material.

b. Optimized X-radiographic exposure techniques for graphic/epoxy specimens were established by comparative analysis of images produced by different exposure techniques and materials. Comparative analysis of exposures was aided by use of fabricated image quality indicators (penetrameters).

The optimized exposure technique consisted of:

- Equipment - "Balteau", 5-50 Kilowatts, 20 milliampere
- Film - "Eastman Kodak, Industrex", Type R, Double Emulsion with automatic processing.
- Exposure parameters.

PLY	KILOVOLTAGE	MILLIAMPERES	TIME	FFD
8	15	20	4 Min.	50 inch
16	15	20	8 Min.	50 inch
24	15	20	16 Min.	50 inch

c. Controlled methods for introducing impact damage in graphite/epoxy composite materials were established using a "Gardner Impact Tester" with modified indenters (punches).

d. Seven candidate x-ray opaque imaging penetrants were identified. No reference for previous use of three (3) of the candidates (Diiodomethane, Amipaque, and Zinc Iodide) were found in a literature search.

e. An optimized stereo-x-radiographic exposure technique was developed which provided control in exposure, ease in viewing depth resolution, and ease in analysis. The technique consisted of:

   1). X-ray exposure using the optimized exposure/processing parameters

   2). Exposure by the object displacement method using a 5:2 shift ratio.

   3). Use of circular step wedge for image analysis and depth estimation.

f. A special circular step wedge was developed for use in stereo image analysis studies.

SECTION III

IMPACT DAMAGE ASSESSMENT

1. General

The purpose of the impact damage assessment studies was to establish methods for introducing controlled impact damage in graphite/epoxy composite materials and to use damaged specimens in evaluating X-ray opaque penetrant materials for imaging impact damage. An iterative process of damage introduction and damage assessment was used to minimize and direct experimental effort.

A Gardner Impact Tester had been shown to be desirable and useful in previous studies. Options for use in graphite/epoxy composite materials included:

- Variation in the shape of the indenter (punch) (four types were selected).
- Variation in the impact energy level. (5 to 80 inch pounds selected from previous work).
- Variation in panel backing during impact.

Initial impact damage was inflicted using a solid metal (stainless steel) backing to simulate impact over an attachment area such as an Aircraft Stringer. Damage inflicted was less severe and was not judged to be as wide as impact over an unsupported area. After initial assessment of impact with solid backing, all damage was inflicted with "no backing".

Unsupported (no backing) area impact was inflicted by positioning the location of impact over the center of a four (4) inch diameter by three and one-eighth (3 1/8) inch thick block with a center hole one and one-quarter (1¼) inch in diameter. The block material was stainless steel. The one and one-quarter (1¼) inch diameter hold was selected as the maximum practical size that would provide edge support for the specimen sizes to be damaged.

Evaluations completed and the results obtained by successive application of various penetrant materials by X-radiographic imaging of specimens containing varying degrees of impact damage are presented in the following:

2. Impact Damaged Specimen Preparation

a. 8 Ply Specimens

1). Specimen 8-29. Impact damage was inflicted on specimen 8-29 with no backing, in four (4) locations using tool (punch) No. 1 at 2, 4, 6 and 8 inch-pound energy levels. Damage locations are shown schematically in Figure 23.

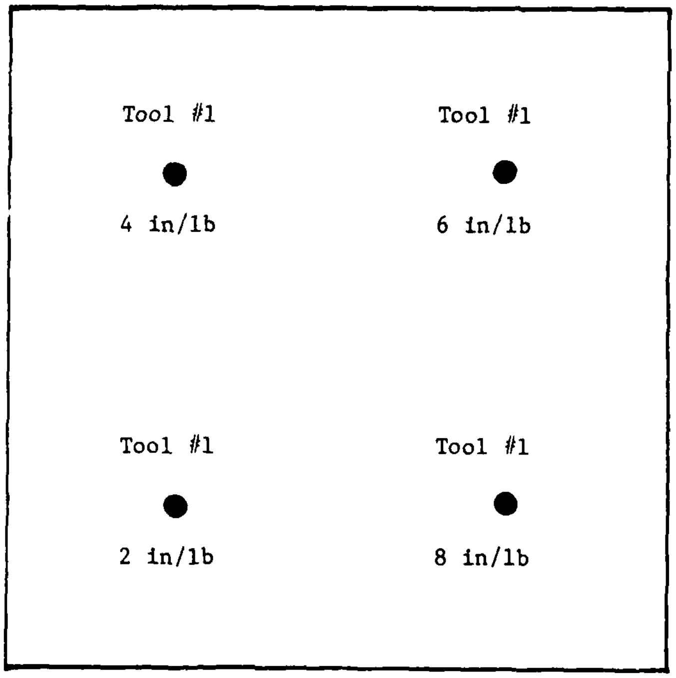

FIGURE 23 DAMAGE LOCATIONS IN SPECIMEN 8-29
(SPECIMEN SHOWN ACTUAL SIZE)

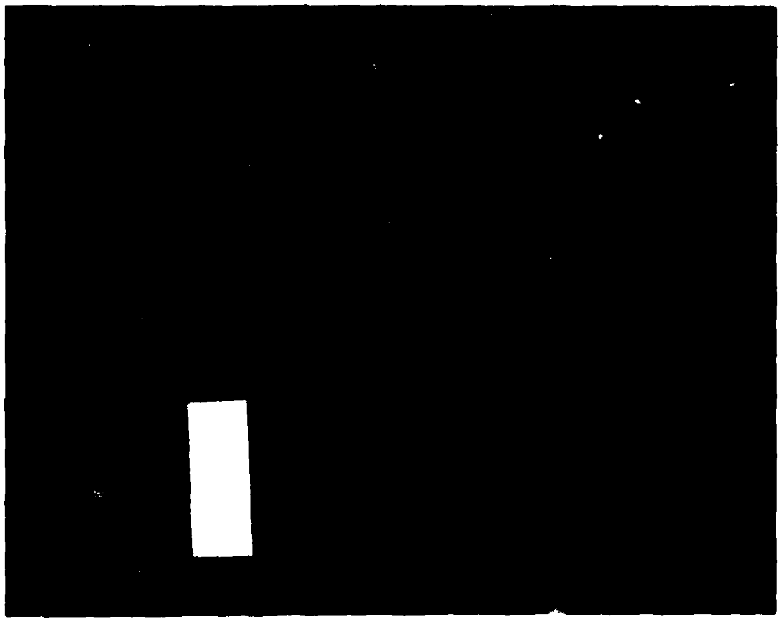

FIGURE 24 CONVENTIONAL X-RADIOGRAPH OF SPECIMEN 8-29
AFTER IMPACT - NO PENETRANT

Conventional X-radiographic inspection without penetrant revealed no evidence of damage in the 2 and 4 inch pound impact areas and revealed cracking the 6 and 8 inch pound impact areas. (Figure 24)

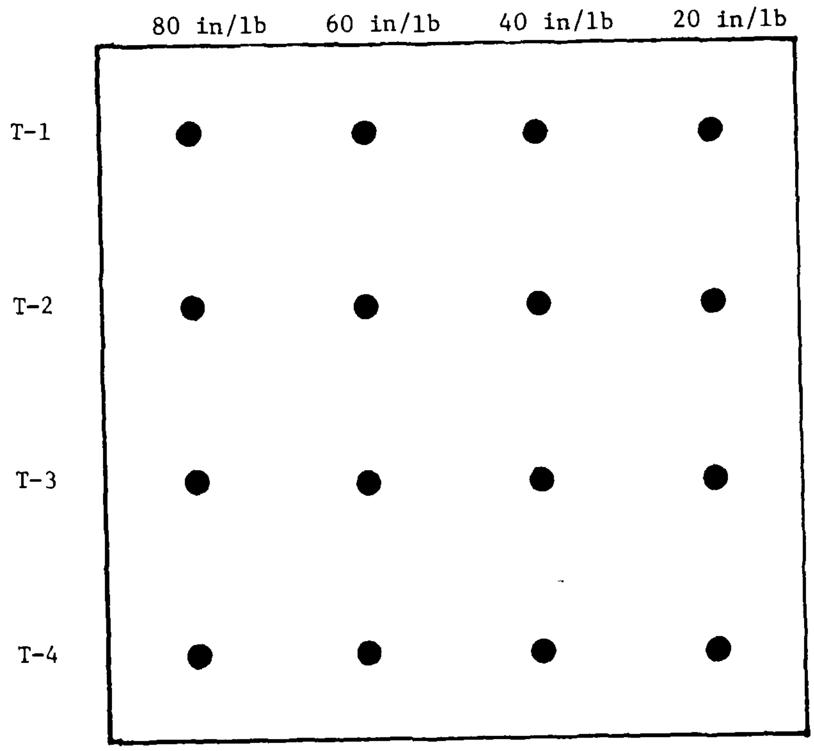

FIGURE 25 DAMAGE LOCATIONS IN SPECIMEN 8-30
(SPECIMEN SHOWN ACTUAL SIZE)

2). Specimen 8-30. Impact damage was inflicted on Specimen 8-30, with solid backing, in sixteen (16) locations using tool (punch) No. 1, 2, 3 and 4 at 20, 40, 60 and 80 inch-pound energy levels. Damage locations are shown schematically in Figure 25. Conventional X-radiography, with no penetrant, revealed extensive damage from tools No. 2, 3 and 4 and slight damage from tool No. 1. (Figure 26)

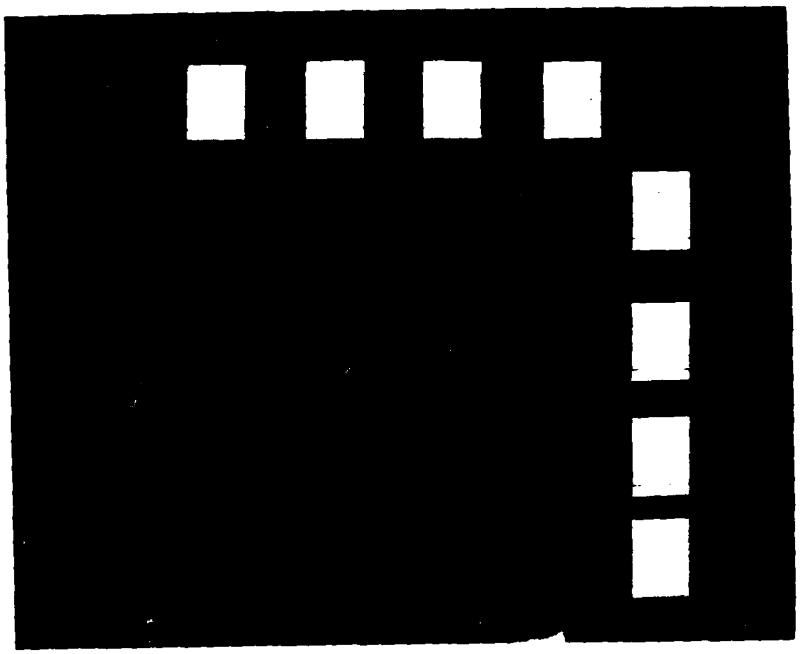

FIGURE 26 CONVENTIONAL X-RADIOGRAPH OF SPECIMEN 8-30 AFTER IMPACT - NO PENETRANT

b. Sixteen (16)- Ply Specimens

1). Specimen 16A10. Impact damage was inflicted on specimen 16A-10, with no backing, in sixteen (16) locations using tool (punch) No. 1, 2, 3 and 4 at 20, 40, 60, and 80 inch-pound energy levels. Damage locations are shown schematically in Figure 27. Conventional X-radiography, with no penetrant, revealed damage from tool No. 2, 3, and 4 at all energy levels. No apparent damage from tool No. 1 was revealed (Figure 28).

2). Specimen X16-20. Impact damage was inflicted on specimen X16-20, with no backing, in three locations, using tool (punch) No. 1 at 10, 15, and 20 inch-pounds. Damage locations are shown schematically in Figure 29. Conventional X-radiography, with no penetrant, revealed no apparent evidence of damage. (Figure 30)

c. Twenty-Four (24)- Ply Specimens

1). Specimen 24-24. Impact damage was inflicted on specimen 24-24, with no backing, in one (1) location using tool (punch) No. 1 at a 15 inch-pound energy level. Damage location is shown schematically in Figure 31. Conventional X-radiography, with no penetrant, revealed no apparent damage (Figure 32).

2). Specimen 24-26. Impact damage was inflicted on specimen 24-26, with no backing, at four (4) locations using tool (punch) No. 1 at a 20 inch-pound energy level. The four (4) locations (A through D) were designated for application of various penetrant materials in subsequent comparative evaluations. Damage locations and penetrant designation are shown schematically in Figure 33. Conventional X-radiography, with no penetrant, revealed no apparent damage (Figure 34).

3). Specimen 24-27. (Specimen 24-27 was identical to specimen 24-26). Impact damage was inflicted on specimen 24-27, with tool (punch) No. 1 at a 20 inch-pound energy level. The four (4) locations (A through D) were designated for application of various penetrant materials in subsequent applications. Damage locations are shown schematically in Figure 35. Conventional X-radiography, with no penetrant, revealed no apparent damage (Figure 36).

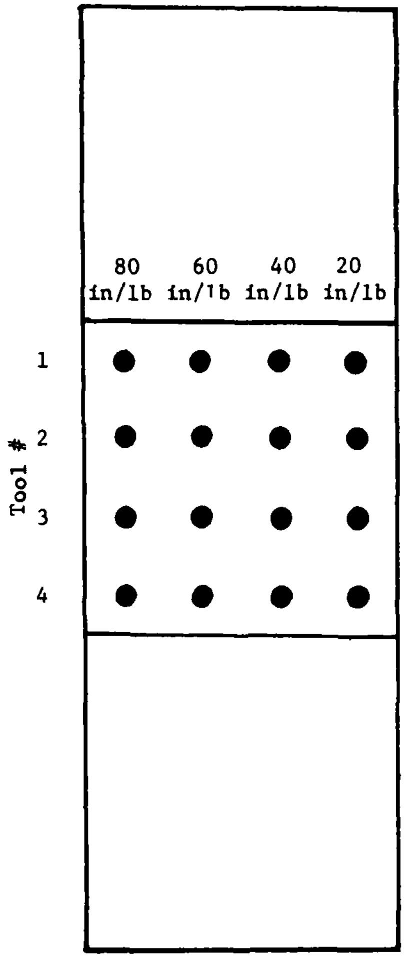

FIGURE 27 DAMAGE LOCATION IN SPECIMEN 16A-10 (SPECIMEN SHOWN HALF-SIZE)

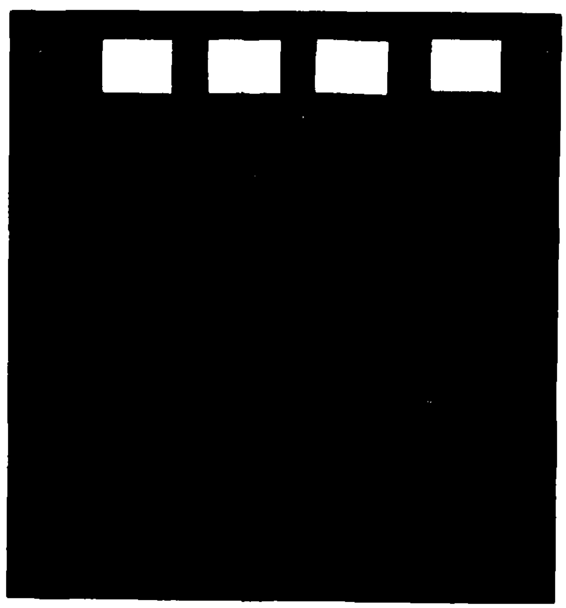

FIGURE 28 CONVENTIONAL X-RADIOGRAPH OF SPECIMEN 16A-10 AFTER IMPACT - NO PENETRANT

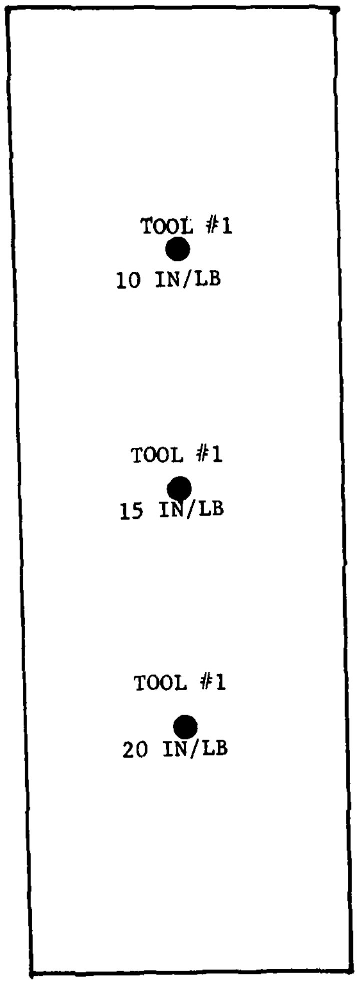

FIGURE 29

DAMAGE LOCATIONS IN SPECIMEN X16-20
(SPECIMEN SHOWN HALF-SIZE)

FIGURE 30

CONVENTIONAL X-RADIOGRAPH
OF SPECIMEN X16-20,
AFTER IMPACT -
NO PENETRANT

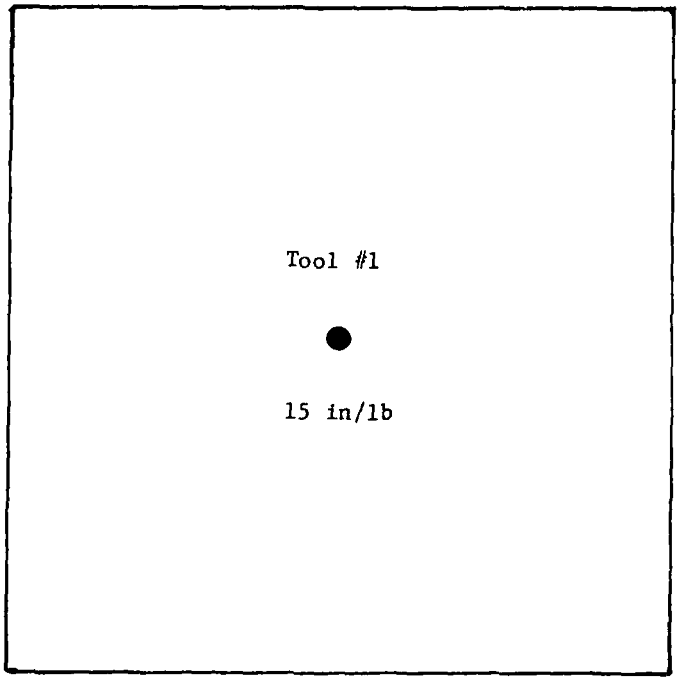

FIGURE 31 DAMAGE LOCATION IN SPECIMEN 24-24
(SPECIMEN SHOWN ACTUAL SIZE)

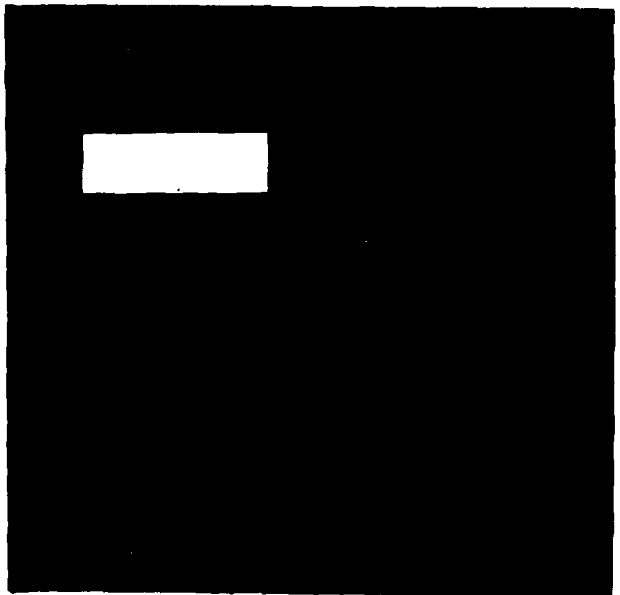

FIGURE 32 CONVENTIONAL X-RADIOGRAPH OF SPECIMEN 24-24,
AFTER IMPACT - NO PENETRANT

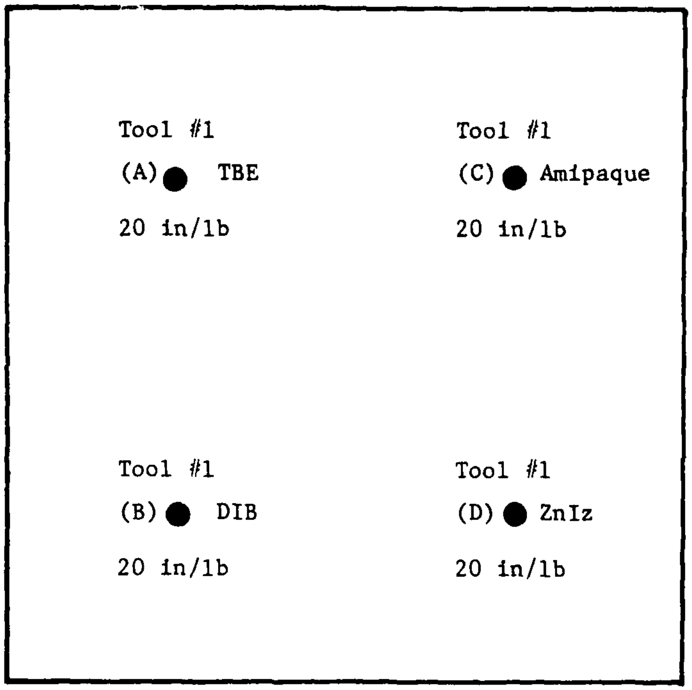

FIGURE 33 DAMAGE LOCATION IN SPECIMEN 24-26 (SPECIMEN SHOWN ACTUAL SIZE)

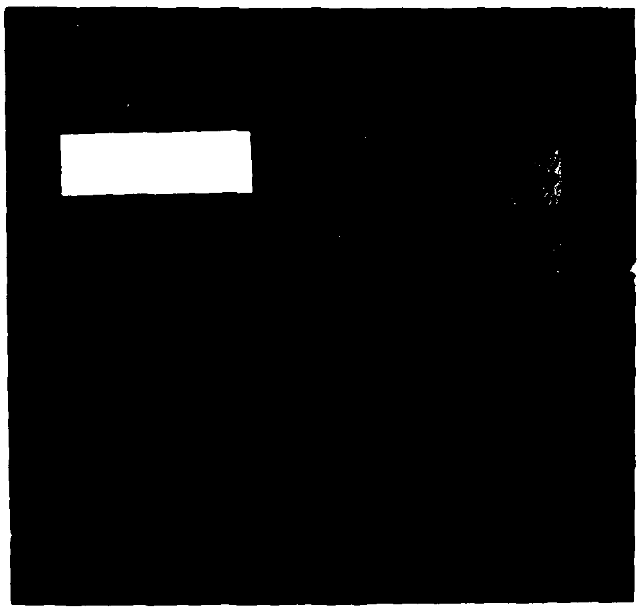

FIGURE 34 CONVENTIONAL X-RADIOGRAPH OF SPECIMEN 24-26 AFTER IMPACT - NO PENETRANT

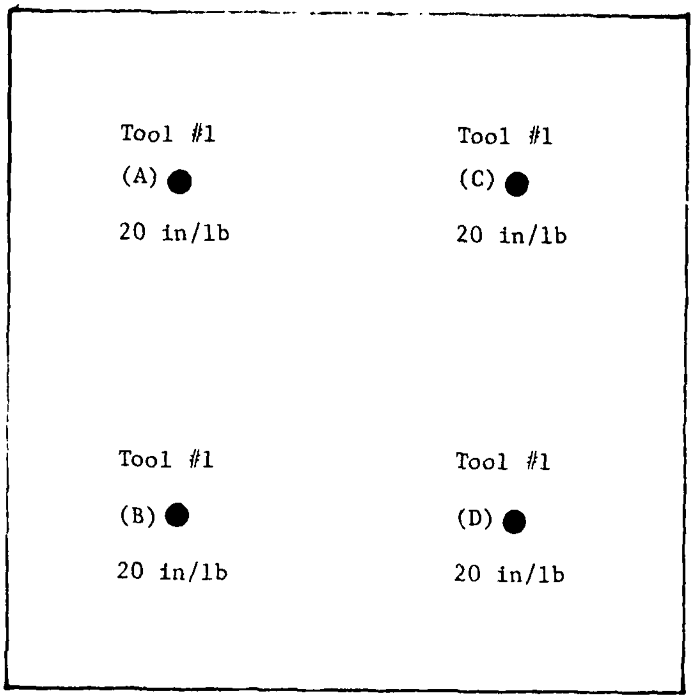

FIGURE 35 DAMAGE LOCATION IN SPECIMEN 24-27
(SPECIMEN SHOWN ACTUAL SIZE)

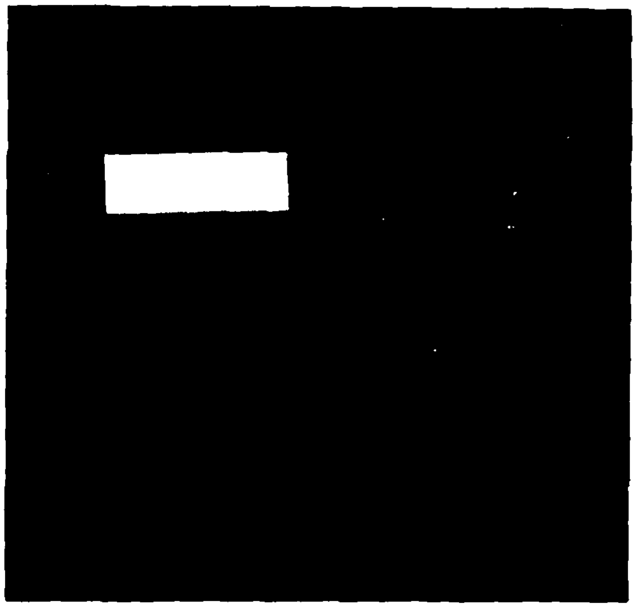

FIGURE 36 CONVENTIONAL X-RADIOGRAPH OF SPECIMEN 24-27
AFTER IMPACT - NO PENETRANT

4.) Specimen 24-28. Impact damage was inflicted on specimen 24-28, with no backing, at four (4) locations using tool (punch) No. 1, 2, 3, and 4 at a 20 inch-pound energy level. Damage locations are shown schematically in Figure 37. Conventional X-radiography, with no penetrant, revealed no apparent damage (Figure 38).

3. X-radiographic Evaluation of Impact Damaged Specimens with Various Penetrants.

Evaluation of impact damage in selected graphite/epoxy composite material specimens were conducted to:

- Select a controlled impact damage method for use in evaluating damage growth;

- Select penetrant for use in materials compatibility evaluations;

- Select a single penetrant for use in fatigue damage growth studies; and

- Establish a penetrant handling, application and removal procedures.

Evaluation consisted of iterative test and analysis as described in the following.

a. Eight (8)- Ply Specimen, 8-29. with ZLX-418B. ZLX-418B was applied to all damaged locations of specimen 8-29 and allowed to dwell for 30 minutes. X-radiographic inspection of the specimen (Figure 39) revealed the following:

1). Little capillary movement of the penetrant and slight damage at the 2 inch-pound location.

2). Good capillary movement of the penetrant and slight damage at the 4 inch-pound location.

3). Good capillary movement and a large amount of damage at the 6 and 8 inch-pound locations.

b. Eight (8)- Ply Specimen, 8-30, with Amipaque. Amipaque Metrizamide was applied to the 80-inch-pound damage locations and allowed to dwell for 30 minutes. X-radiographic inspection of the specimen (Figure 40) revealed the following:

1). Extensive damage at Tool No. 1, 2, and 3 locations.

2). Slight damage at the Tool No. 4 location.

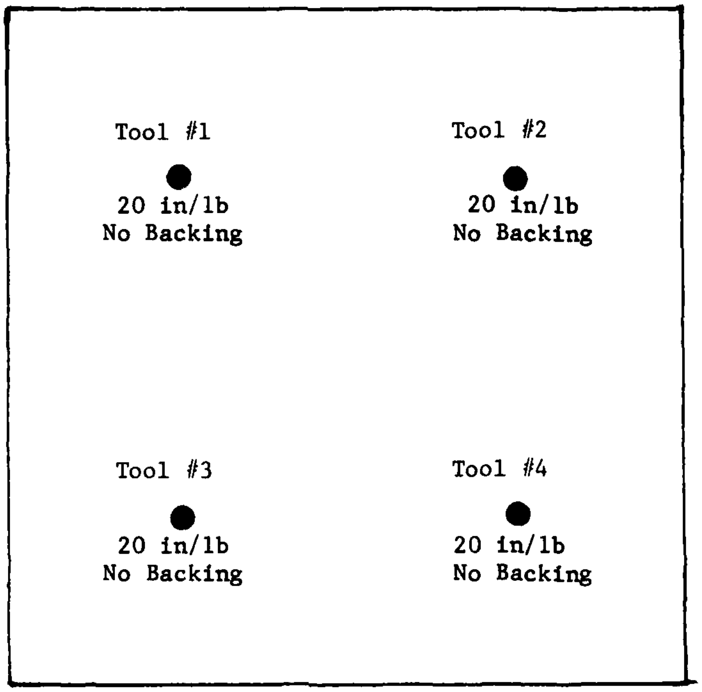

FIGURE 37 DAMAGE LOCATION IN SPECIMEN 24-28
(SPECIMEN SHOWN ACTUAL SIZE)

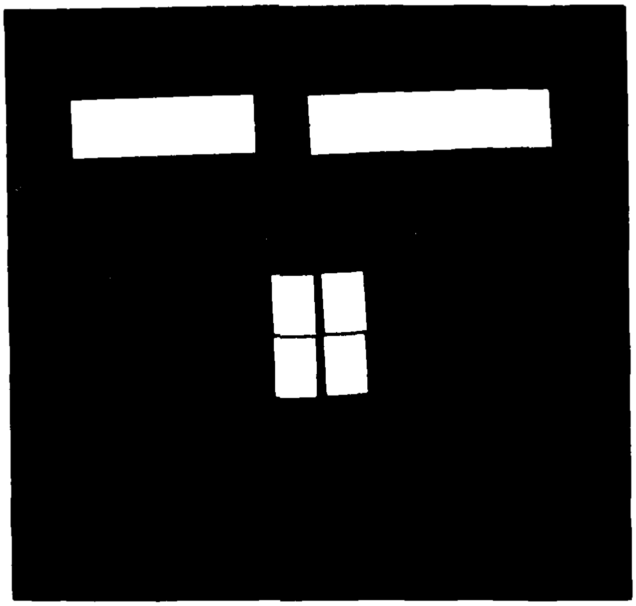

FIGURE 38 CONVENTIONAL X-RADIOGRAPH OF SPECIMEN 24-28
AFTER IMPACT - NO PENETRANT

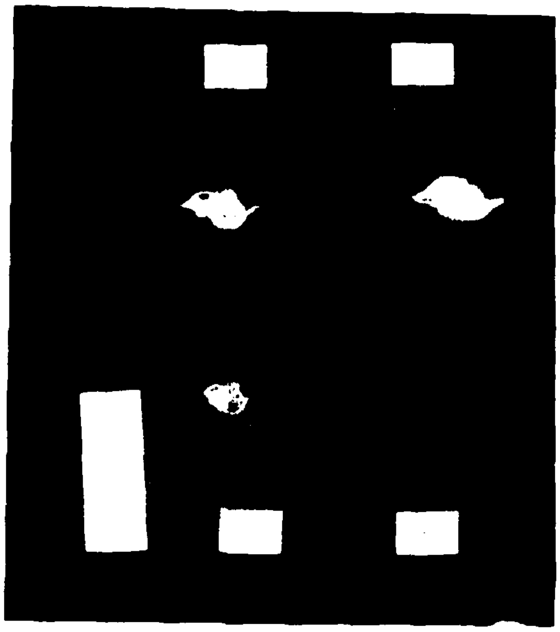

FIGURE 39 X-RADIOGRAPH OF SPECIMEN 8-29
WITH ZLX-418B AT ALL LOCATIONS

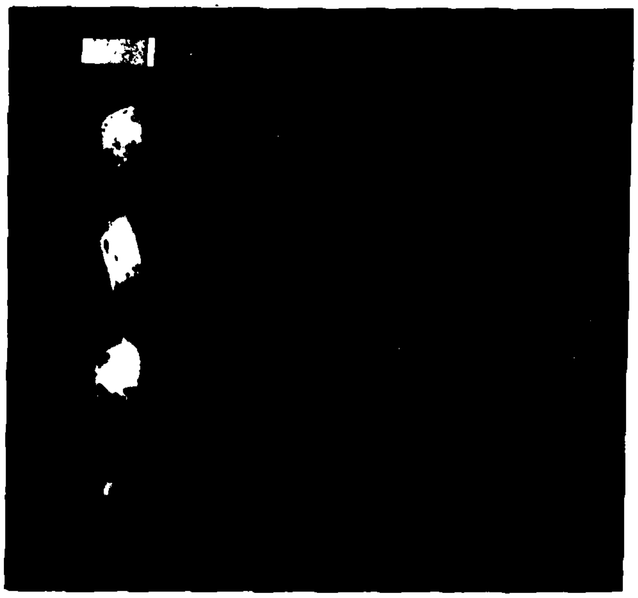

FIGURE 40 X-RADIOGRAPH OF SPECIMEN 8-30 WITH AMIPAQUE IN THE
80 INCH-POUND DAMAGE LOCATIONS

c. Sixteen (16)- Ply Specimen, 16A-10, with Amipaque.

NOTE: 80 inch-pound damage locations were selected for evaluation of all penetrant materials since damage was believed to be severe enough to provide assessment of poor as well as good materials.

Amipaque Metrizamide was applied to the 80 inch-pound damage locations and allowed to dwell for 30 minutes. X-radiographic inspection of the specimen (Figure 41) revealed the following:

1). Good capillary movement into damaged locations from Tool No. 2, 3, and 4.

2). Slight capillary movement and damage in the No. 1 Tool location.

The specimen was washed with water and re-radiographed to assess penetrant removal. The X-radiograph (Figure 42) revealed little penetrant residue after washing.

d. Sixteen (16)- Ply Specimen, 16A-10, with ZnI_2.

Zinc Iodide (ZnI_2) penetrant solution was applied to the 80 inch-pound damage locations and allowed to dwell for 30 minutes. X-radiographic inspection of the specimen (Figure 43) revealed the following:

1). Good capillary movement into all damage locations.

2). Slight damage in the No. 1 Tool location.

The specimen was water washed and re-radiographed to verify penetrant removal (Figure 44).

e. Sixteen (16)- Ply Specimen, 16A-10, with ZLX-418B.

ZLX-418B penetrant was applied to the 80 inch-pound damage locations and allowed to dwell for 30 minutes X-radiographic inspection of the specimen (Figure 45) revealed good capillary movement into all locations. The part was cleaned with "Tracer Tek K-410E remover and re-radiographed. The X-radiograph showed penetrant retention in locations 1, 3, and 4 (Figure 46). The specimen was ultrasonically cleaned in trichlorethane for one hour and re-radiographed. Most of the residual penetrant was removed.

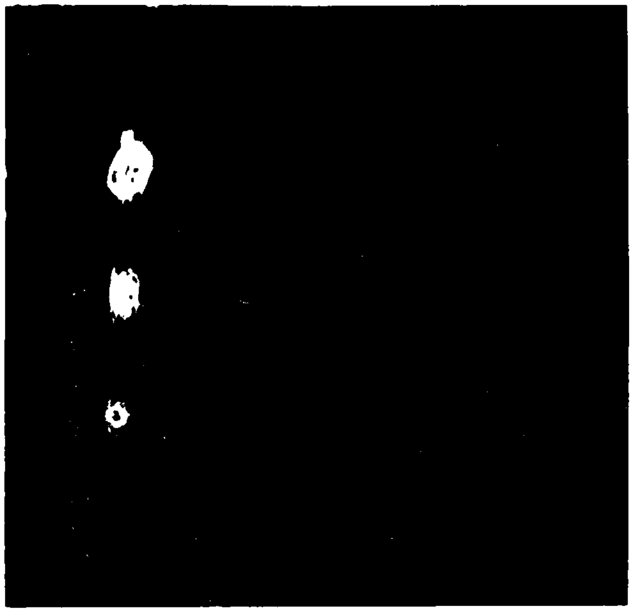

FIGURE 41 X-RADIOGRAPH OF SPECIMEN 16A-10, WITH AMIPAQUE IN THE 80 INCH-POUND DAMAGE LOCATION

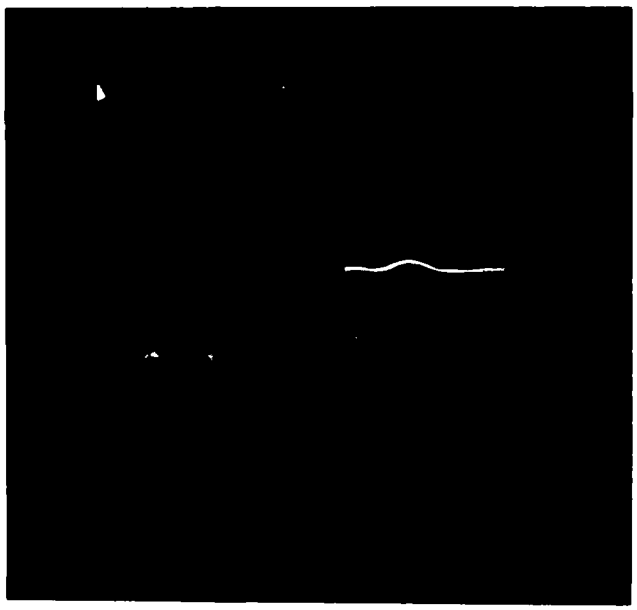

FIGURE 42 X-RADIOGRAPH OF SPECIMEN 16A-10 (AMIPAQUE) AFTER WATER WASH

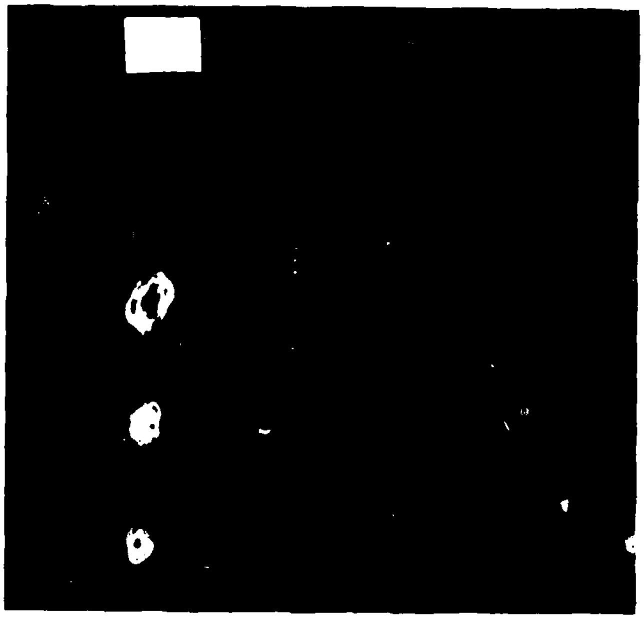

FIGURE 43 X-RADIOGRAPH OF SPECIMEN 16A-10, WITH ZINC IODIDE IN THE 80 INCH-POUND DAMAGE LOCATIONS

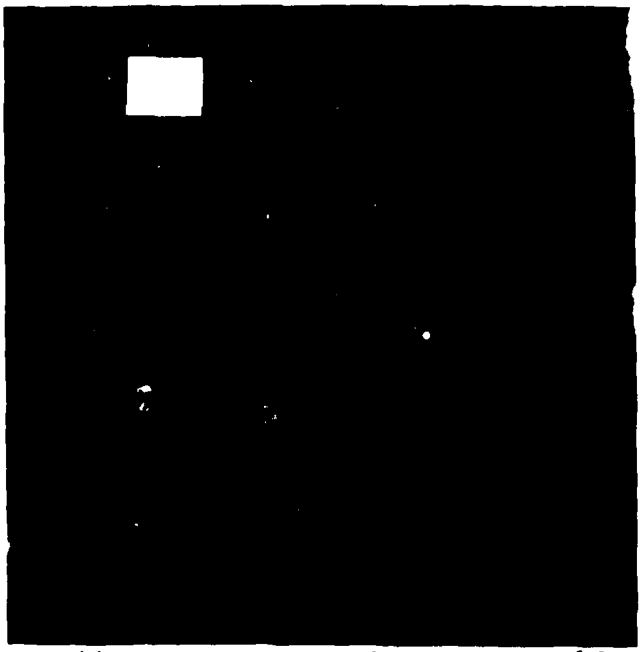

FIGURE 44 X-RADIOGRAPH OF SPECIMEN 16A-10, (ZINC IODIDE) AFTER WATER WASH

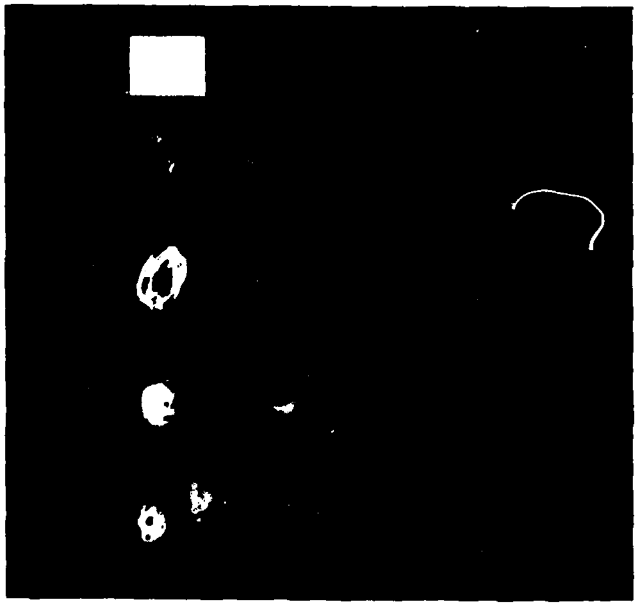

FIGURE 45 X-RADIOGRAPH OF SPECIMEN 16A-10, WITH ZLX-418B in the 80 INCH-POUND DAMAGE LOCATIONS

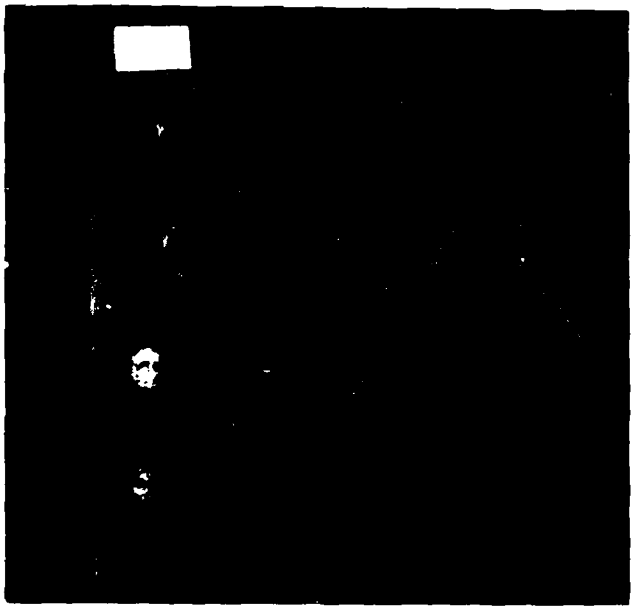

FIGURE 46 X-RADIOGRAPH OF SPECIMEN 16A-10, (ZLX-418B) AFTER CLEANING WITH TRACER TEK K-410E

f. Sixteen (16)- Ply Specimen, 16A-10, with TBE.

Tetrabromoethane (TBE) was applied to the 80 inch-pound damage locations and allowed to dwell for 30 minutes. X-radiographic inspection of the specimen (Figure 47) revealed good capillary movement into all locations. The specimen was ultrasonically cleaned in trichloroethane for one hour and re-radiographed. Most of the penetrant was removed.

g. Sixteen (16)- Ply Specimen, X16-20, with ZLX-418B

ZLX-418B penetrant was applied to all damage locations and allowed to dwell for 30 minutes. X-radiographic inspection of the specimen (Figure 48) revealed:

1). Good capillary movement into all locations;

2). Slight damage in the 10 inch pound location; and

3). A large amount of damage at the 15 and 20 inch-pound locations.

h. Twenty-four (24)- Ply Specimen, 24-24, with ZnI_2

Zinc Iodide (ZnI_2) was applied to the specimen and allowed to dwell for 30 minutes. X-radiographic inspection of the specimen (Figure 49) showed slight impact and good capillary movement into the damaged area.

i. Twenty-Four (24)- Ply Specimen, 24-26 with Various Penetrants

Tetrabromoethane (TBE) was applied to damage location A;

Diiodobutane (DIB) was applied to damage location B;

Amipaque Metrizamide was applied to damage location C; and

Zinc Iodide (ZnI_2) penetrant was applied to damage location D. Penetrant was allowed to dwell for 30 minutes. X-radiographic inspection of the specimen (Figure 50) revealed the following:

1). Good capillary movement into locations A, B, and D.

2). The Amipaque did not move well into the damage location but instead crystallized on the surface of the specimen.

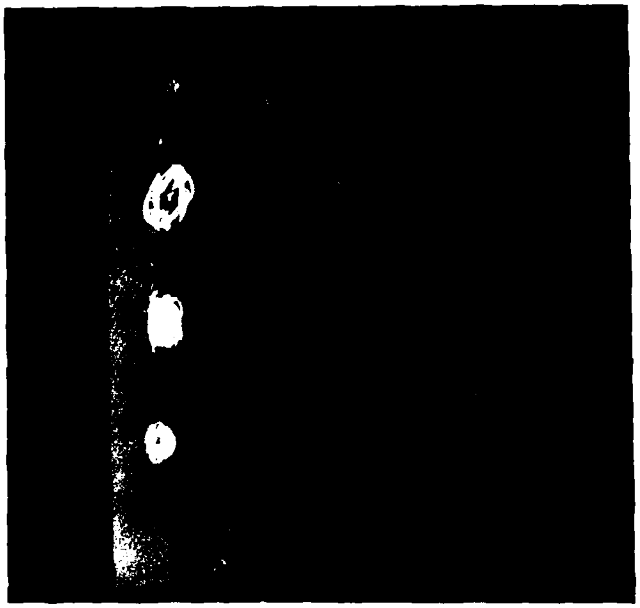

FIGURE 47 X-RADIOGRAPH OF SPECIMEN 16A-10, WITH TETRABROMOETHANE IN THE 80 INCH-POUND DAMAGE LOCATIONS

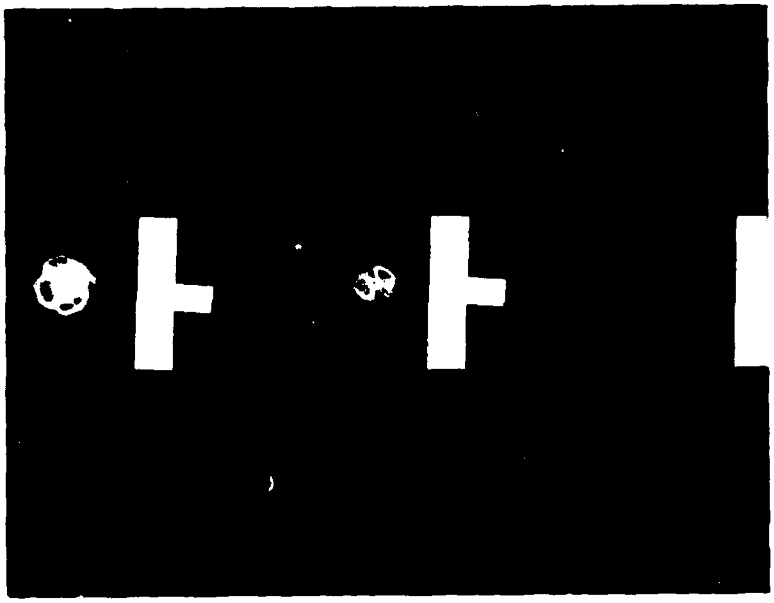

FIGURE 48 X-RADIOGRAPH OF SPECIMEN X16-20, WITH ZLX-418B IN ALL DAMAGE LOCATIONS

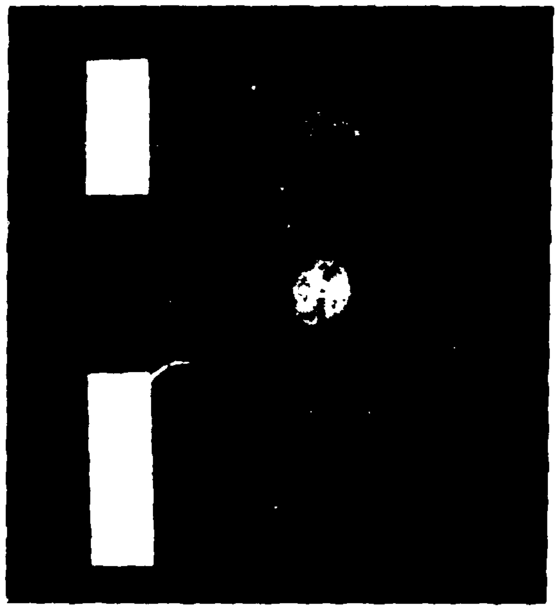

FIGURE 49 X-RADIOGRAPH OF SPECIMEN 24-24, WITH ZnI_2 IN THE DAMAGE LOCATION

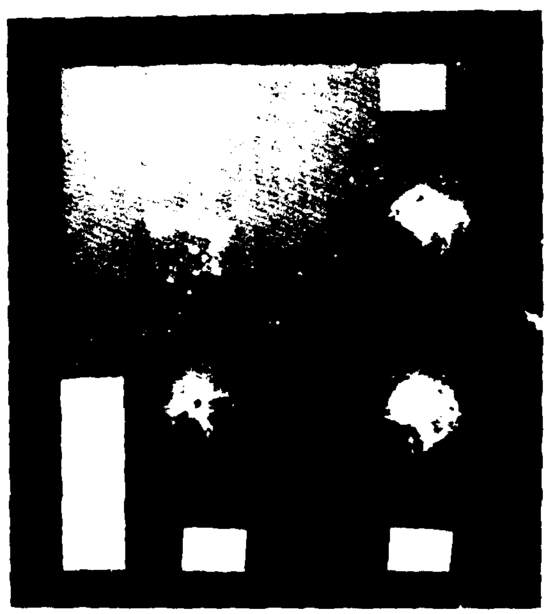

FIGURE 50 X-RADIOGRAPH OF SPECIMEN 24-26 WITH VARIOUS PENETRANTS

j. Twenty-Four (24)- Ply Specimen, 24-27, with Various Penetrants

1). Effects on penetration and removal properties at various concentrations of X-ray opaque additives was evaluated by dilution of the T-100X opaque penetrant with P-149 fluorescent penetrant (Uresco).

A mixture of 10% (by volume) T-100X with 90% P-149 was applied to damage location A; and

A mixture of 50% T-100X with 50% P-149 was applied to damage location B. The mixtures were allowed to dwell for 30 minutes. X-radiographic inspection (Figure 51) showed no evidence of capillary movement into the damage locations.

2). The specimen was ultrasonically cleaned for three (3) hours in trichloroethance; T-100X applied full strength to damage locations A and B; and allowed to dwell for 30 minutes. X-radiographic inspection (Figure 52) showed some capillary movement into the damage locations.

3). The specimen was ultrasonically cleaned for one and one-half (1½) hours in trichloroethane. X-radiographic inspection showed little movement of opaque materials.

T-100X was re-applied to damage location B;

ZLX418B was applied to damage location C; and

Diiodomethane (DIM) was applied to damage location D. Penetrants were allowed to dwell for 30 minutes.

X-radiographic inspection of the specimen (Figure 53) showed good capillary movement into damage locations C and D and some movement into location B. The DIM material tended to bead up on the specimen surface and was somewhat more difficult to apply.

The specimen was ultrasonically cleaned for five (5) hours in trichloroethane. X-radiography showed that most of the penetrants remained in the damage locations (Figure 54).

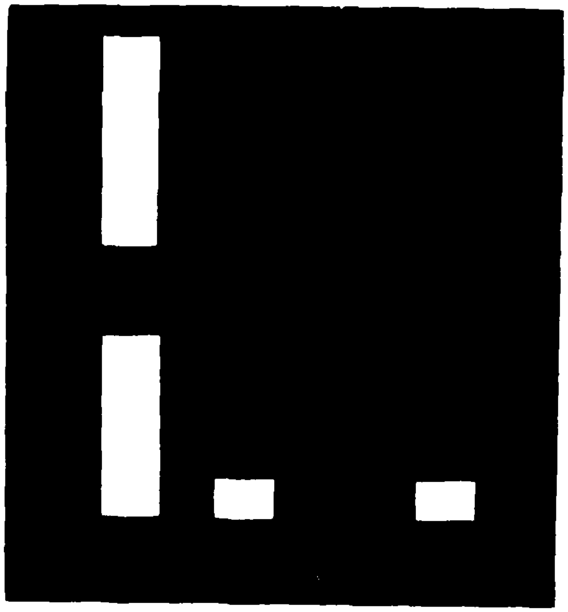

FIGURE 51 X-RADIOGRAPH OF SPECIMEN 24-27 WITH VARIOUS MIXED PENETRANTS

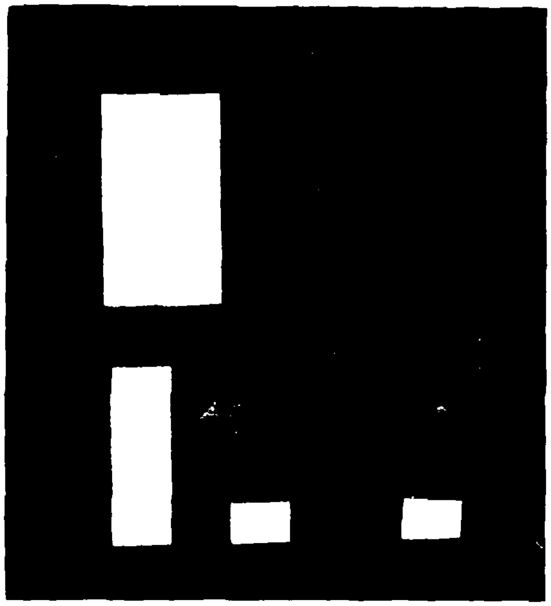

FIGURE 52 X-RADIOGRAPH OF SPECIMEN 24-27 AFTER REAPPLICATION OF T-100X TO DAMAGE LOCATIONS A AND B

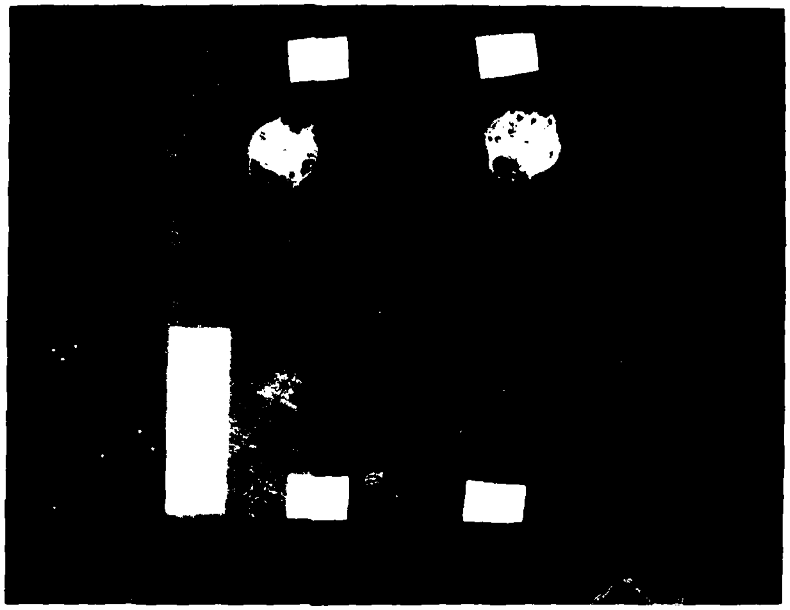

FIGURE 53 X-RADIOGRAPH OF SPECIMEN 24-27
WITH VARIOUS PENETRANTS

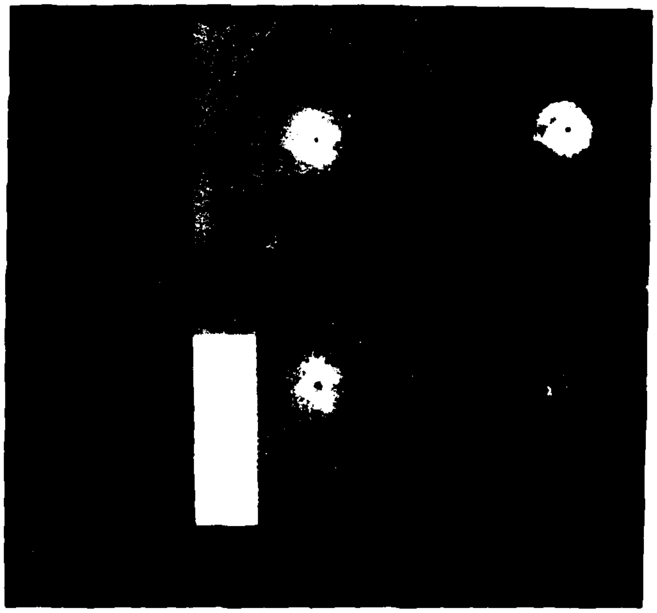

FIGURE 54 X-RADIOGRAPH OF SPECIMEN 24-27
AFTER ULTRASONIC CLEANING

k. Twenty-Four (24)- Ply Specimen, 24-28,

ZLX-418B penetrant was applied to all damage areas on the top (bleeder cloth) side only and allowed to dwell for 30 minutes. X-radiographic inspection of the specimen (Figure 55) revealed no evidence of damage at locations 1 or 2; a slight amount of damage at location 3; and a large amount of damage at location 4.

ZLX-418B penetrant was then applied to all damage areas on the bottom (platen) side and allowed to dwell for 30 minutes. X-radiographic inspection (Figure 56) showed damage in the form of cracks in all ply directions (0, $\pm$ 45, 90 degree) and delaminations at locations 1, 3, and 4. There was no evidence of damage at location 2.

4. Conclusions:

Conclusions from the impact damage studies were as follows:

a. Low energy impact, in-service, damage was most closely simulated by use of Tool No. 1, a blunt nose, large radius indenter (punch). Damage from Tool No. 1 was not readily visible in radiographs taken with no penetrant enhancement. Damage from Tool No. 1 was not as pronounced as that from Tool No. 2, 3, and 4.

b. Penetrants selected for compatibility studies were:

Tetrabromoethane (TBE)
Diiodobutane
ZLX-418B
Zinc Iodide (ZnI_2)

Tetrabromoethane and diiodobutane were selected for their proven image contrast enhancement properties in this study and in previous studies (Ref. 3-4).

ZLX-418B and Zinc Iodide solutions were selected for their surface wetting properties, ease of handling and image contrast enhancement properties.

c. Zinc Iodide solution was selected as the single penetrant to be used for subsequent damage studies due to its ease in handling, ease of mixing, image contrast enhancement properties, surface wetting, and capillary properties and ease of removal and clean up. It was also predicted to have the least potential of all materials evaluated for deterioration of the graphite/epoxy matrix.

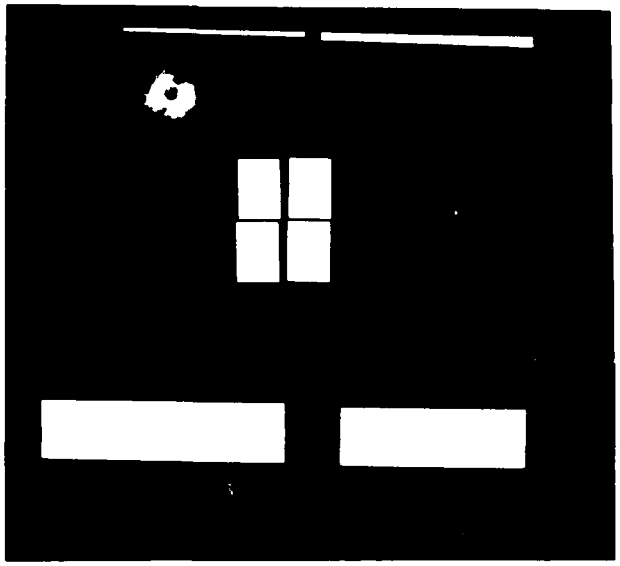

FIGURE 55 X-RADIOGRAPH OF SPECIMEN 24-28, WITH ZLX-418B APPLIED TO TOP SIDE ONLY

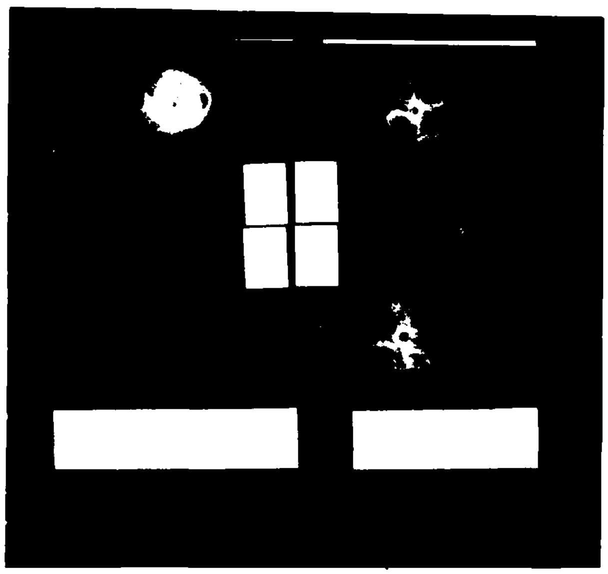

FIGURE 56 X-RADIOGRAPH OF SPECIMEN 24-28, WITH ZLX-418B APPLIED TO BOTH SIDES

d. Procedures for use of X-ray opaque penetrant enhancement materials were established to include application to the bottom side (opposite impact point) side of all test specimens.

SECTION IV

MATERIAL COMPATIBILITY ASSESSMENT

AT

ROOM TEMPERATURE AND AT ELEVATED TEMPERATURE

1. GENERAL

X-ray opaque penetrant enhanced x-radiography has been shown to be a valuable tool for documenting damage initiation and damage accumulation processes in resin-matrix composite materials (Ref. 5-6). Its use has, however, been limited due to unknown effects of penetrant materials on post-inspection behavior of a composite material. Previous experimental work and analysis has addressed tetrabromoethane (TBE) (Ref. 5) and diiodobutane (Ref. 6) and has concluded that these materials do not alter post inspection behavior. Additional experimental work was indicated for investigation of the effects of extended exposure of candidate penetrants on the integrity of graphite-epoxy material. The experimental work described in the following was intended to support previously reported work and to provide comparison of behavior for additional x-ray opaque penetrant materials.

Four penetrant materials selected for evaluation were:

- Tetrabromoethane (TBE)
- Diiodobutane (DIB)
- ZLX-418B (Diiodomethane base)
- Zinc Iodide Penetrant

2. Test Specimen Preparation

a. Impact Damaged Specimens

8, 16, and 24 ply specimens were subjected to impact damage, at a location near the center of a 4 inch by 4 inch area, using Tool No. 1. Eight (8) ply specimens were subjected to a 4 inch-pound energy level. Sixteen (16) ply specimens were subjected to a 10 inch-pound energy level. Twenty-four (24) ply specimens were subjected to a 15 inch-pound energy level. All impact damage was conducted with no backing.

Specimens were x-radiographically inspected, with no penetrant enhancement to document the initial condition.

b. Six (6) Ply Control Specimens

Six (6) Ply sheet material for control specimens was prepared using a 0, 90, 0, 0, 90, 0 degree lay-up sequence. One inch by four inch specimens were out from the prepared sheet with the 0 degree axis was oriented along the length of the specimen. The 1 inch by 4 inch by (6 ply control specimens) were delaminated on one end with an "x-acto" knife.

3. Room Temperature Specimen Exposure

A specimen set consisting of one 8 ply, one 16 ply and one 24 ply panel was subjected to each of the selected penetrants and allowed to dwell for 30 minutes. All specimens were re-x-radiographically inspected after the initial penetrant dwell.

Specimens were then stored at room temperature and were re-inspected at weekly intervals for six-weeks. Radiographs and visual notes of specimen condition were compared to the initial and to prior inspections and differences were noted.

Subsequent to sequence 1 (inspection after one week) the 8 and 16 ply specimens were hand flexed 10 times each after penetrant application. Flexure was repeated as noted. The results of the exposure and evaluations are summarized in Tables 5. 6, 7, and 8. Before (initial penetrant enhanced and after 6 weeks) exposure x-radiographs of test specimens are shown in Figures 57 through 64.

TABLE 5

ROOM TEMPERATURE EXPOSURE OF IMPACT DAMAGED GRAPHITE/EPOXY SPECIMENS TO TETRABROMOETHANE

	CONVENTIONAL X-RADIOGRAPHY	INITIAL	AFTER 1 WEEK	AFTER 2 WEEKS	AFTER 3 WEEKS	AFTER 4 WEEKS	AFTER 5 WEEKS	AFTER 6 WEEKS
8 PLY 4 IN-LBS	1 CRACK AT 90^o	CRACKS AT $\pm 45^o, 90^o$ NO DELAMINATION	CRACKS AT $0^o, +45^o$, 90^o 3/16x1/8 INCH DELAMINATION	NO CHANGE	90^o CENTER CRACKS APPEAR LONGER STEREO - CRACK AT BOTTOM LAYER 0.012	NO CHANGE	NO CHANGE	PANEL FLEXED CRACKS APPEAR LONGER EDGE CRACKS APPEARED
16 PLY 10 IN-LBS	2 CRACKS AT 90^o	CRACKS AT $0^o, \pm 45^o, 90^o$ ½x½ INCH DELAMINATION	NO CHANGE	NO CHANGE	NO CHANGE	NO CHANGE	NO CHANGE	PANEL FLEXED NO CHANGE
24 PLY 15 IN-LBS	SCATTERED VOIDS	CRACKS AT $0^o, \pm 45^o, 90^o$ 3/4x1 INCH DELAMINATION	NO CHANGE	NO CHANGE	NO CHANGE	NO CHANGE	NO CHANGE	NO CHANGE

TABLE 6

ROOM TEMPERATURE EXPOSURE OF IMPACT DAMAGED GRAPHITE/EPOXY

SPECIMENS TO DIIODOBUTANE

	CONVENTIONAL X-RADIOGRAPHY	INITIAL	AFTER 1 WEEK	AFTER 2 WEEKS	AFTER 3 WEEKS	AFTER 4 WEEKS	AFTER 5 WEEKS	AFTER 6 WEEKS
8 PLY 4 IN-LBS	1 CRACK AT 90^o	CRACKS AT $0^o, \pm 45^o, 90^o$ 3/8x1/4 INCH DELAMINATION	NO CHANGE	PANEL FLEXED NO CHANGE	PANEL FLEXED NUMEROUS CRACKS AT 90^o IN DAMAGE AND AWAY FROM DAMAGED AREA STEREO-DELAMINATION AT 0.012 IN	NO CHANGE	NO CHANGE	PANEL FLEXED MORE CRACKS MORE CRACK GROWTH
16 PLY 10 IN-LBS	2 CRACKS AT 90^o	CRACKS AT $0^o, \pm 45^o, 90^o$ 7/16x1/2 INCH DELAMINATION 2 CRACKS 90^o	NO CHANGE	NO CHANGE	NO CHANGE	NO CHANGE	NO CHANGE	NO CHANGE
24 PLY 15 IN-LBS	NO ANOMALIES	CRACKS AT $0^o, \pm 45^o, 90^o$ 1/2x5/8 IN. DELAMINATION 2 CRACKS IN CENTER OF DELAMINATION	NO CHANGE	NO CHANGE	NO CHANGE	NO CHANGE	NO CHANGE	NO CHANGE

TABLE 7

ROOM TEMPERATURE EXPOSURE OF IMPACT DAMAGED GRAPHITE/EPOXY SPECIMENS TO ZLX-418B

	CONVENTIONAL X-RADIOGRAPHY	INITIAL	AFTER 1 WEEK	AFTER 2 WEEKS	AFTER 3 WEEKS	AFTER 4 WEEKS	AFTER 5 WEEKS	AFTER 6 WEEKS
8 PLY 4 IN-LBS	2 CRACKS AT 90°	LITTLE PENETRANT MOVEMENT SOME CRACKS VISIBLE	CRACKS AT $0 \pm 45^{\circ}$ $\frac{1}{2}$x$\frac{1}{4}$ INCH DELAMINATION	NO CHANGE LESS PENETRANT VISIBLE	PANEL WAS FLEXED NO CHANGE	PANEL WAS FLEXED NO CHANGE	ADDITIONAL CRACKS DELAMINATION GROWTH	PANEL FLEXED GROWTH OF 10° CRACK
16 PLY 10 IN-LBS	1 SMALL CRACK AT 90°	CRACKS AT $0, \pm 45^{\circ}, 90^{\circ}$ 1/2x5/8 INCH DELAMINATION	NO CHANGE	PANEL WAS FLEXED NO CHANGE	PANEL WAS FLEXED GROWTH IN LENGTH OF 90° CRACK BEYOND DELAMINATION	NO CHANGE	NO CHANGE	NO CHANGE
24 PLY 15 IN-LBS	NO ANOMALIES	CRACKS AT $0, \pm 45^{\circ}, 90^{\circ}$ 5/8 x 3/4 INCH DELAMINATION	NO CHANGE	NO CHANGE	NO CHANGE	NO CHANGE	NO CHANGE	NO CHANGE

TABLE 8

ROOM TEMPERATURE EXPOSURE OF IMPACT DAMAGED GRAPHITE/EPOXY SPECIMENS TO ZINC IODIDE

	[illegible]NVENTIONAL X-RADIOGRAPHY	INITIAL	AFTER 1 WEEK	AFTER 2 WEEKS	AFTER 3 WEEKS	AFTER 4 WEEKS	AFTER 5 WEEKS	AFTER 6 WEEKS
[illegible] PLY [illegible] IN-LBS	1 CRACK AT 90^o	CRACKS AT $0,\pm45^o,90^o$ / 3/8x3/8 INCH DELAMINATION / 2 CRACKS BEYOND DELAMINATION	NO CHANGE / SOME ZINC IODIDE	NO CHANGE	PANEL WAS FLEXED / CRACK GROWTH / CRACKS FROM EDGES	PANEL WAS FLEXED / SOME CRACK GROWTH	PANEL WAS FLEXED / SOME CRACK GROWTH	NO CHANGE
16 PLY 10 IN-LBS	VOIDS 1 CRACK	CRACKS AT $0,\pm45^o,90^o$ ½x½ INCH DELAMINATION	NO CHANGE	PANEL WAS FLEXED / NO CHANGE	NO CHANGE	PANEL WAS FLEXED / NO CHANGE	PANEL WAS FLEXED / NO CHANGE	PANEL WAS FLEXED / NO CHANGE
24 PLY 15 IN-LBS	NO ANOMALIES	CRACKS AT $0,\pm45^o, 90^o$ / 5/8x5/8 IN. DELAMINATION	NO CHANGE	NO CHANGE	NO CHANGE	NO CHANGE	NO CHANGE	NO CHANGE

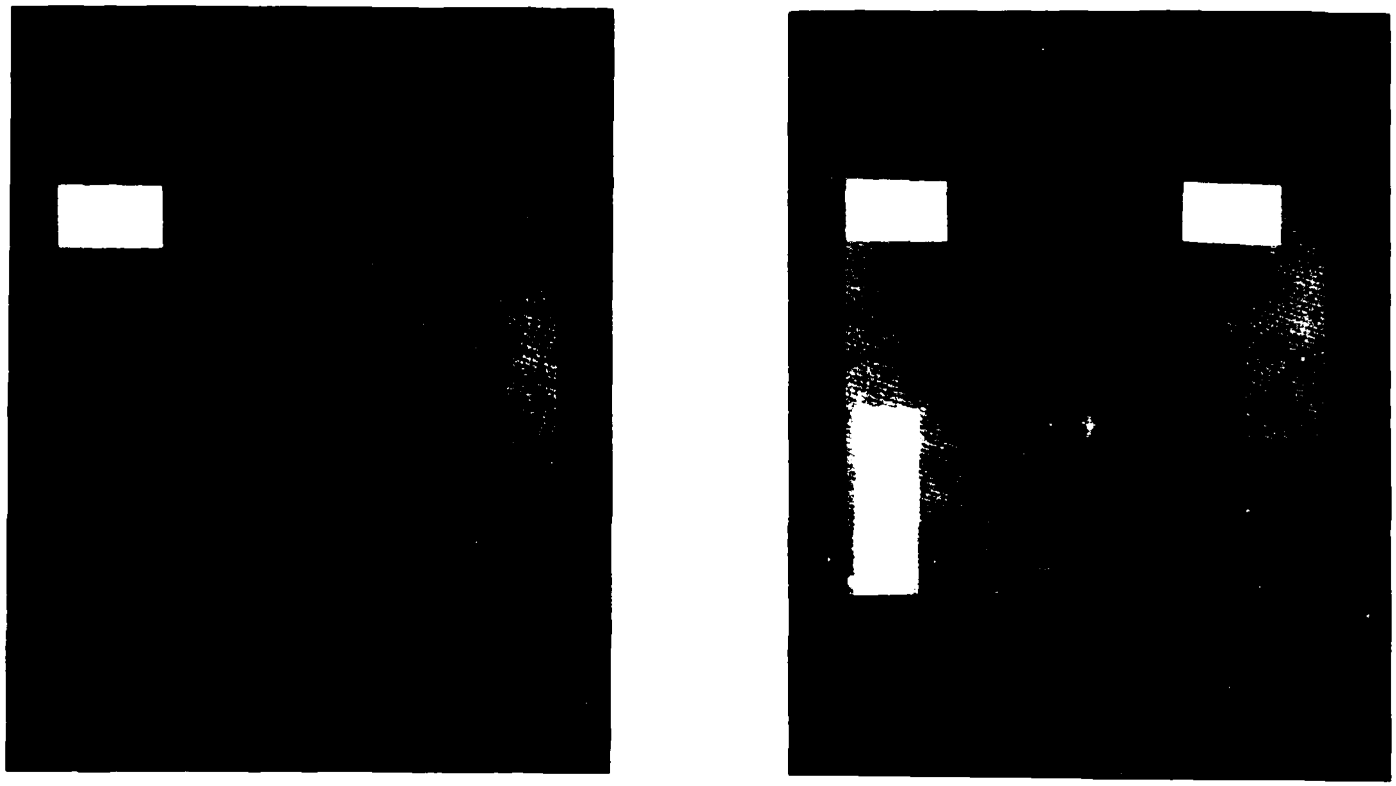

FIGURE 57 X-RADIOGRAPHS OF SPECIMEN 8-8 (PENETRANT ENHANCED) SHOWING THE INITIAL AND FINAL CONDITION AFTER ROOM TEMPERATURE EXPOSURE TO TETROBROMOETHANE

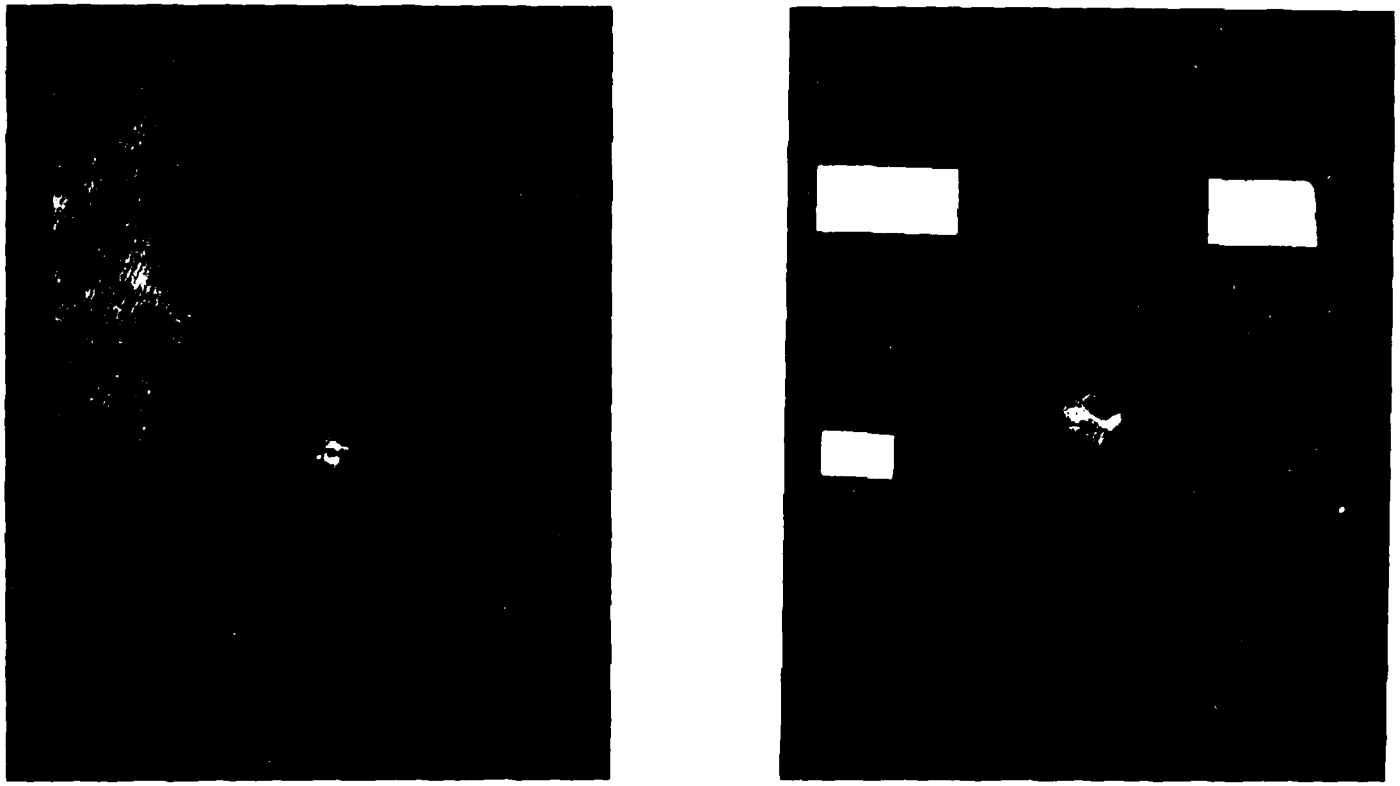

FIGURE 58 X-RADIOGRAPHS OF SPECIMENS 16-7 AND 24-7 (PENETRANT ENHANCED) AFTER ROOM TEMPERATURE EXPOSURE TO TETRABROMOETHANE

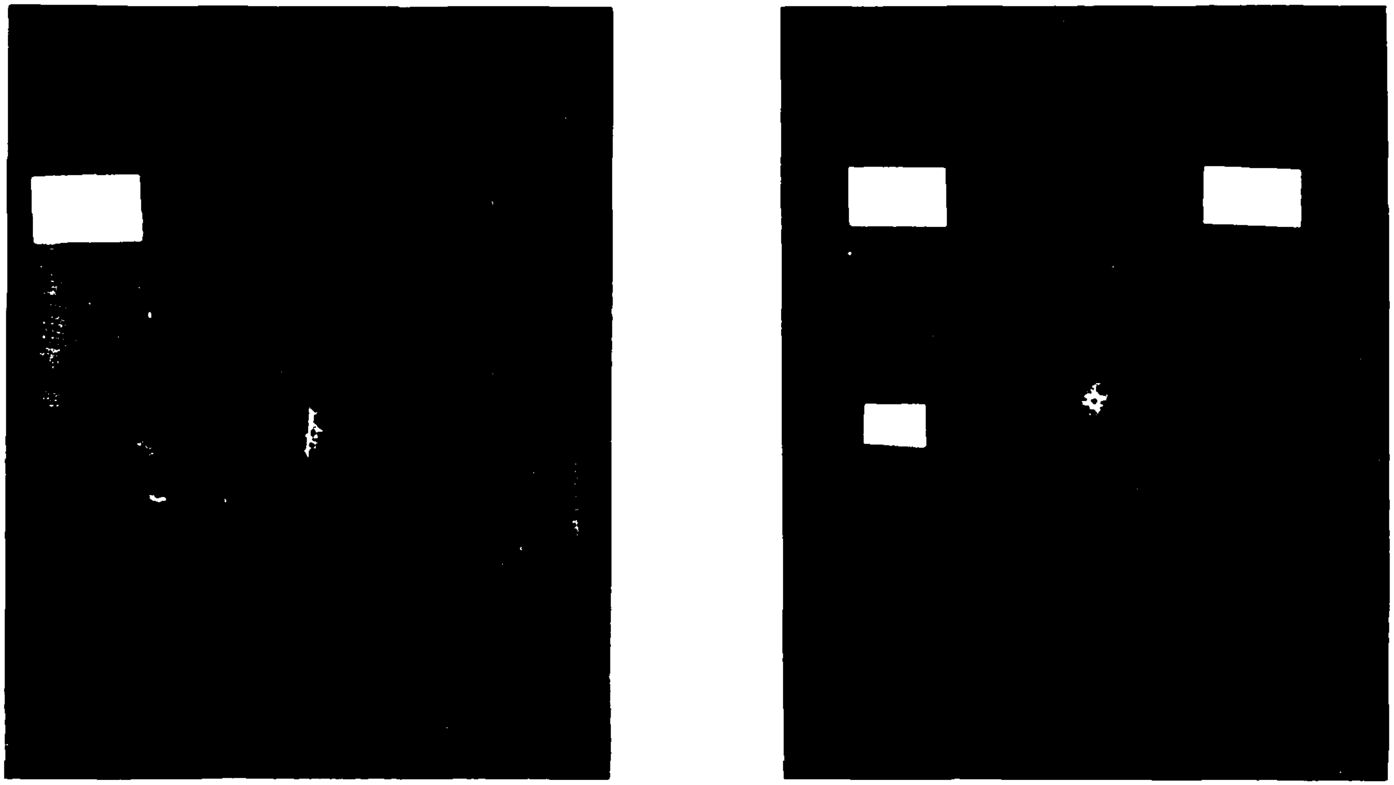

FIGURE 59 X-RADIOGRAPHS OF SPECIMEN 8-6 (PENETRANT ENHANCED) SHOWING THE INITIAL AND FINAL CONDITION AFTER ROOM TEMPERATURE EXPOSURE TO DIIODOBUTANE

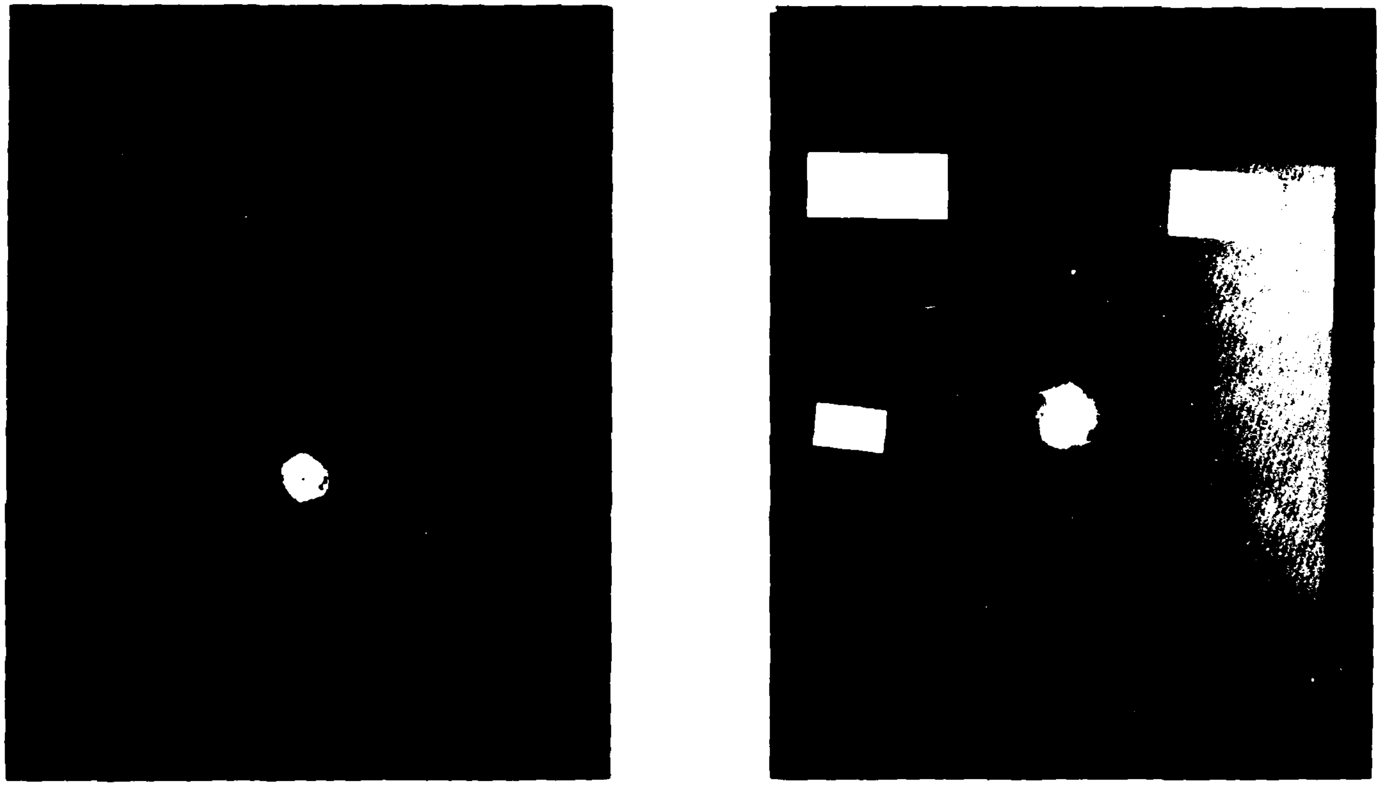

FIGURE 60 X-RADIOGRAPHS OF SPECIMENS 16A-6 AND 24-6 (PENETRANT ENHANCED) AFTER ROOM TEMPERATURE EXPOSURE TO DIIODOBUTANE

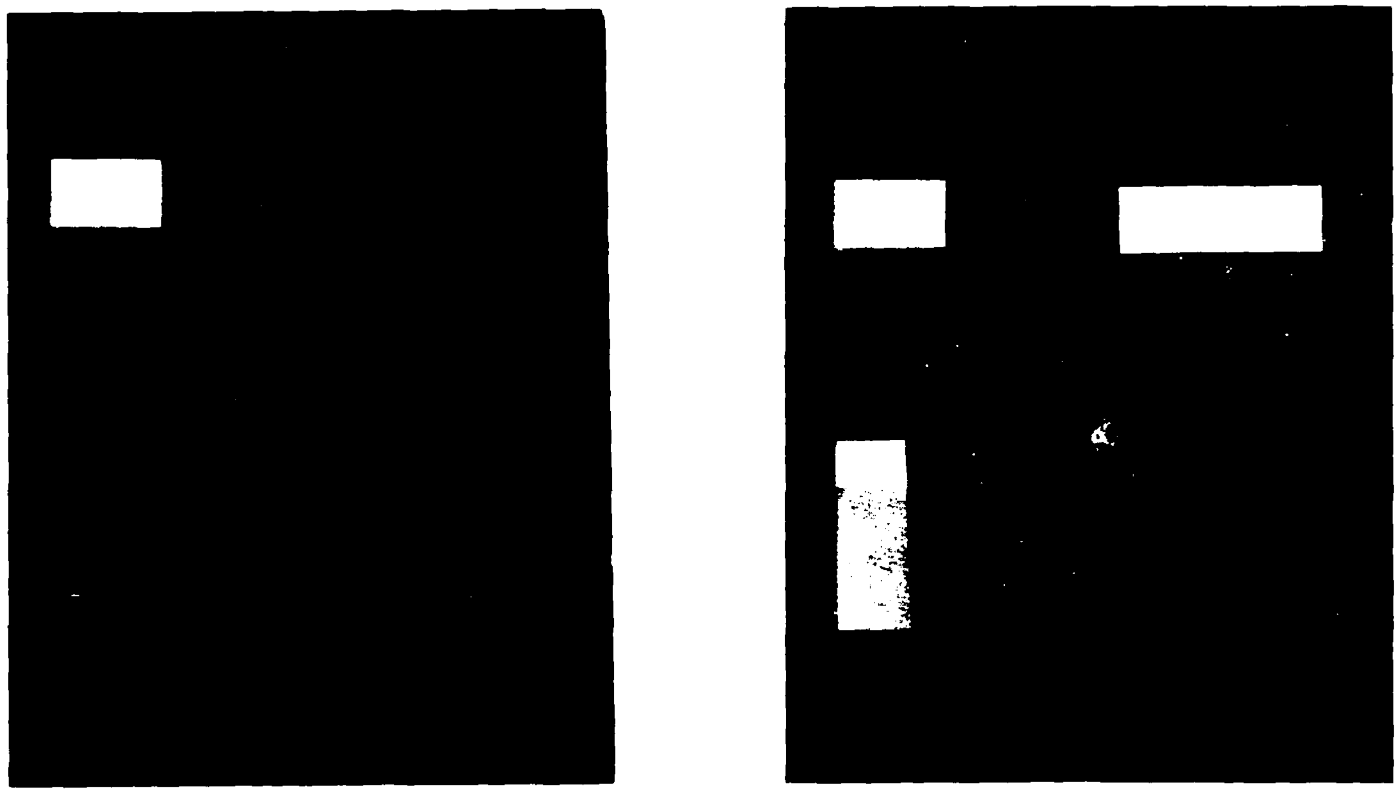

FIGURE 61 X-RADIOGRAPHS OF SPECIMEN 8-4 (PENETRANT ENHANCED) SHOWING THE INITIAL AND FINAL CONDITIONS AFTER ROOM TEMPERATURE EXPOSURE TO ZLX-418B

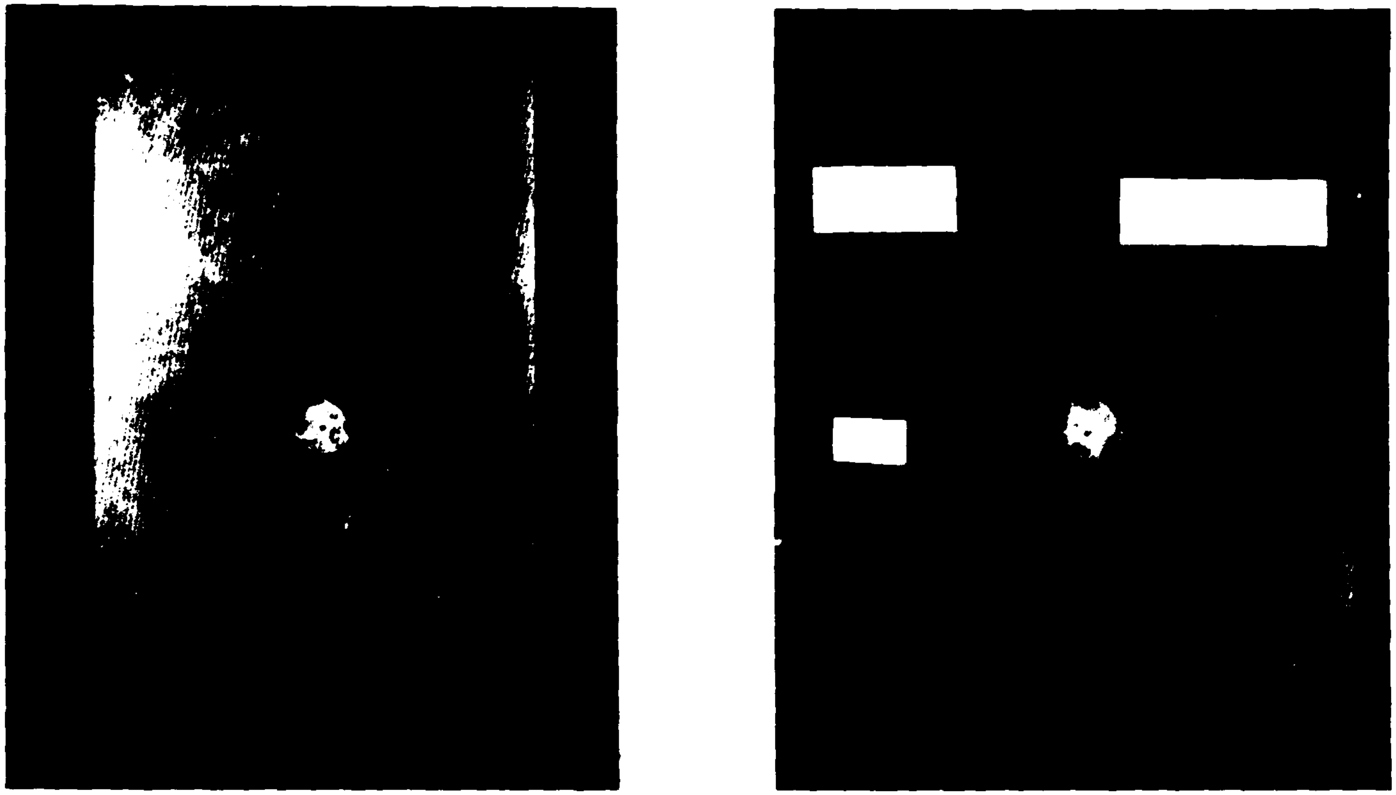

FIGURE 62 X-RADIOGRAPHS OF SPECIMENS 16A-4 AND 24-4 (PENETRANT ENHANCED) AFTER ROOM TEMPERATURE EXPOSURE TO ZLX-418B

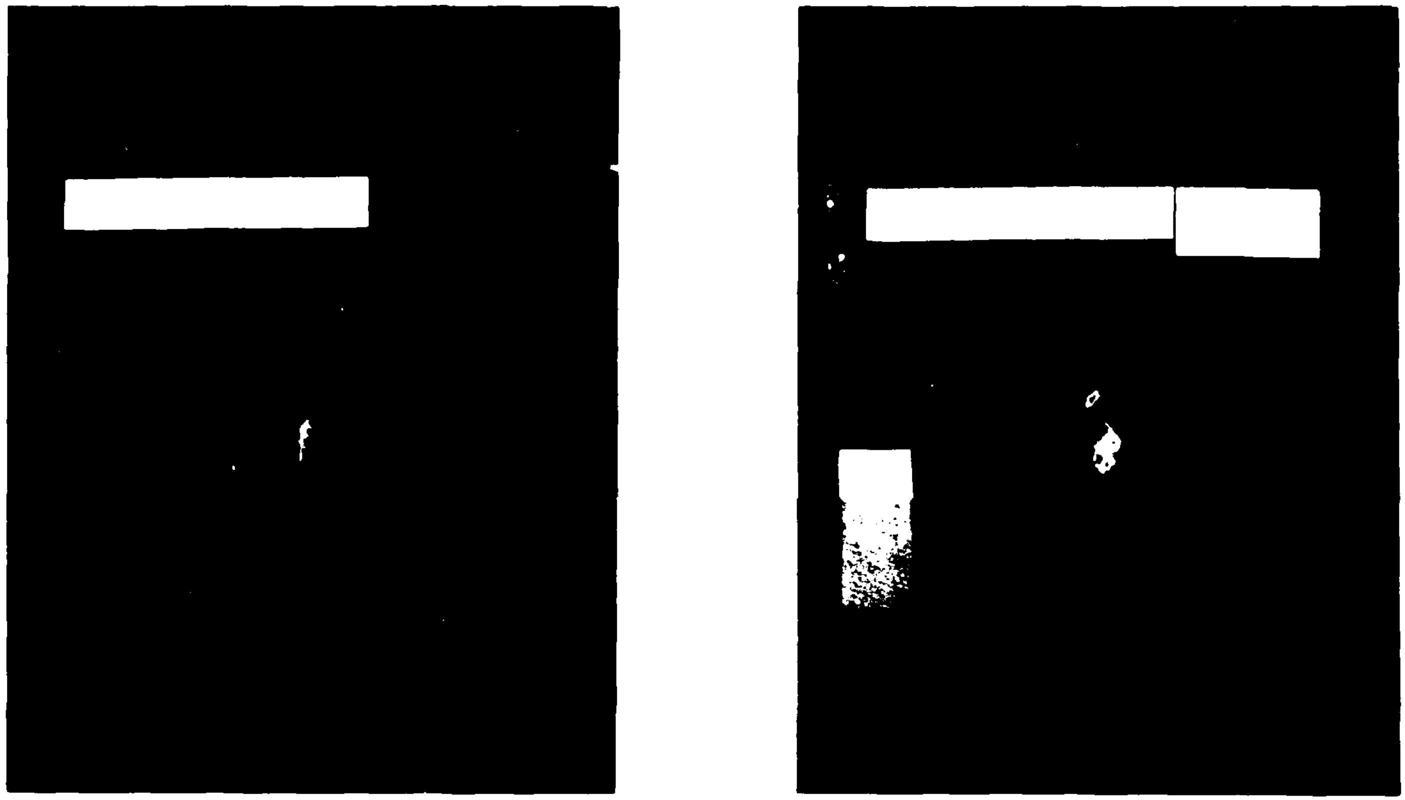

FIGURE 63 X-RADIOGRAPHS OF SPECIMEN 8-2 (PENETRANT ENHANCED) SHOWING THE INITIAL AND FINAL CONDITIONS AFTER ROOM TEMPERATURE EXPOSURE TO ZnI_2

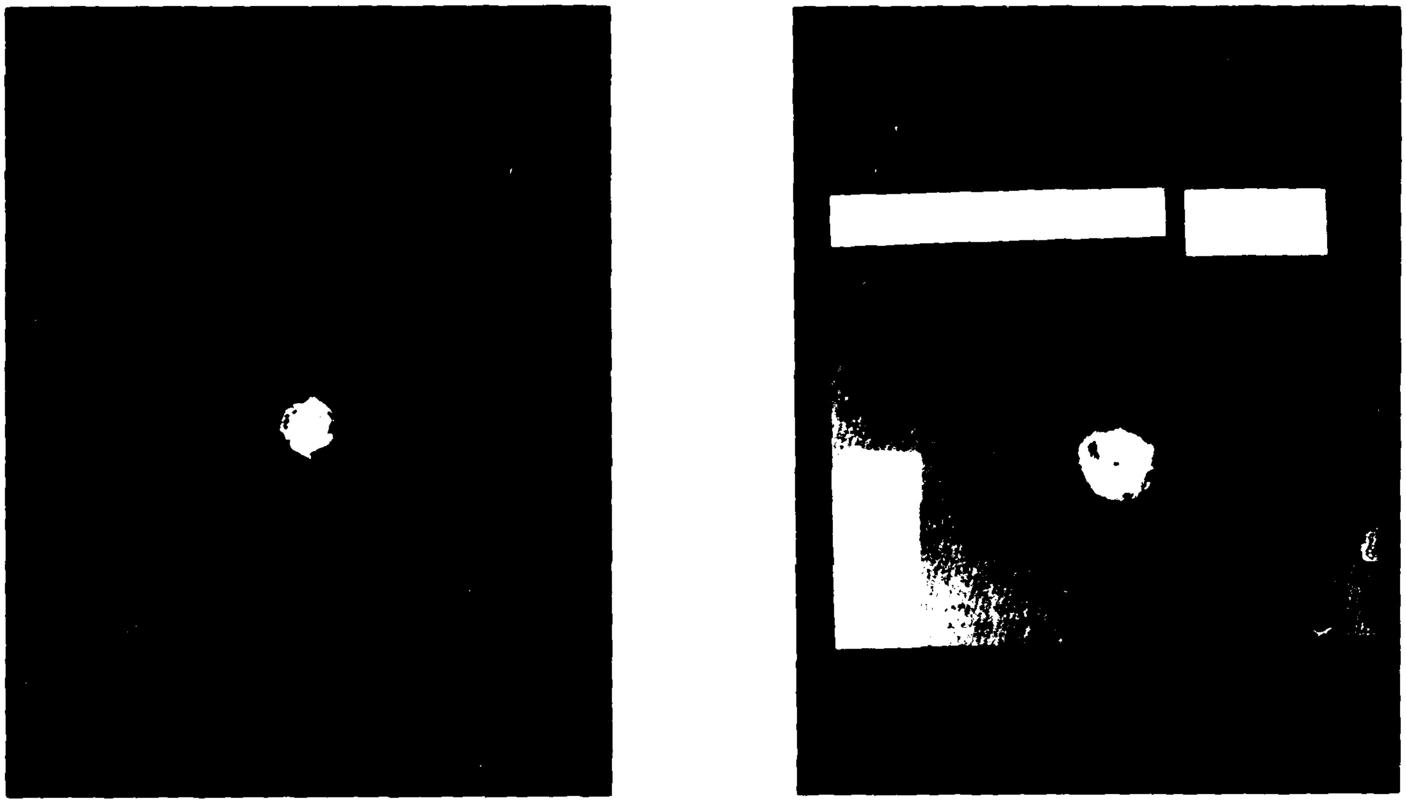

FIGURE 64 X-RADIOGRAPHS OF SPECIMENS 16A-2 AND 24-2 (PENETRANT ENHANCED) AFTER ROOM TEMPERATURE EXPOSURE TO ZnI_2

4. Elevated Temperature Specimen Exposure

A specimen set consisting of one 8 ply, one 16 ply, one 24 ply and one edge delaminated control specimen was subjected to each of the selected penetrants and allowed to dwell for 30 minutes. All specimens were re-x-radiographically inspected after the initial penetrant dwell.

Specimen sets were placed into a shallow pyrex container along with small samples of the respective penetrants. A glass lid was used to cover each container thereby establishing an equilibrium exposure with volatile components of each respective penetrant. The containers were placed in a "Blue M" thermostatically controlled and electrically heated oven (equipped with oven temperature protection) and the temperature was raised to 100°F. (See Figure 65)

Specimens were re-inspected at weekly intervals for six-weeks. Radiographs and visual notes of specimen condition were compared to the initial and to prior inspections and differences were noted. Panels were flexed during the exposure sequence as noted.

The results of the exposures and evaluations are summarized in Tables 9, 10, 11, and 12. Before (initial penetrant enhanced) and after (6 weeks) exposure radiographs of test specimens are shown in Figures 66 through 74.

FIGURE 65 BLUE M - ELECTRIC OVEN WITH PYREX CONTAINERS IN PLACE

TABLE 9

ELEVATED TEMPERATURE EXPOSURE OF IMPACT DAMAGED GRAPHITE/EPOXY SPECIMENS TO TETRABROMOETHANE

	CONVENTIONAL X-RADIOGRAPHY	INITIAL	AFTER 1 WEEK	AFTER 2 WEEKS	AFTER 3 WEEKS	AFTER 4 WEEKS	AFTER 5 WEEKS	AFTER 6 WEEKS
8 PLY 4 IN-LBS	2 CRACKS AT 90°	CRACKS AT $\pm 45^{\circ}$, 90° NO DELAMINATIONS	CRACKS AT 0°, $\pm 45^{\circ}$, 90° 5/16x5/16 INCH DELAMINATION	PANEL WAS FLEXED CRACK GROWTH CRACK EXTENDED BEYOND DELAMINATION	PANEL WAS FLEXED CONTINUED CRACK GROWTH	PANEL WAS FLEXED POOR PENETRANT MOVEMENT NO CHANGE	PANEL WAS FLEXED CRACK GROWTH	PANEL WAS FLEXED NO CHANGE
16 PLY 10 IN-LBS	NO ANOMALIES	CRACKS AT 0° $\pm 45^{\circ}$, 90° 7/16 INCH DIAMETER DELAMINATION	NO CHANGE	PANEL WAS FLEXED NO CHANGE	PANEL WAS FLEXED NO CHANGE	PANEL WAS FLEXED NO CHANGE	PANEL WAS FLEXED NO CHANGE	PANEL WAS FLEXED NO CHANGE
24 PLY 15 IN-LBS	VOIDS	CRACKS AT 0, $\pm 45^{\circ}$, 90° 9/16 INCH DIAMETER DELAMINATION	NO CHANGE	NO CHANGE	NO CHANGE	NO CHANGE	NO CHANGE	NO CHANGE

TABLE 10

ELEVATED TEMPERATURE EXPOSURE OF IMPACT DAMAGED GRAPHITE/EPOXY SPECIMENS TO DIIODOBUTANE

	CONVENTIONAL X-RADIOGRAPHY	INITIAL	AFTER 1 WEEK	AFTER 2 WEEKS	AFTER 3 WEEKS	AFTER 4 WEEKS	AFTER 5 WEEKS	AFTER 6 WEEKS
8 PLY 4 IN-LBS	1 CRACK AT 90°	3 LARGE CRACKS 90° SMALLER 0° $\pm 45^{\circ}, 90^{\circ}$ 3/16x3/8 INCH DELAMINATION	NO CHANGE	PANEL WAS FLEXED SOME CRACK GROWTH	PANEL WAS FLEXED NO CHANGE	PANEL WAS FLEXED NO CHANGE	PANEL WAS FLEXED NO CHANGE	PANEL WAS FLEXED NO CHANGE
16 PLY 10 IN-LBS	NO ANOMALIES	CRACKS AT 0, $\pm 45^{\circ}, 90^{\circ}$ ½ INCH DIAMETER DELAMINATION WITH CRACKS 90°	NO CHANGE	PANEL WAS FLEXED NO CHANGE	PANEL WAS FLEXED NO CHANGE	PANEL WAS FLEXED NO CHANGE	PANEL WAS FLEXED NO CHANGE	PANEL WAS FLEXED NO CHANGE
24 PLY 15 IN-LBS	NO ANOMALIES	CRACKS AT 0, $\pm 45^{\circ}, 90^{\circ}$ 11/16 INCH DIAMETER DELAMINATION	NO CHANGE SOME IMPROVED PENETRANT	NO CHANGE	NO CHANGE	NO CHANGE	NO CHANGE	NO CHANGE

TABLE 11

ELEVATED TEMPERATURE EXPOSURE OF IMPACT DAMAGED GRAPHITE/EPOXY SPECIMENS TO ZLX-418B

	CONVENTIONAL X-RADIOGRAPHY	INITIAL	AFTER 1 WEEK	AFTER 2 WEEKS	AFTER 3 WEEKS	AFTER 4 WEEKS	AFTER 5 WEEKS	AFTER 6 WEEKS
8 PLY 4 IN-LBS	1 CRACK AT 90^o	CRACKS AT 0^o, $+45^o$, 90^o ¼ INCH DIAMETER DELAMINATION	NO CHANGE	PANEL WAS FLEXED NO CHANGE	PANEL WAS FLEXED NO CHANGE	PANEL WAS FLEXED NO CHANGE	PANEL WAS FLEXED NO CHANGE	PANEL WAS FLEXED NO CHANGE
16 PLY 10 IN-LBS	VOIDS	CRACKS AT 0^o, $\pm 45^o$, 90^o ½ INCH DIAMETER DELAMINATION	NO CHANGE	PANEL WAS FLEXED NO CHANGE	PANEL WAS FLEXED NO CHANGE	PANEL WAS FLEXED NO CHANGE	PANEL WAS FLEXED NO CHANGE	PANEL WAS FLEXED NO CHANGE
24 PLY 15 IN-LBS	VOIDS $\pm 45^o$, 90^o	CRACKS AT 0^o, $\pm 45^o$, 90^o DELAMINATION	NO CHANGE	NO CHANGE	NO CHANGE	NO CHANGE	NO CHANGE	NO CHANGE

AD-A111 303 MARTIN MARIETTA AEROSPACE DENVER CO QUALITY ASSURANC--ETC F/G 11/4
ENHANCED X-RAY STEREOSCOPIC NDE OF COMPOSITE MATERIALS.(U)
JUN 80 W D RUMMEL, T TEDROW, H D BRINKERHOFF F33615-79-C-3220

UNCLASSIFIED AFWAL-TR-80-3053 NL

2 OF 3
AD
A111303

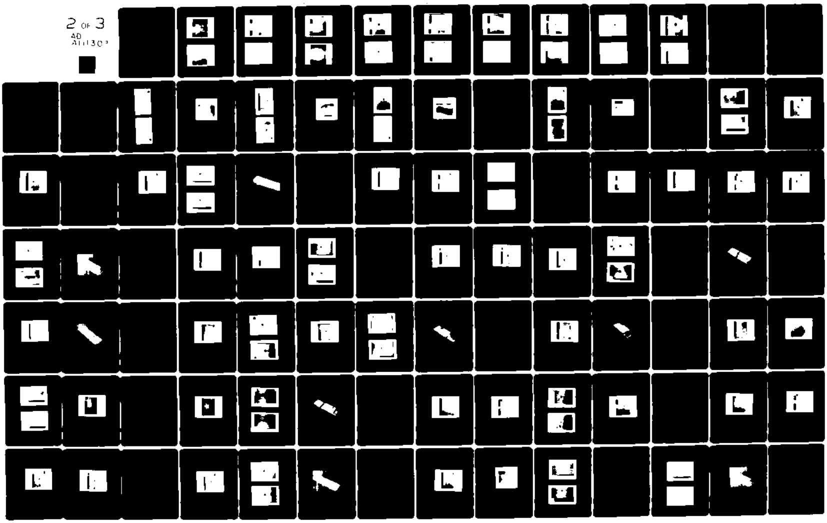

TABLE 12

ELEVATED TEMPERATURE EXPOSURE OF IMPACT DAMAGED GRAPHITE/EPOXY SPECIMENS TO ZINC IODIDE

	CONVENTIONAL X-RADIOGRAPHY	INITIAL	AFTER 1 WEEK	AFTER 2 WEEKS	AFTER 3 WEEKS	AFTER 4 WEEKS	AFTER 5 WEEKS	AFTER 6 WEEKS
8 PLY 4 IN-LBS	1 CRACK AT 90°	CRACKS AT 0°, $\pm 45^{\circ}, 90^{\circ}$ DELAMINATION CRACKS BEYOND DELAMINATION	NO CHANGE	PANEL WAS FLEXED GROWTH OF ONE CRACK	PANEL WAS FLEXED CRACK GROWTH AND NEW CRACKS	PANEL WAS FLEXED CRACK GROWTH	PANEL WAS FLEXED SOME CRACK GROWTH	PANEL WAS FLEXED NO CHANGE
16 PLY	NO ANOMALIES	CRACKS AT 0°, $\pm 45^{\circ}, 90^{\circ}$ 7/16 INCH DIAMETER DELAMINATION CRACKS BEYOND DELAMINATION	NO CHANGE	PANEL WAS FLEXED NO CHANGE SOME CRYSTAL-LIZATION	PANEL WAS FLEXED NO CHANGE	PANEL WAS FLEXED NO CHANGE	PANEL WAS FLEXED NO CHANGE	PANEL WAS FLEXED NO CHANGE
24 PLY 15 IN-LBS	VOIDS AT $\pm 45^{\circ}$	CRACKS AT 0°, $\pm 45^{\circ}, 90^{\circ}$ DELAMINATION	NO CHANGE SOME CRYSTAL-LIZATION	NO CHANGE	NO CHANGE	NO CHANGE	NO CHANGE	NO CHANGE

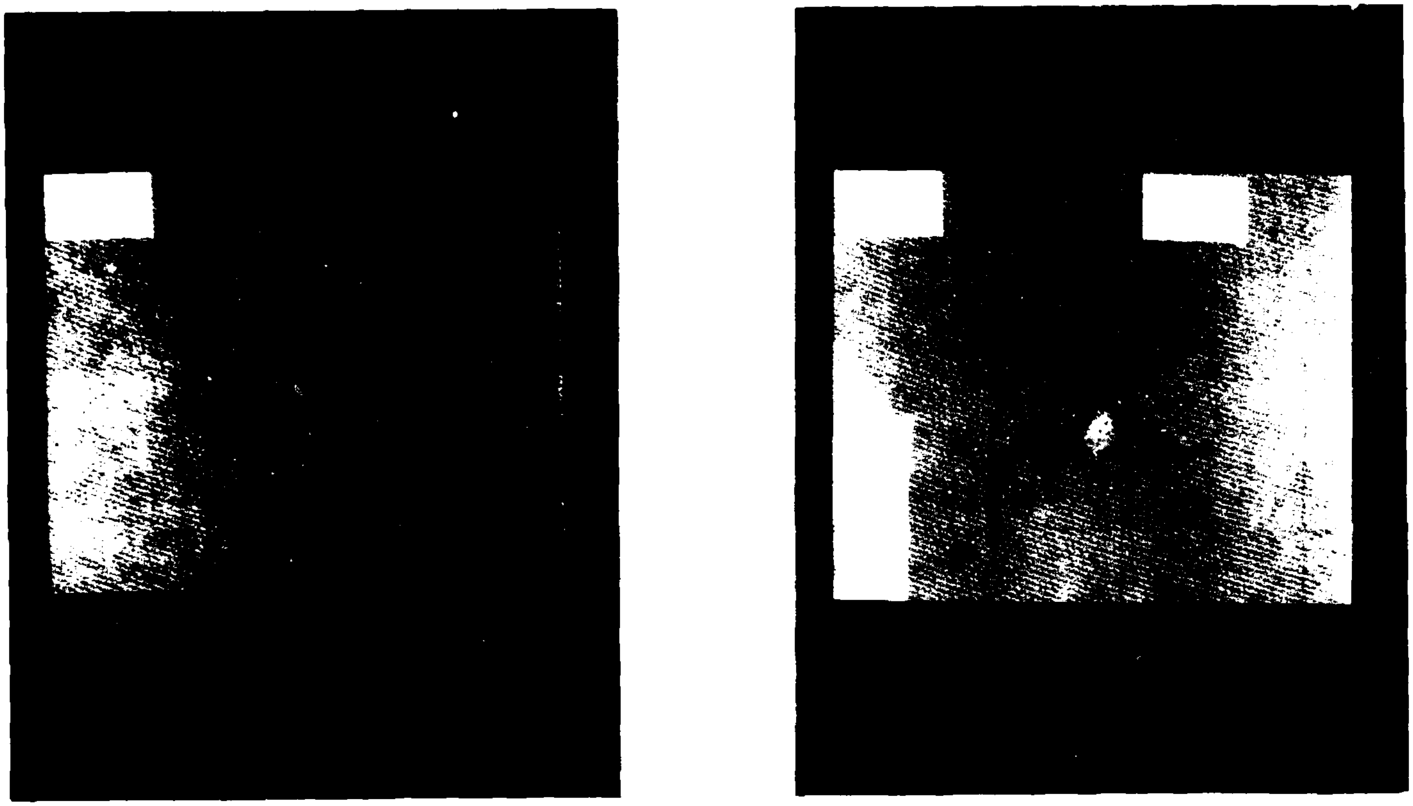

FIGURE 66 X-RADIOGRAPHY OF SPECIMEN 8-7 (PENETRANT ENHANCED) SHOWING THE INITIAL AND FINAL CONDITION AFTER ELEVATED TEMPERATURE EXPOSURE TO TETROBROMOETHANE

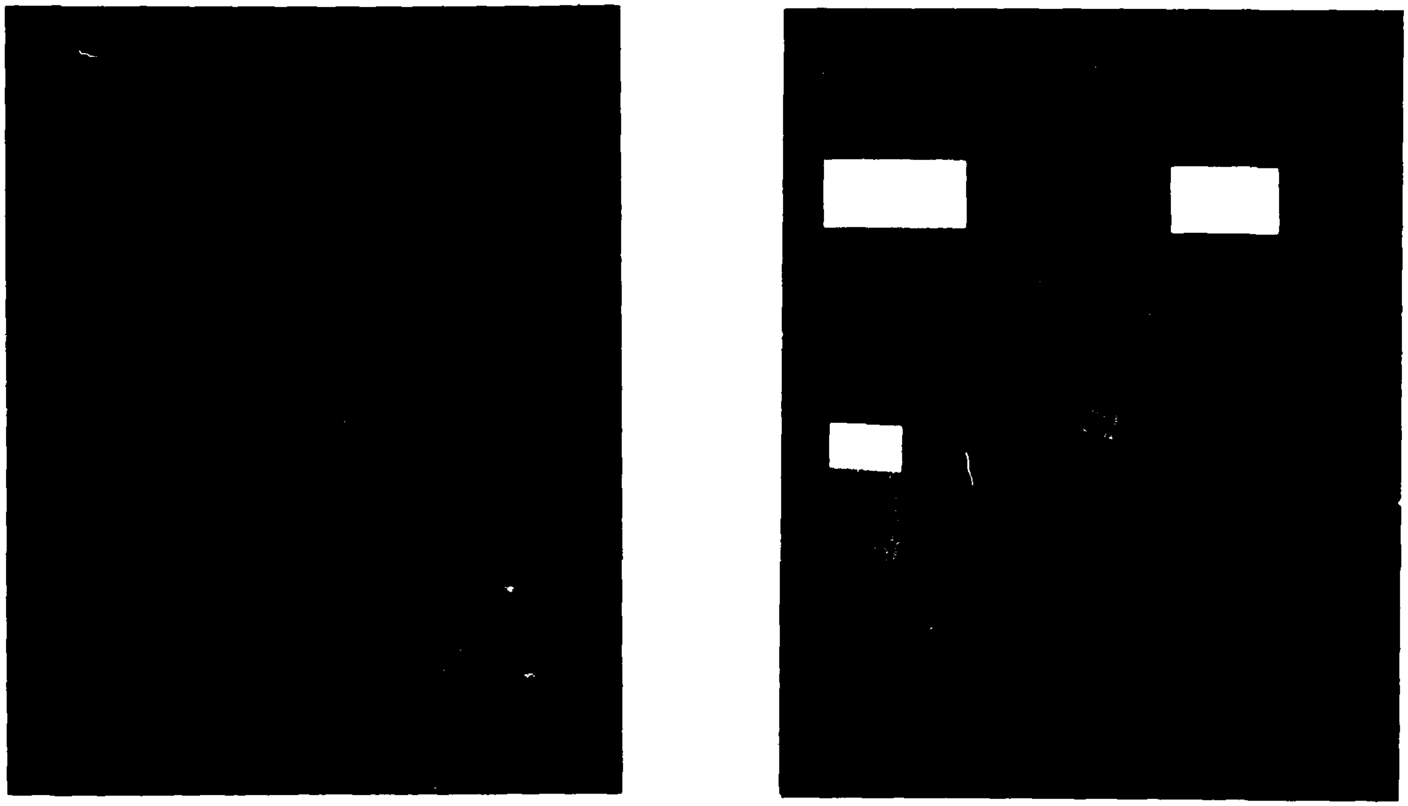

FIGURE 67 X-RADIOGRAPHS OF SPECIMENS 16-7 and 24-7 (PENETRANT ENHANCED) AFTER ELEVATED TEMPERATURE EXPOSURE TO TETRABROMOETHANE

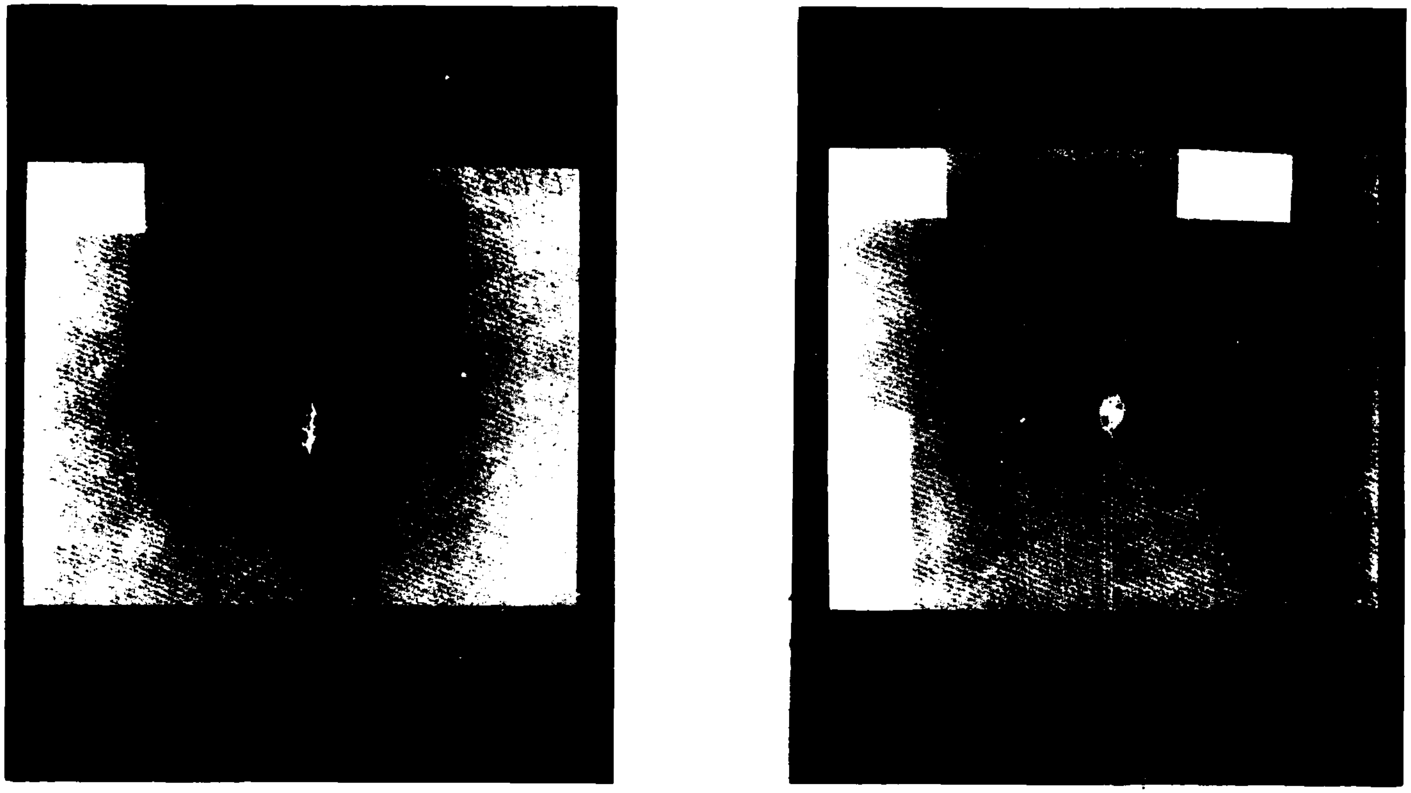

FIGURE 68 X-RADIOGRAPHS OF SPECIMEN 8-5 (PENETRANT ENHANCED) SHOWING THE INITIAL AND FINAL CONDITION ELEVATED TEMPERATURE EXPOSURE TO DIIODOBUTANE

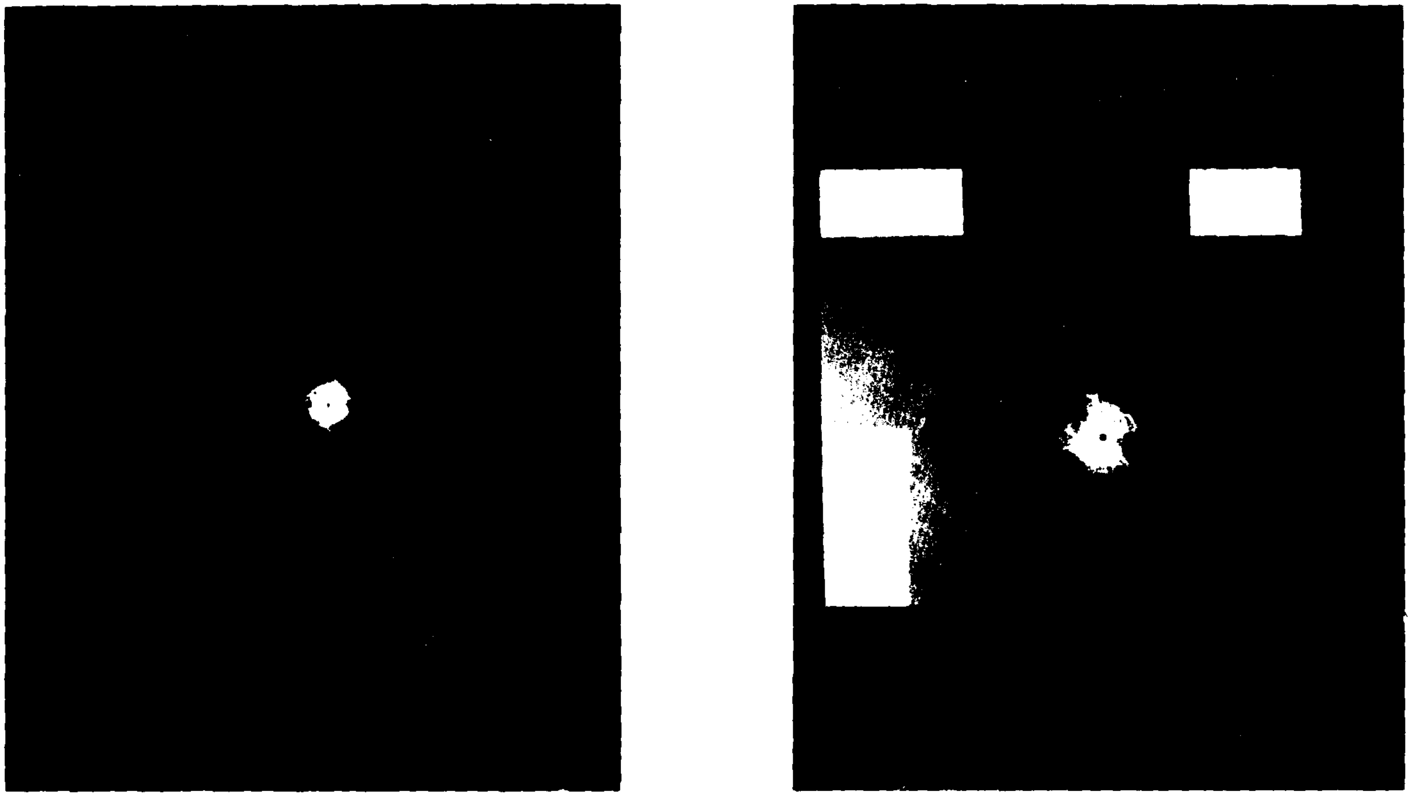

FIGURE 69 X-RADIOGRAPHS OF SPECIMENS 16A-6 AND 24-6 (PENETRANT ENHANCED) AFTER ELEVATED TEMPERATURE EXPOSURE TO DIIODOBUTANE

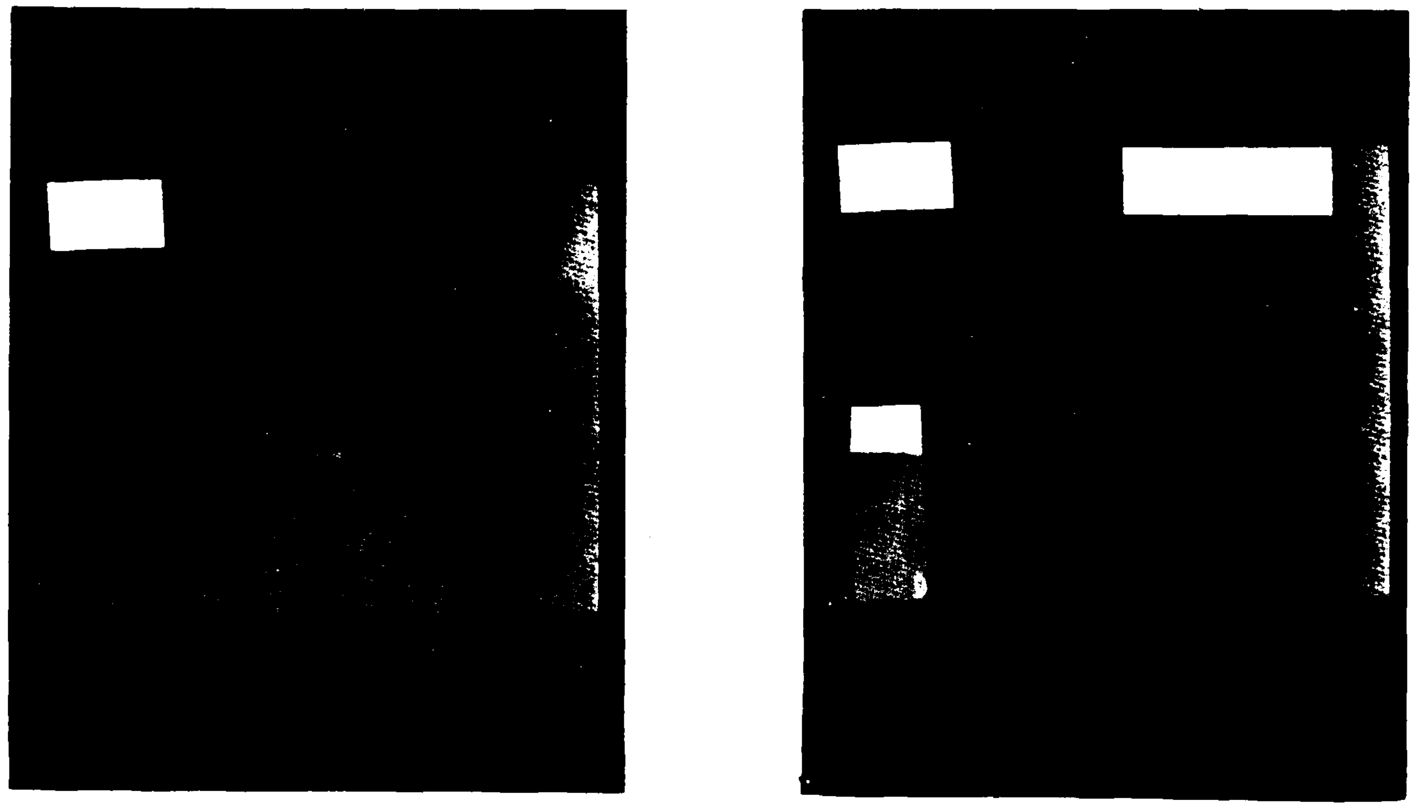

FIGURE 70 X-RADIOGRAPHS OF SPECIMEN 8-3 (PENETRANT ENHANCED) SHOWING THE INITIAL AND FINAL CONDITIONS AFTER ELEVATED TEMPERATURE EXPOSURE TO ZIX-418B

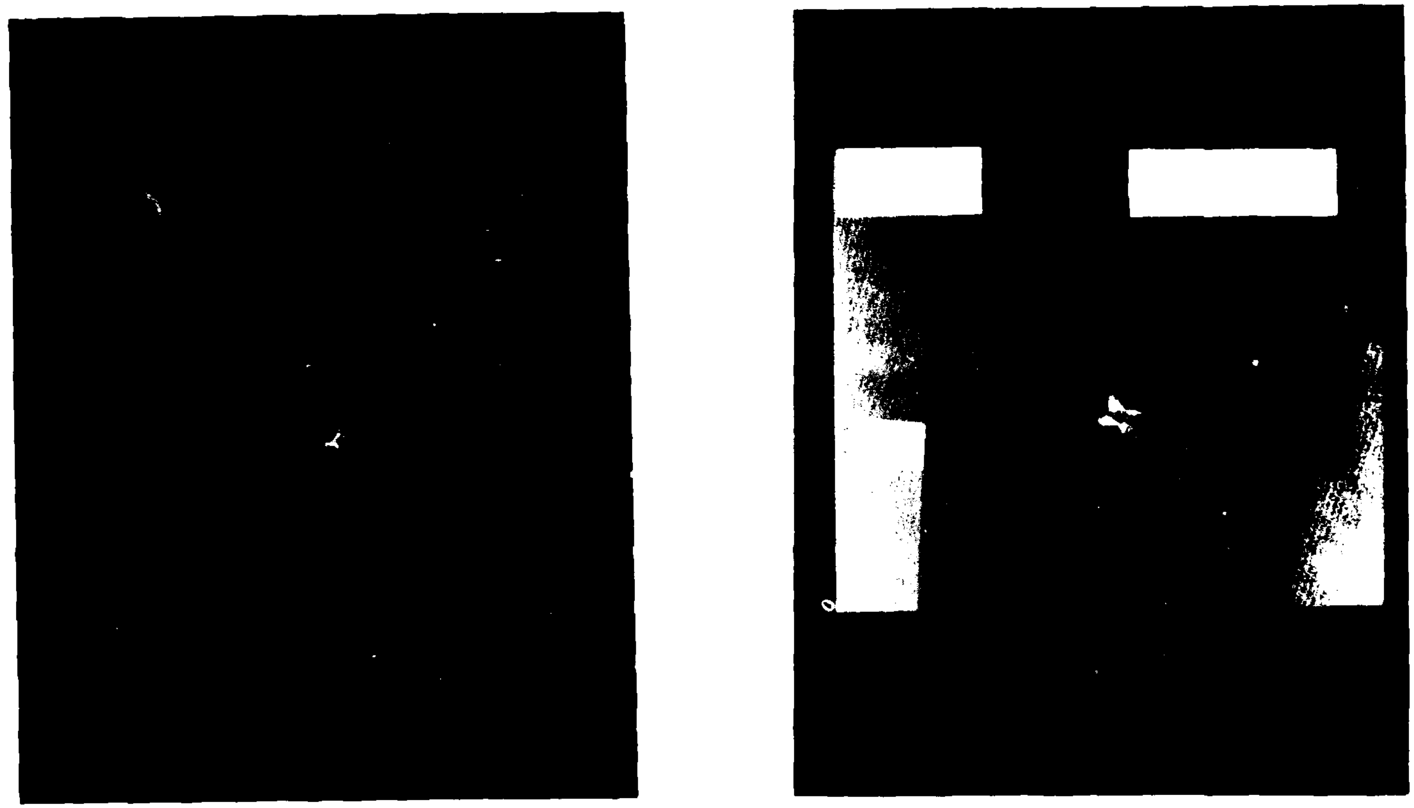

FIGURE 71 X-RADIOGRAPHS OF SPECIMENS 16A-3 AND 24-3 (PENETRANT ENHANCED) AFTER ELEVATED TEMPERATURE EXPOSURE TO ZLX-418B

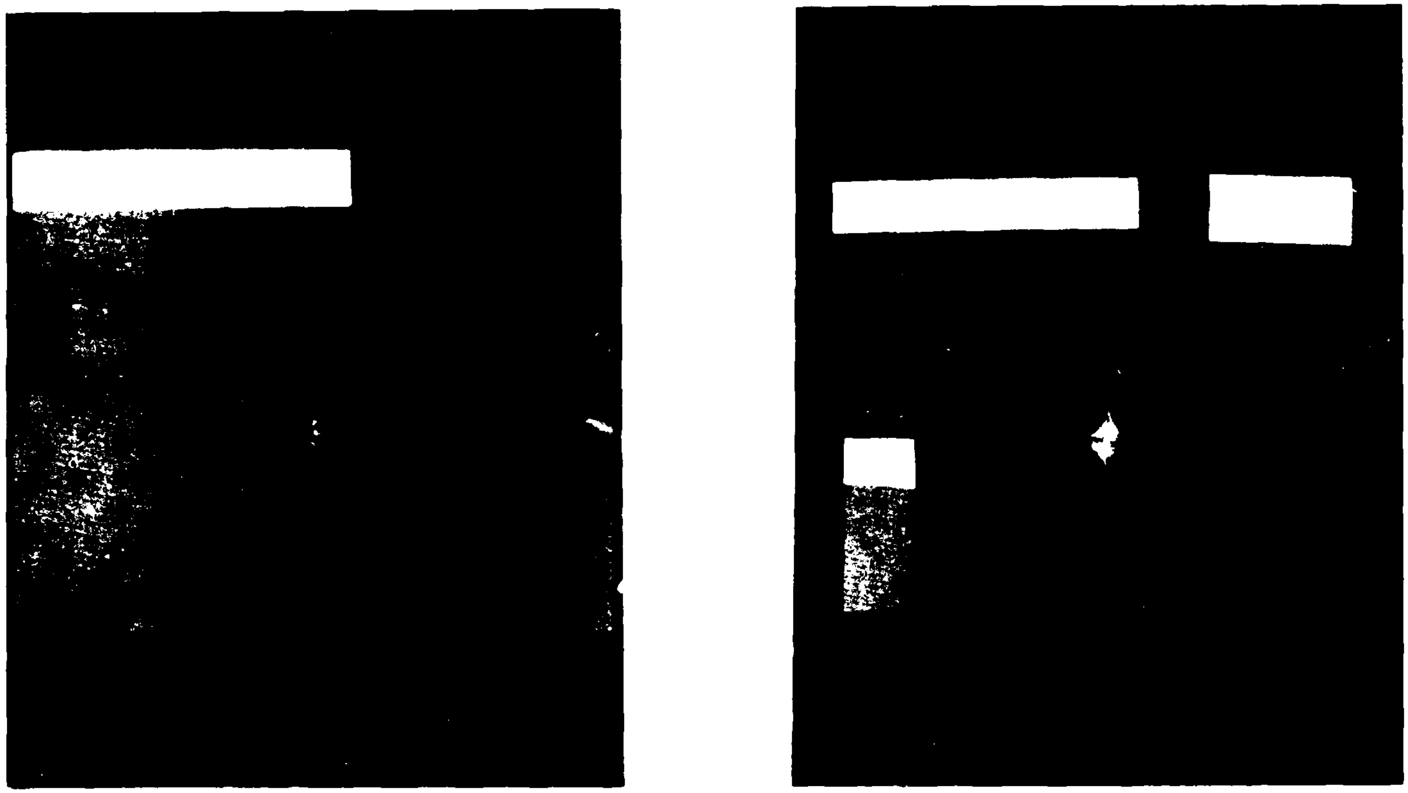

FIGURE 72 X-RADIOGRAPHS OF SPECIMEN 8-1 (PENETRANT ENHANCED) SHOWING THE INITIAL AND FINAL CONDITIONS ELEVATED ROOM TEMPERATURE EXPOSURE TO ZnI_2

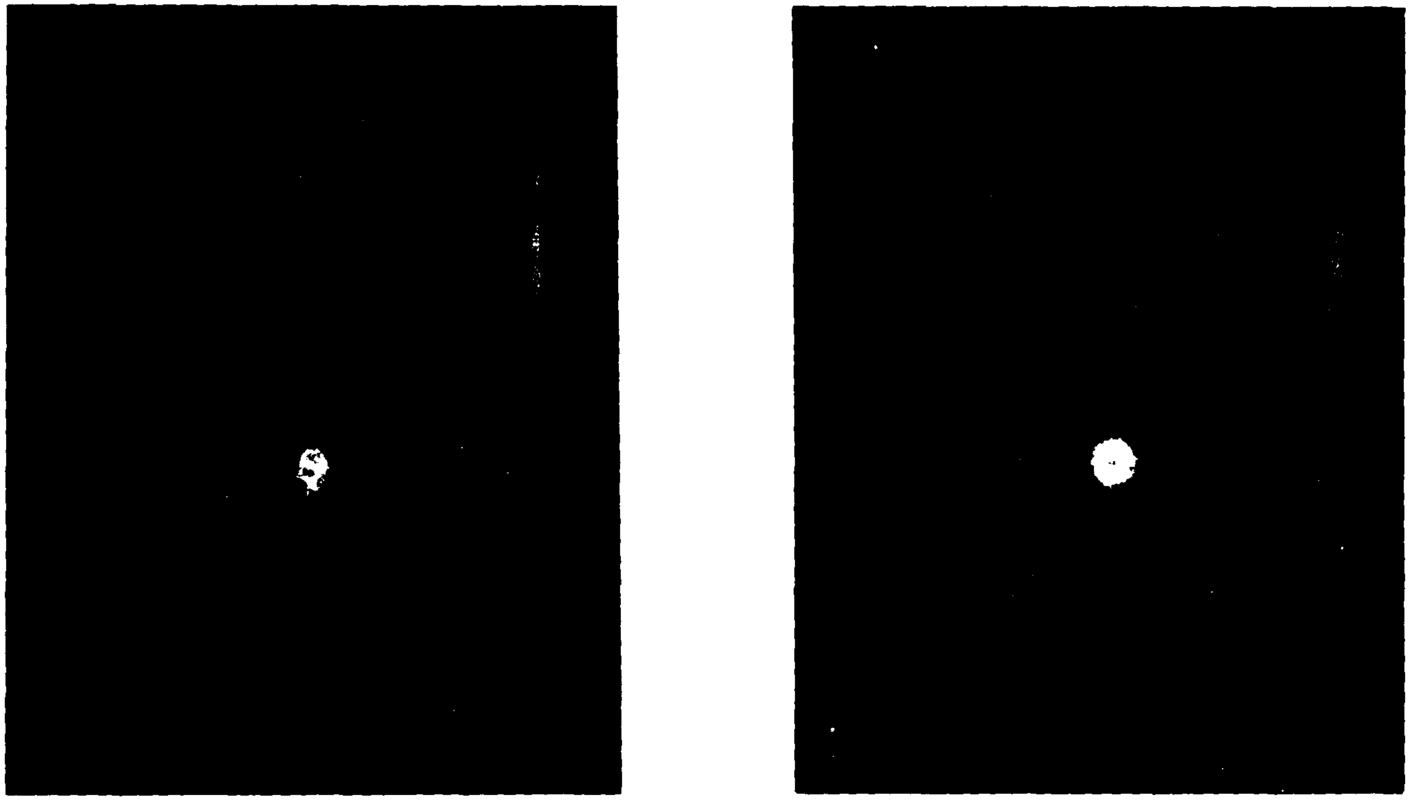

FIGURE 73 X-RADIOGRAPHS OF SPECIMENS 16A-1 (PENETRANT ENHANCED) SHOWING INITIAL AND FINAL CONDITIONS AFTER ELEVATED TEMPERATURE EXPOSURE TO ZnI_2

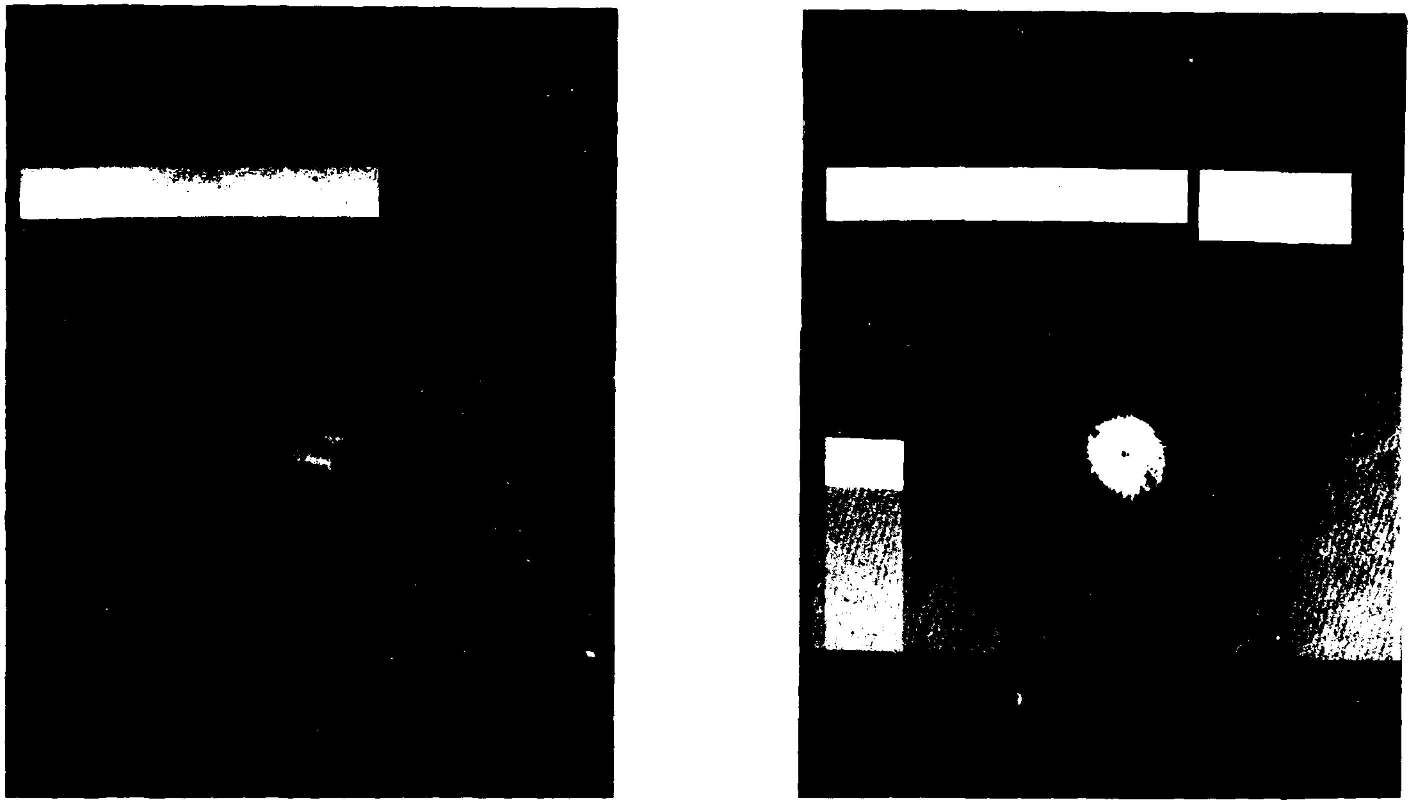

FIGURE 74 X-RADIOGRAPHS OF SPECIMEN 24-1 (PENETRANT ENHANCED) SHOWING THE INITIAL AND FINAL CONDITION AFTER ELEVATED ROOM TEMPERATURE EXPOSURE TO TETROBROMOETHANE

5. Conclusions:

Conclusions from the material compability studies were as follows:

a. X-radiographic inspection showed little significant change in the impact damage location. It was the opinion of test personnel that cracks that were detected subsequent to the initial inspection were caused primarily by hand flexing to aid in penetrant movement. This opinion agrees with results for the 24 ply specimens that did not undergo flexure.

b. Visual inspection did not reveal changes during the test.

c. There appeared to be no difference between the results with those exposed at room temperature and those specimens exposed at elevated temperature.

d. No change or degradation of any of the specimens could be attributed to exposure to penetrants.

SECTION V

STEREO-X-RADIOGRAPHIC INSPECTION DEMONSTRATION

1. GENERAL

The sensitivity and capability for stereo X-radiograph inspection and analysis was demonstrated on specimens subjected to impact damage and fatigue loading. Twelve (12) 16 ply symmetric quasi-isotropic specimens were selected from those previous fabricated. Three of the specimens were selected at random for use in determining the average tensile strength. Impact damage was inflicted at the center of all twelve specimens using Tool No. 1 at a 15 in.-pound level.

Damage assessment and quantification was made by stereo-x-radiography, with zinc iodide penetrant solution, using the established technique. Impact/fatigue damage depth was estimated by reference to the circular step wedges that were imaged with the specimen. Damage accumulation was sized and located within the specimen by plies (levels within the panel). The bottom of the specimen was the platen side. Impact was inflicted from the top side. Damage was documented by progression from Level 1 (bottom side) to level 8 (top side) as described in the following:

16 PLY	
level 1	0.012 in.
level 2	0.024 in.
level 3	0.036 in.
level 4	0.048 in.
level 5	0.060 in.
level 6	0.072 in.
level 7	0.084 in.
level 8	0.096 in.

2. Determination of Average Tensile Strength

Three randomly selected specimens were used to determine average tensile strength of the material as an aid in selecting stress levels for fatigue tests. Specimens were identified as 16B-4, 16B-7, and 16B-11 respectively.

Conventional x-radiography (no penetrant) revealed no evidence of cracks or delaminations. Zinc Iodide solution was applied to each specimen and allowed to dwell for 30 minutes. Stereo-x-radiographs were made at damage locations to document panel condition prior to tensile loading. Specimens were loaded to failure at a rate of 0.50 inches per minute.

Zinc Iodide solution was reapplied to damaged areas and allowed to dwell for 30 minutes. Stereo-x-radiographs were made at damage locations to document post-test conditions. Results of testing are summarized in Table 13. Stereo x-radiographic pairs taken before and after test are shown in Figures 75 and 76; 77 and 78; and 79 and 80.

TABLE 13

TENSILE TEST PARAMETERS AND RESULTS

SPECIMEN	WIDTH	THICKNESS	AREA (SQ.-IN.)	INITIAL CONDITION	ULTIMATE LOAD (LB)	ULTIMATE STRENGTH (PSI)	FINAL CONDITION
16B-4	3.900 INCH	0.094 INCH	0.366 SQ. IN.	CRACKS AT $\pm 45^{o}$, 90^{o}. SMALL DELAMINATION AT LEVEL 1. (FIGURE 75)	29,000 POUNDS	79,234 POUNDS PER SQUARE INCH	VISUAL INSPECTION SHOWED THAT THE FAILURE SITE WAS NOT ASSOCIATED WITH THE DAMAGED AREA. STEREO-X-RADIOGRAPHY SHOWED NO CHANGE IN THE DAMAGE AREA (FIGURE 76)
16B-7	3.800 INCH	0.095 INCH	0.369 SQ. IN.	CRACKS AT 0^{o}, $\pm 45^{o}$, 90^{o}. DELAMINATIONS AT LEVEL 1, 2, AND 3. (FIGURE 77)	28,500 POUNDS	77,236 POUNDS PER SQUARE INCH	VISUAL INSPECTION SHOWED THAT THE FAILURE SITE WAS NOT ASSOCIATED WITH THE DAMAGE AREA. STEREO-X-RADIOGRAPHY SHOWED SOME CRACK GROWTH IN THE DAMAGED AREA (FIGURE 78)
16B-11	3.900 INCH	0.097 INCH	0.379 SQ. IN.	CRACKS AT 0^{o}, $\pm 45^{o}$,90^{o} DELAMINATIONS AT LEVEL 1 THROUGH 5. (FIGURE 79)	29,000 POUNDS	76,517 POUNDS PER SQUARE INCH	VISUAL INSPECTION SHOWED THAT THE FAILURE EXTEND-ED THROUGH THE DAMAGE AREA STEREO-X-RADIOGRAPHY WAS INCONCLUSIVE DUE TO THE EXCESS PENETRANT IN THE FAILURE SITE (FIGURE 80)
MACHINE SPEED - 0.050 INCHES/MINUTE - TENSILE AVERAGE - 77,622 p.s.i.							

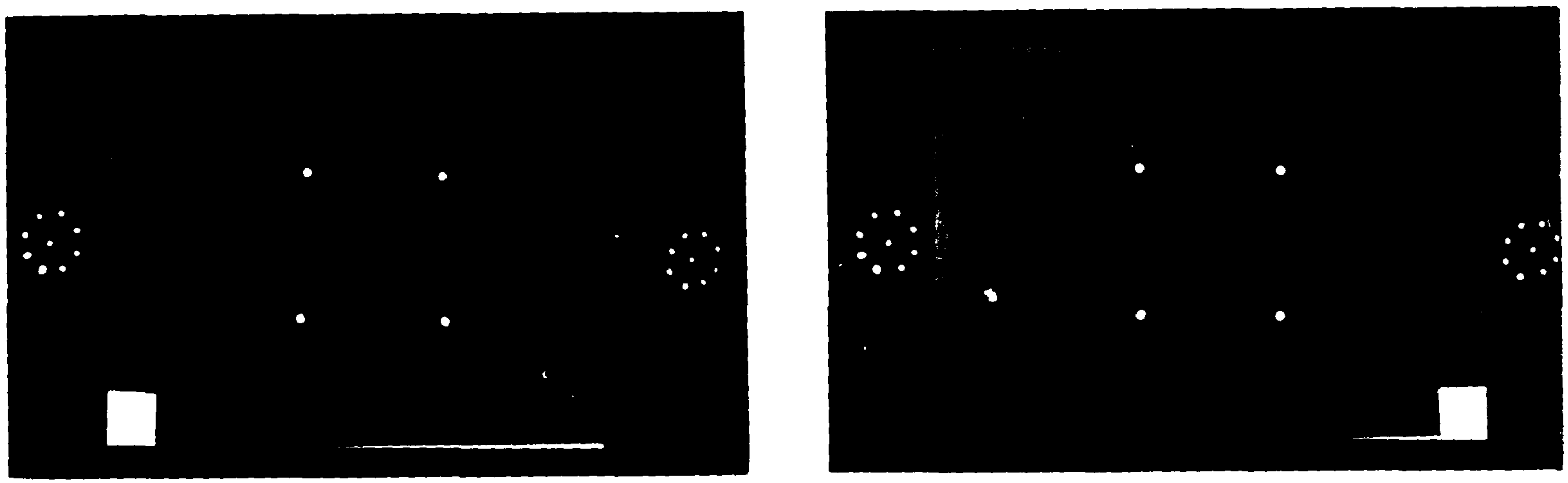

FIGURE 75 X-RADIOGRAPH OF SPECIMEN 16B-4 (ZnI_2 ENHANCED) BEFORE TENSILE LOADING

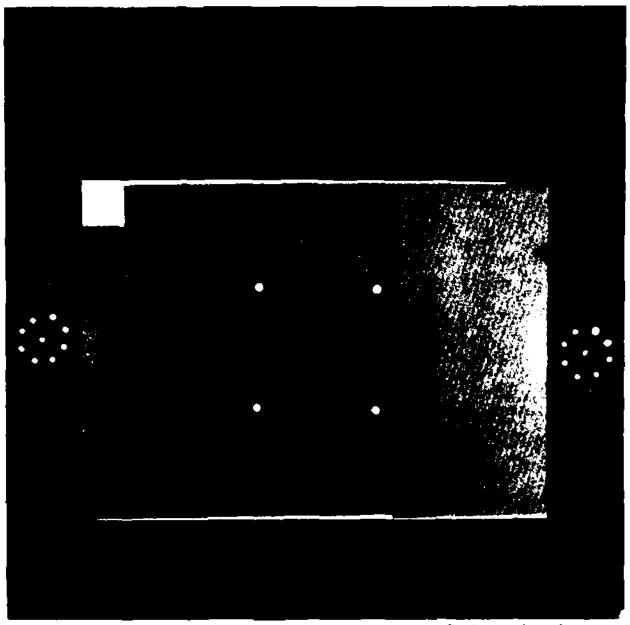

FIGURE 76 X-RADIOGRAPH OF SPECIMEN 16B-4 (ZnI_2 ENHANCED) AFTER TENSILE LOADING

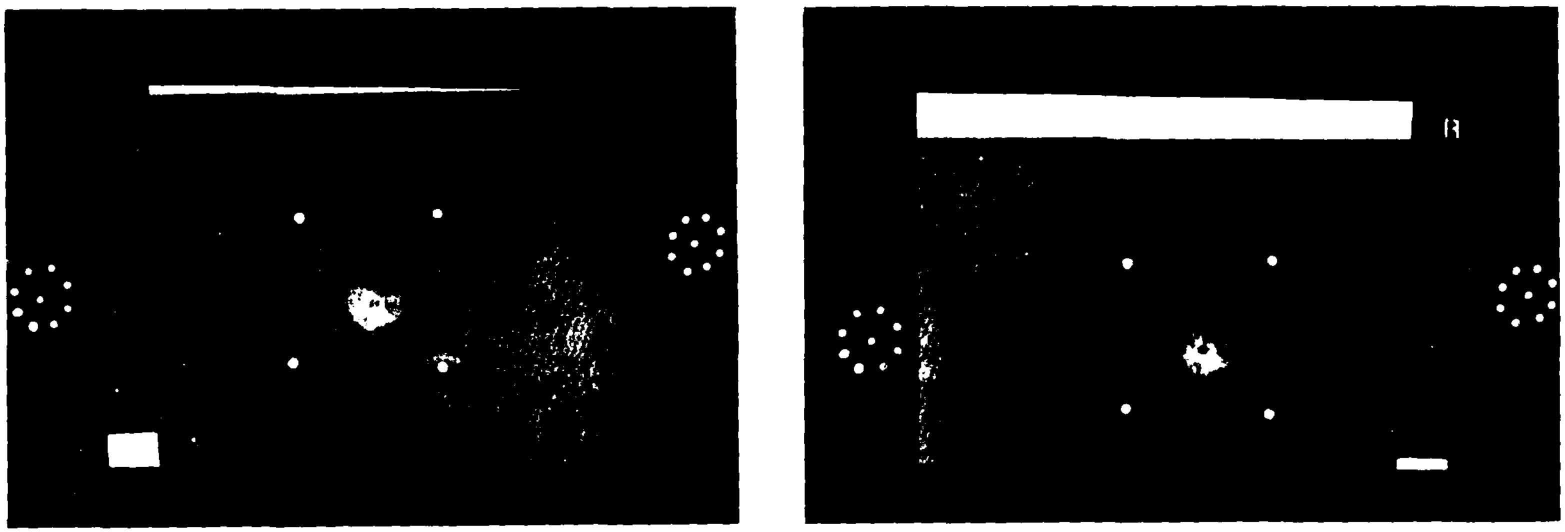

FIGURE 77 X-RADIOGRAPH OF SPECIMEN 16B-7 (ZnI_2 ENHANCED) BEFORE TENSILE LOADING

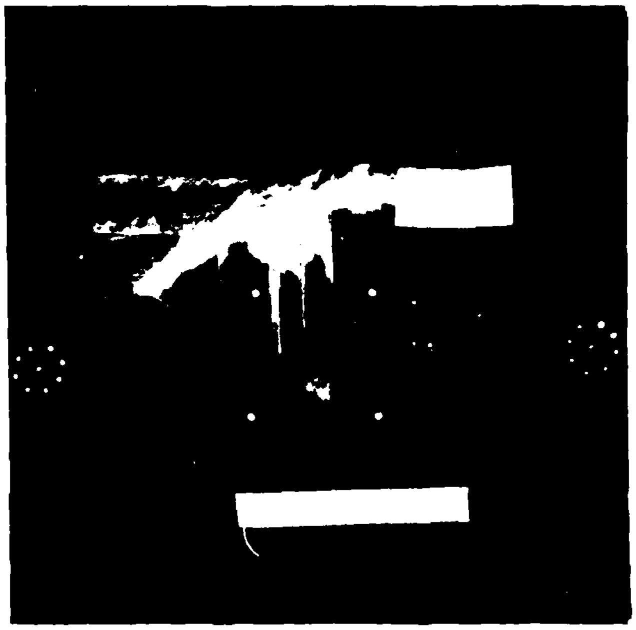

FIGURE 78 X-RADIOGRAPH OF SPECIMEN 16B-7 (ZnI_2 ENHANCED) AFTER TENSILE LOADING

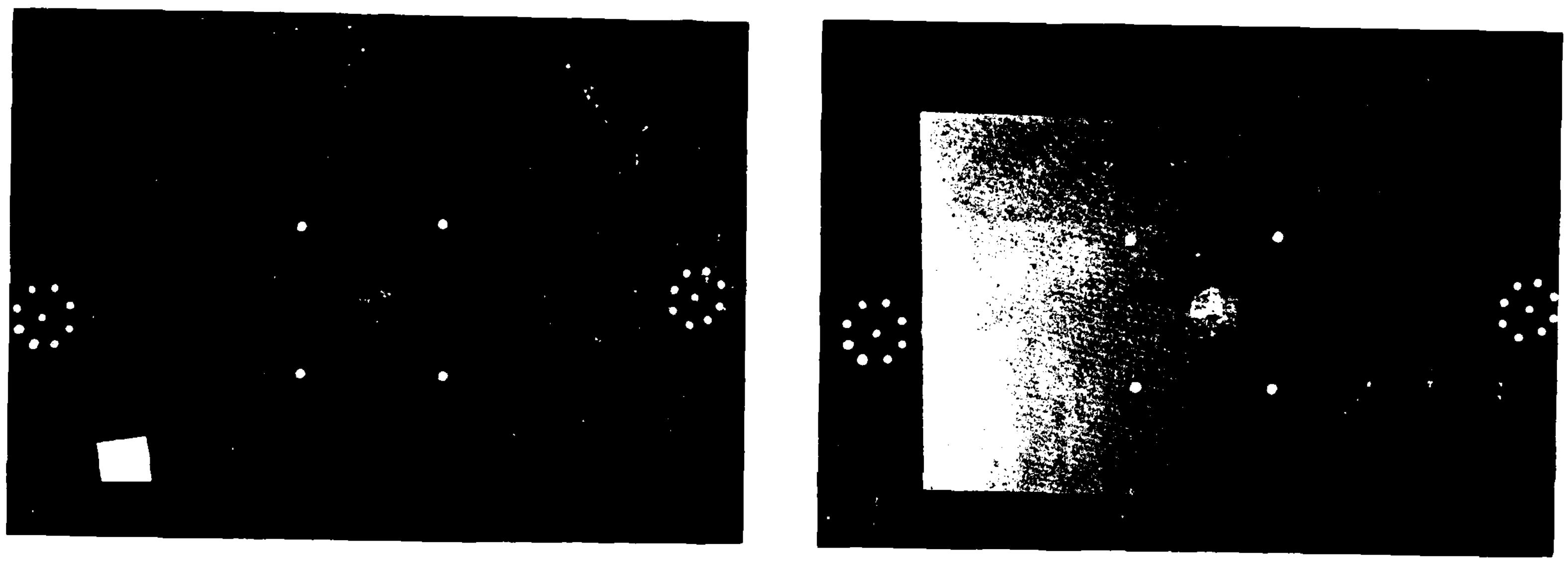

FIGURE 79 X-RADIOGRAPH OF SPECIMEN 16B-11 (ZnI_2 ENHANCED) BEFORE TENSILE LOADING

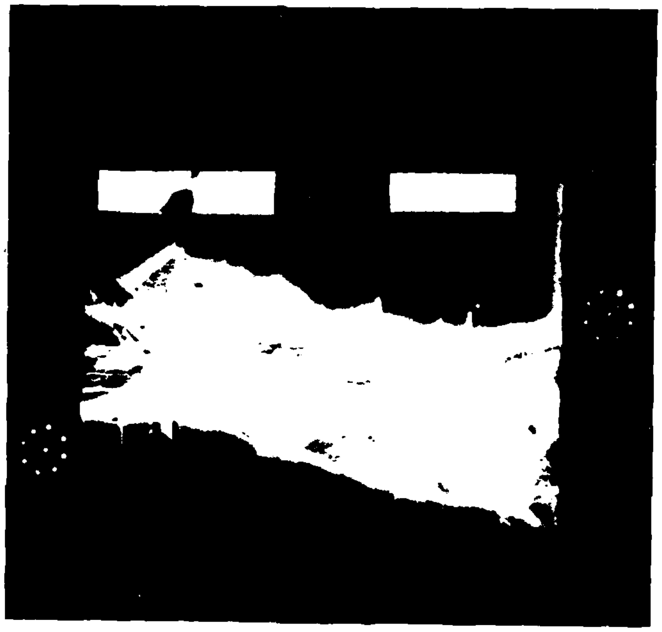

FIGURE 80 X-RADIOGRAPH OF SPECIMEN 16B-11 (ZnI_2 ENHANCED) AFTER TENSILE LOADING

3. Fatigue Life Tests

Nine specimens identified for fatigue test, were initially inspected by stereo-x-radiography with and without penetrant enhancement. Three specimens each were designated for test at 60, 70, and 80 percent of the average static tensile failure stress.

Incremental inspection by the stereo-x-radiographic technique was performed to document damage accumulation due to fatigue loading. The frequency of inspections was gaged to the rate of damage accumulation. One (1) x-radiographic inspection was performed on-site, in the fatigue machine to demonstrate portability of the technique.

All failures were documented by visual observation and by photography.

After test of initial specimens, the aluminum doublers were modified to a longer taper, thereby, reducing failures at the junction to the doubler area. Tapers were modified to extend back 3/4 inch by hand filing on Panels 16B1-2, 16B-2, 16B-3, 16B-6, 16B-9, and 16B-10.

4. Fatigue Test of Specimens 16B-1-2

a. Initial Condition

Stereo-x-radiography, after impact damage, with no penetrant showed numerous voids (0°, $+45^\circ$, 90°). There was no evidence of cracks or delaminations. The damaged area does not show in the radiograph.

ZnI_2 was applied to the damaged areas and allowed to dwell for 30 minutes. Stereo-x-radiographic inspection showed cracks (0°, $+45^\circ$, 90°) associated with delaminations at levels 1 and 2. (Figure 81).

ZnI_2 was then applied to the edges of the specimen, and allowed to dwell for 30 minutes. The specimen was then radiographically inspected using the standard optimum technique. The purpose of this inspection was to determine if any cracks existed at the edges prior to fatigue test. No evidence of cracks was detected. (Figure 82).

Fatigue Test

The specimen was fatigued at 60% of average tensile failure load. (60% of 77.7 = 46.6KSI)
(Area = 0.388) (46.6 KSI)= 18,088 lbs maximum load

b. Fatigue Sequence - No. 1

Cycles	KSI stress	Total
7	46.6	7

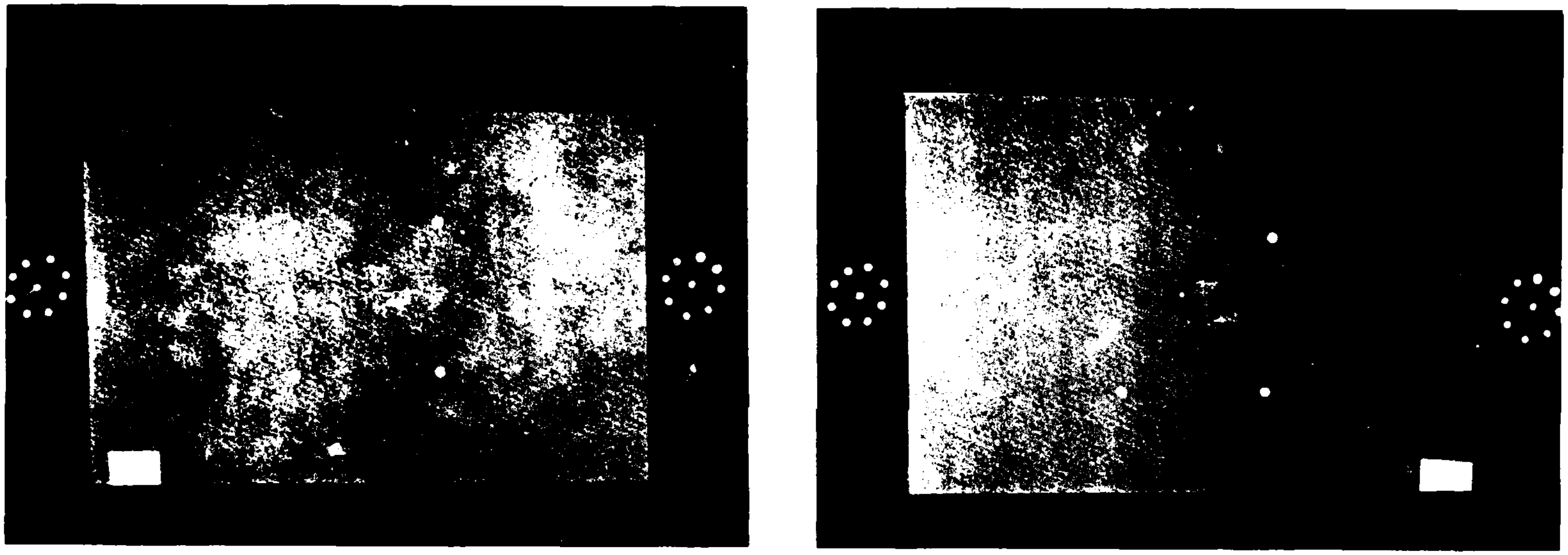

FIGURE 81 X-RADIOGRAPH OF SPECIMEN 16B-1-2 SHOWING INITIAL CONDITION (ZnI_2) ENHANCED

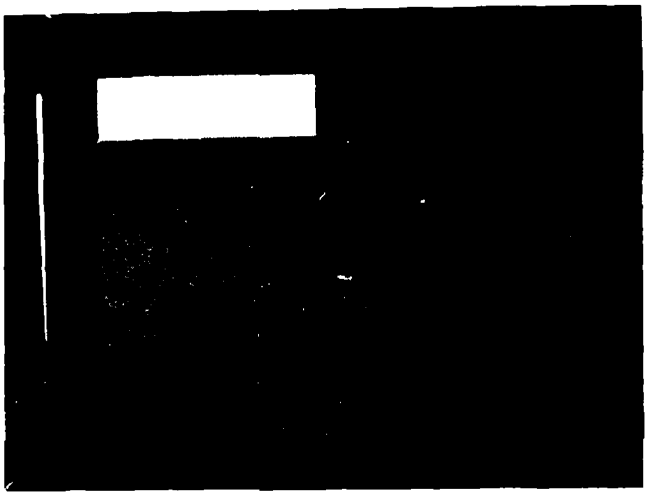

FIGURE 82 X-RADIOGRAPH OF SPECIMEN 16B-1-2 AFTER APPLICATION OF ZnI_2 TO THE EDGES INITIAL CONDITION

After cycling, 1 visual inspection showed no evidence of cracks or delaminations. There was a slight amount of lifting of the doubler (grip) at opposite end from the specimen identification and on the same side.

ZnI_2 was applied to the edges and to the damaged areas and allowed to dwell for 30 minutes. The specimen was radiographed (stereo) and showed extensive cracking from the edges in the area between the grips. These cracks did not exist prior to the start of fatigue test. (Figure 82). There was no change in the impact damage area. (Figure 83).

c. Fatigue Sequence - No. 2

Cycles	KSI stress	Total
43	46.6	50

After cycling, visual inspection showed no change from the condition during Sequence 1.

The specimen was put in a plastic bag with the zinc iodide penetrant solution sealed, evacuated and allowed to dwell for 3 days.

The specimen was radiographed (stereo) and showed considerable growth in crack length from the specimen edges. The cracks (0) through the delamination extend to the edge of the specimen.

The cracks were at all levels through the specimen thickness. The delamination and matrix cracks now extended up to Levels 7 and 8. (Figure 84).

d. Fatigue Sequence - No. 3

Cycles	KSI stress	Total
450	46.6	500

After cycling, visual inspection showed no change from the inspection of Sequence 2.

ZnI_2 was applied to the damaged areas and allowed to dwell for 30 minutes. The specimen was radiographed (stereo) and showed no change from Sequence 2 condition. (Figure 85).

e. Fatigue Sequence - No. 4

Cycles	KSI stress	Total
500	46.6	1000

After cycling, visual inspection showed no change from the Sequence 3 condition.

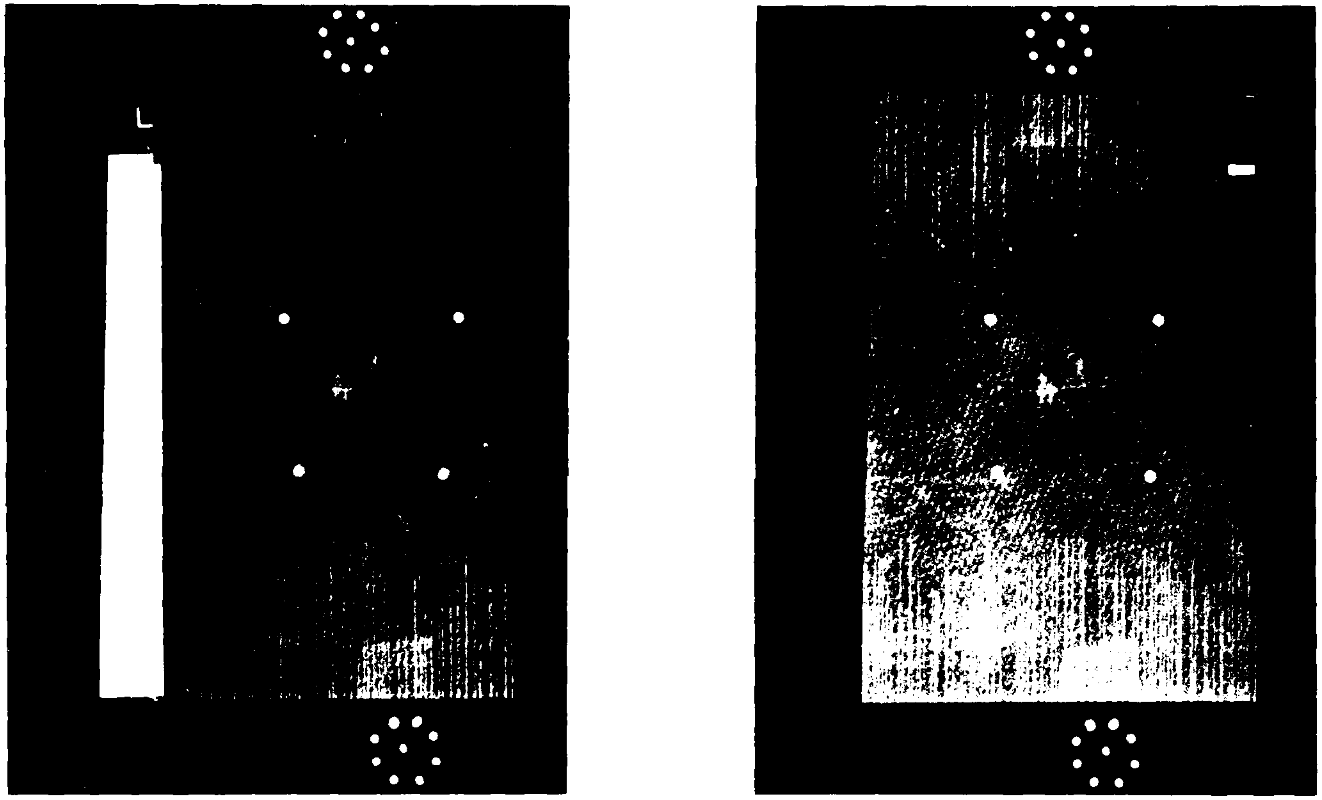

FIGURE 83 SPECIMEN 16B-1-2 AFTER INITIAL FATIGUE SEQUENCE (ZnI_2 ENHANCED)

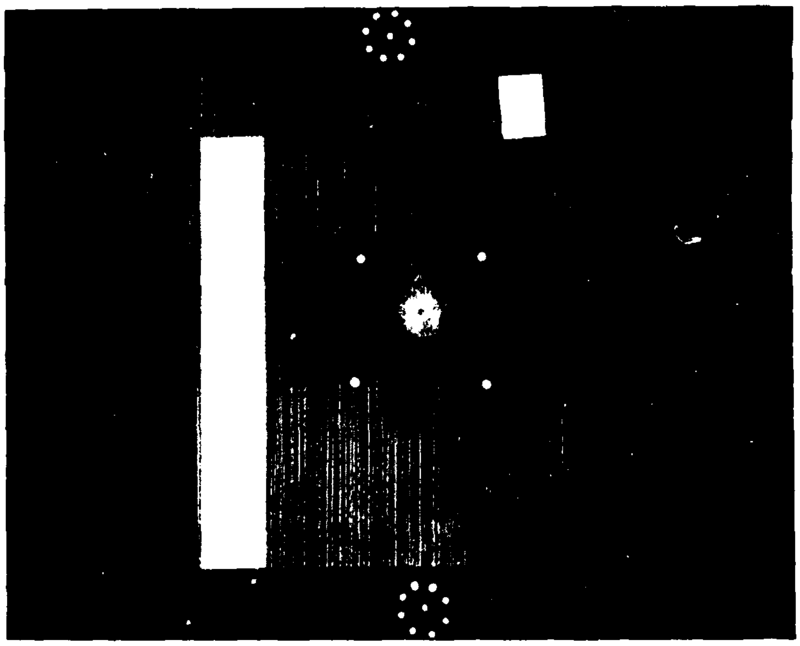

FIGURE 84 SPECIMEN 16B-1-2 AFTER FATIGUE SEQUENCE 2 (ZnI_2 ENHANCED)

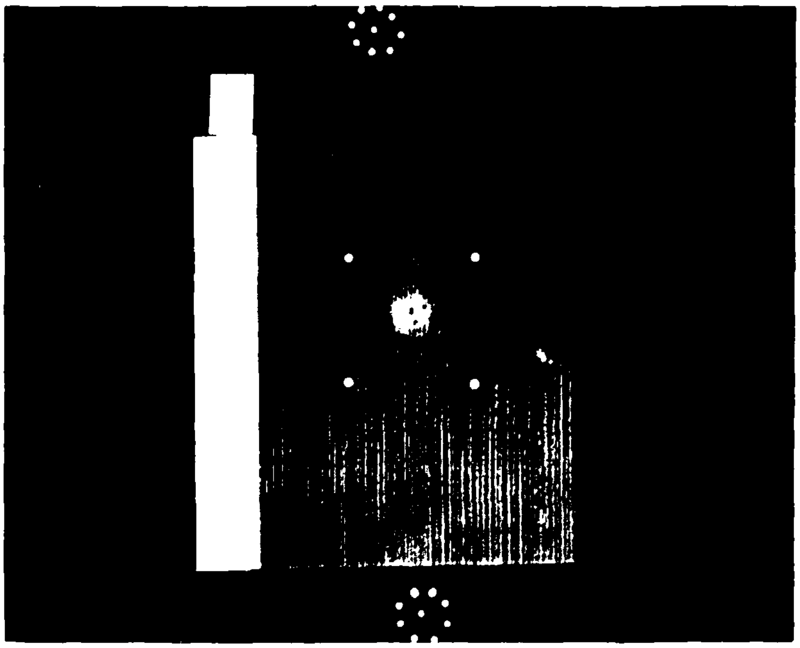

FIGURE 35 SPECIMEN 16B-1-2 AFTER FATIGUE SEQUENCE 3 (ZnI_2 ENHANCED)

ZnI_2 was applied to the damaged areas and allowed to dwell for 30 minutes. The specimen was radiographed (stereo) and showed no change from the radiograph from Sequence 3. (Figure 86).

f. <u>Fatigue Sequence - No. 5</u>

Cycles	KSI stress	Total
2000	46.6	3000

After cycling, visual inspection showed a separation of the grip doubler at the specimen identification end and on the same side the identification. There was a separation of the grips on both ends.

ZnI_2 was applied to the damaged areas and allowed to dwell for 30 minutes. The specimen was radiographed (stereo) and showed no change from the radiographs from Sequence 4. (Figure 87)

g. <u>Fatigue Sequence - No. 6</u>

Cycles	KSI stress	Total
3700	46.6	6700

The panel failed after a total of 6700 cycles.

After failure, visual inspection showed failure at the grip doubler, panel identification end. The composite material had pulled out from under the grip. There was no failure in the impact damage area. No further inspection was accomplished.

Figure 88 shows the location of failure for this specimen.

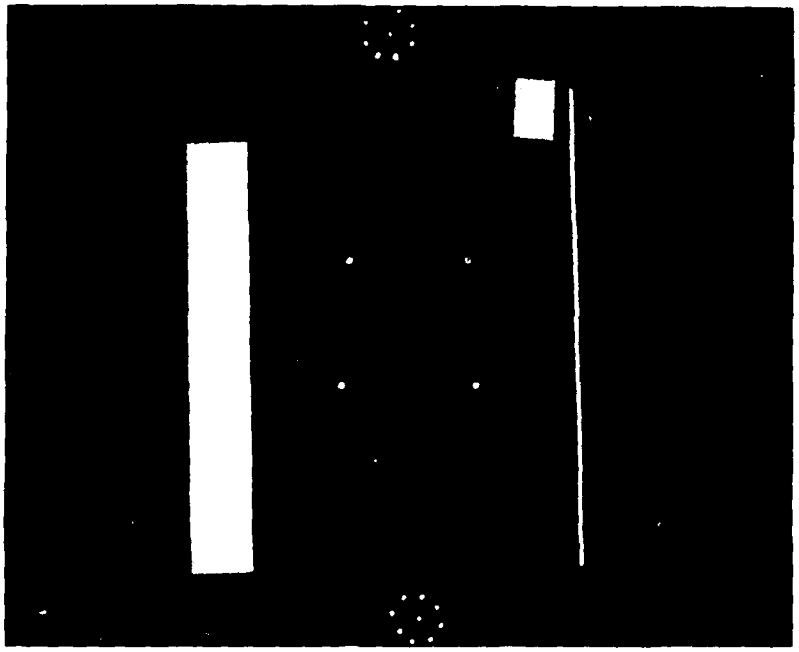

FIGURE 86 SPECIMEN 16B-1-2 AFTER FATIGUE SEQUENCE 4 (ZnI_2 ENHANCED)

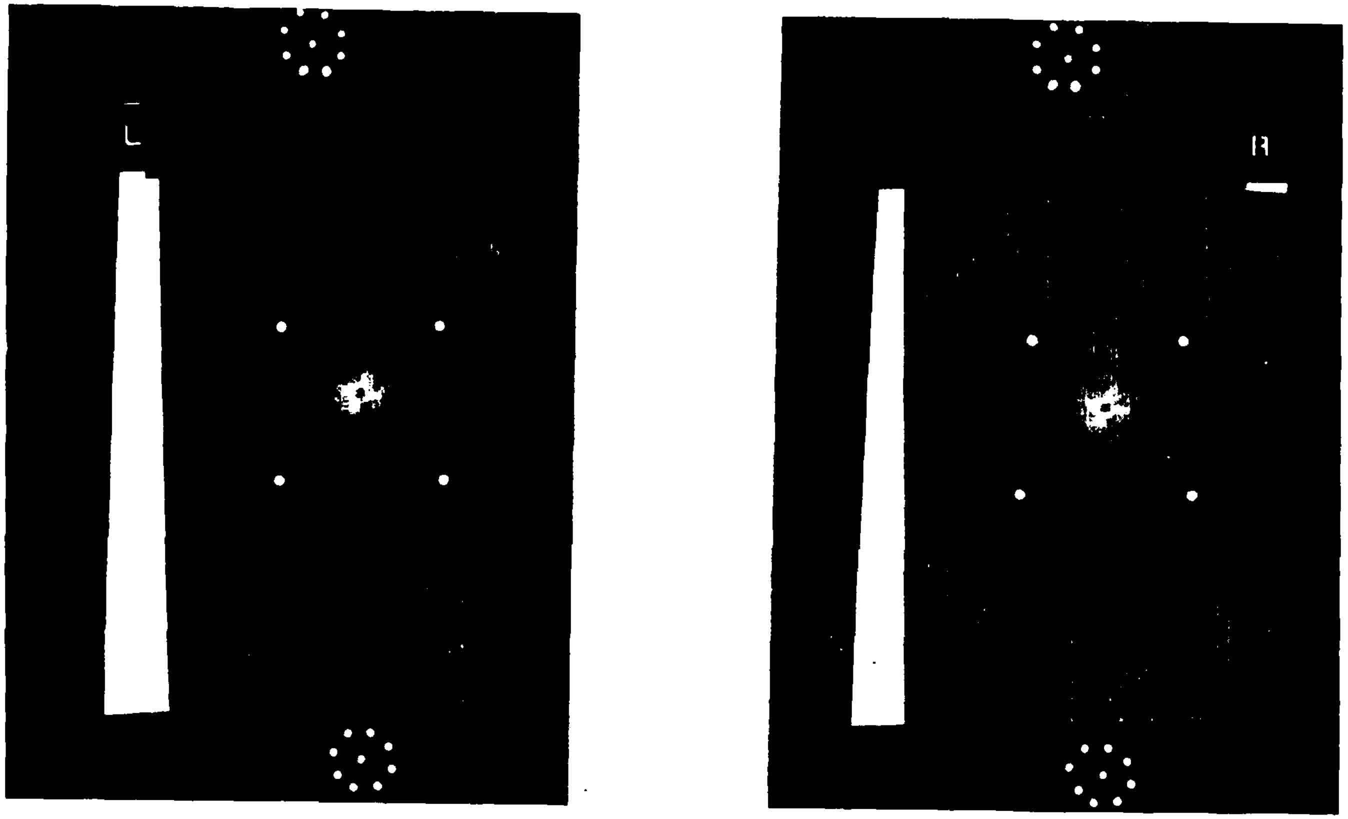

FIGURE 87 SPECIMEN 16B-1-2 AFTER FATIGUE SEQUENCE 5
(ZnI_2 ENHANCED)

FIGURE 88 SPECIMEN 16B-1-2 AFTER FATIGUE FAILURE

5. Fatigue Test of Specimen - 16B-2

a. Initial Condition

Radiography (stereo), after impact damage, with no penetrant, showed numerous voids. The voids tend to follow fiber lay up direction. There was no evidence of cracks or delaminations in the impact damage area.

ZnI_2 was applied to the damaged areas and allowed to dwell for 30 minutes. The specimen was radiographed (stereo) and showed $(0^\circ, \pm 45^\circ, 90^\circ)$ cracks and delamination 1/2 in. diameter at Level -1. (Figure 89)

Fatigue Test

The specimen was fatigued at 60% average tensile failure load (60% of 77.7 = 46.6)
(Area = 0.375) (46.6 KSI) = 17,475 lbs maximum load

b. Fatigue Sequence - No. 1

Cycles	KSI stress	Total
2000	46.6	2000

After cycling, visual inspection showed grip doubler separation at both ends. There were no delaminations.

ZnI_2 was applied to the damaged areas and allowed to dwell for 60 minutes. The panel was radiographed (stereo) and showed cracks transverse to the damage area at Levels 1 and 2. (Figure 90)

ZnI_2 was then applied to the edges of the specimen and allowed to dwell for 4.5 hours. The specimen was radiographed (stereo) and showed numerous cracks from both panel edges at all levels. The cracks occupy all the area between the grips and extend toward center of the panel for approximately 1 1/4 inches. (Figure 91)

c. Fatigue Sequence - No. 2

Cycles	KSI stress	Total
2000	46.6	4000

After cycling, visual inspection showed a delamination under the grip doubler at the identification end.

ZnI_2 was applied to the damaged areas and allowed to dwell for 30 minutes. The specimen was radiographed (stereo) and showed more cracks; (4) in the damaged area at levels 1 and 2. There was no change in the delamination.

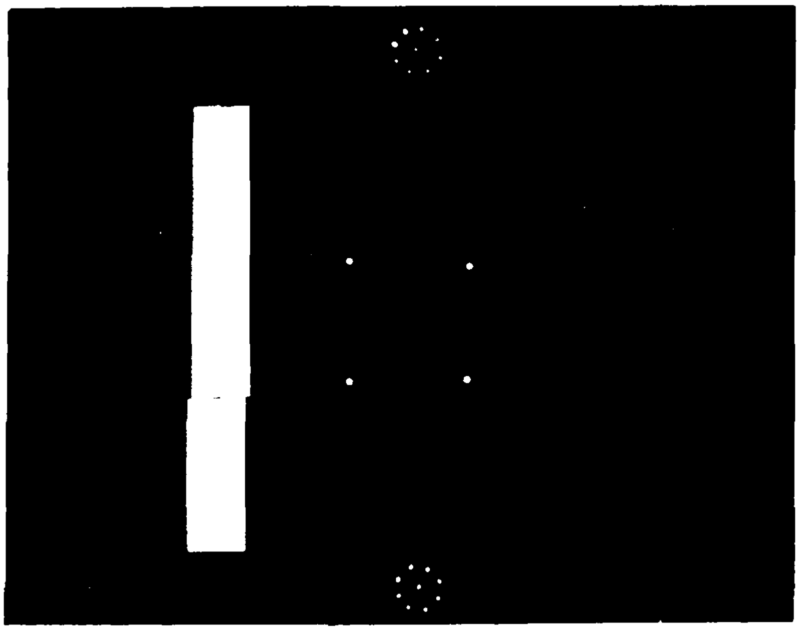

FIGURE 89 X-RADIOGRAPH OF SPECIMEN 16B-2. INITIAL CONDITION (ZnI_2 ENHANCED)

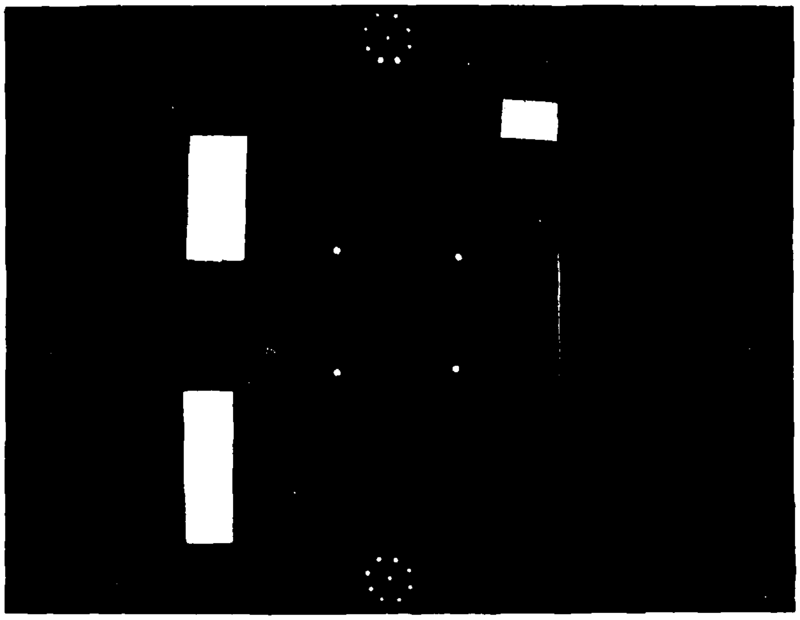

FIGURE 90 SPECIMEN 16B-2 AFTER FATIGUE SEQUENCE 1 (ZnI_2 ENHANCED)

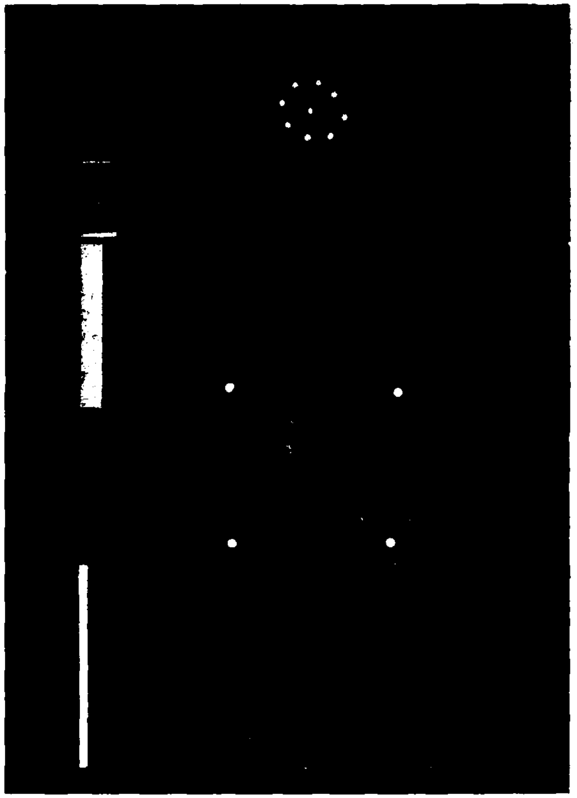

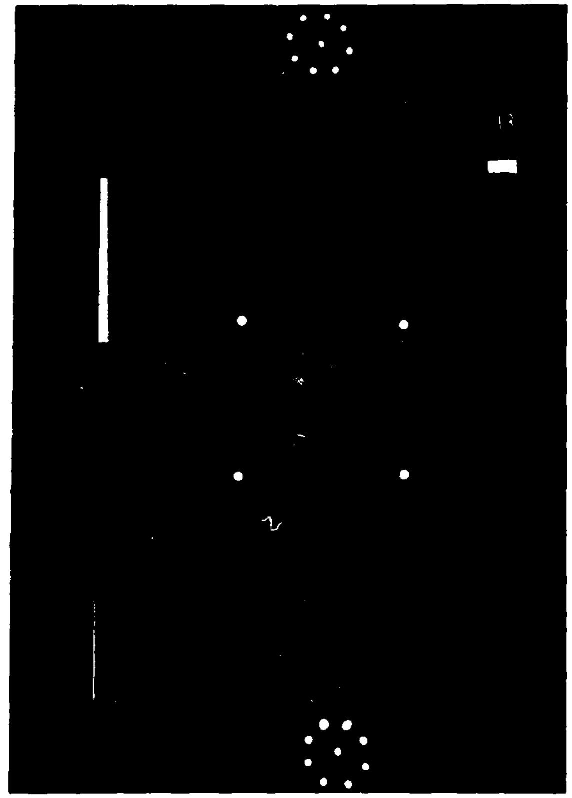

FIGURE 91 SPECIMEN 16B-2 AFTER FATIGUE SEQUENCE 1
(ZnI_2 ENHANCED EDGES)

There was no change in the cracks from the edges. (Figure 92)

d. Fatigue Sequence - No. 3

Cycles	KSI stress	Total
2000	46.6	6000

After cycling, visual inspection showed no change from the inspection in Sequence 2.

ZnI_2 was applied to the damaged areas and allowed to dwell for 30 minutes. The specimen was radiographed (stereo) and showed no change in the damaged area. (Figure 93)

e. Fatigue Sequence - No. 4

Cycles	KSI stress	Total
2000	46.6	8000

After cycling, visual inspection showed a crack and delamination on opposite sides from specimen identification and at the grip opposite from the identification. The delamination extended under the grip. The crack was between the grips.

ZnI_2 was applied to the damaged areas and allowed to dwell for 30 minutes. The specimen was radiographed (stereo) and showed more cracks through the damaged area at levels 1, 2, and 3. The delaminations were also at levels 1, 2, and 3. (Figure 94)

The specimen was put in a plastic bag with ZnI_2, sealed, evacuated, and allowed to dwell for 16 hours.

The specimen was radiographed (stereo) and showed more cracks through the damaged area. The cracks were too numerous to determine depths. The delaminations are at levels 1, 2, 3, and 4. (Figure 95)

f. Fatigue Sequence - No. 5

Cycles	KSI stress	Total
2000	46.6	10,000

After cycling, visual inspection showed a crack under the grip doubler at the identification end and on the side opposite from the identification. There was also a growth in the cracks at the opposite end on the same side.

ZnI_2 was applied to the damaged areas and allowed to dwell for 30 minutes. The specimen was radiographed (stereo) and showed no change from Sequence 4. (Figure 96).

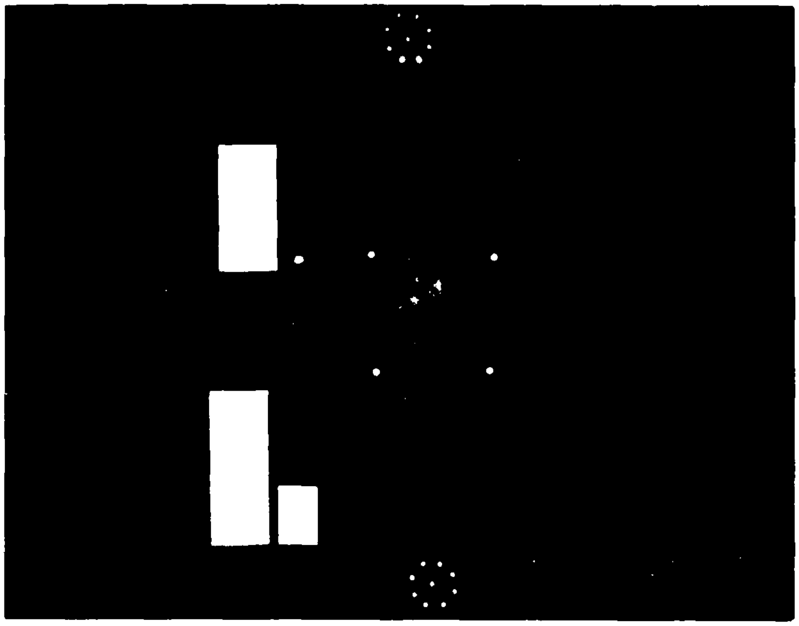

FIGURE 92 SPECIMEN 16B-2 AFTER FATIGUE SEQUENCE 2 (ZnI_2 ENHANCED)

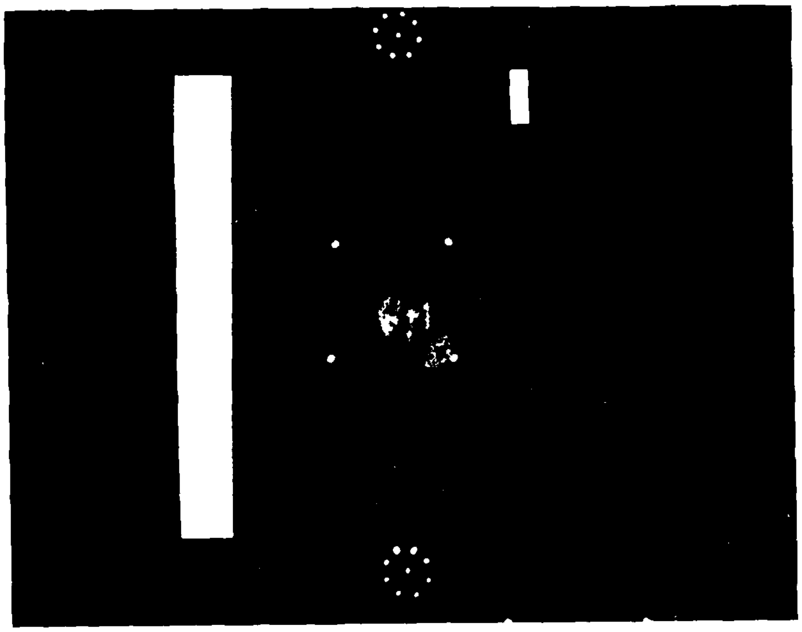

FIGURE 93 SPECIMEN 16B-2 AFTER FATIGUE SEQUENCE 3 (ZnI_2 ENHANCED)

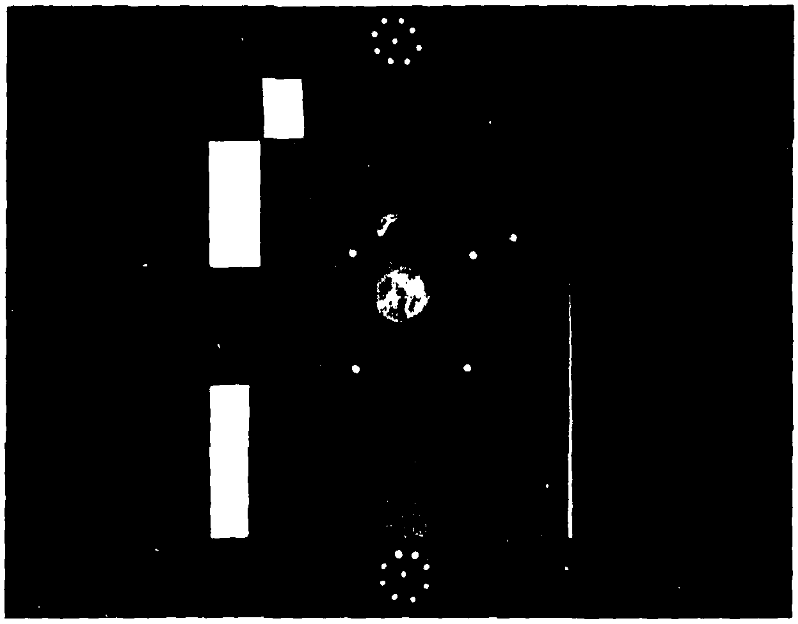

FIGURE 94 SPECIMEN 16B-3 AFTER FATIGUE SEQUENCE 4 (ZnI_2 ENHANCED)

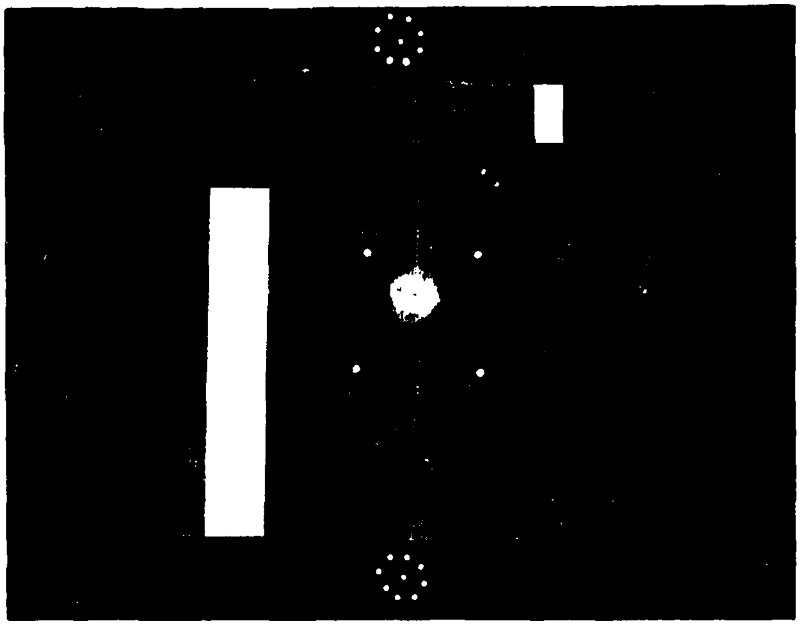

FIGURE 95 SPECIMEN 16B-1-2 AFTER FATIGUE SEQUENCE 5
AND ADDITIONAL ZnI_2 EXPOSURE

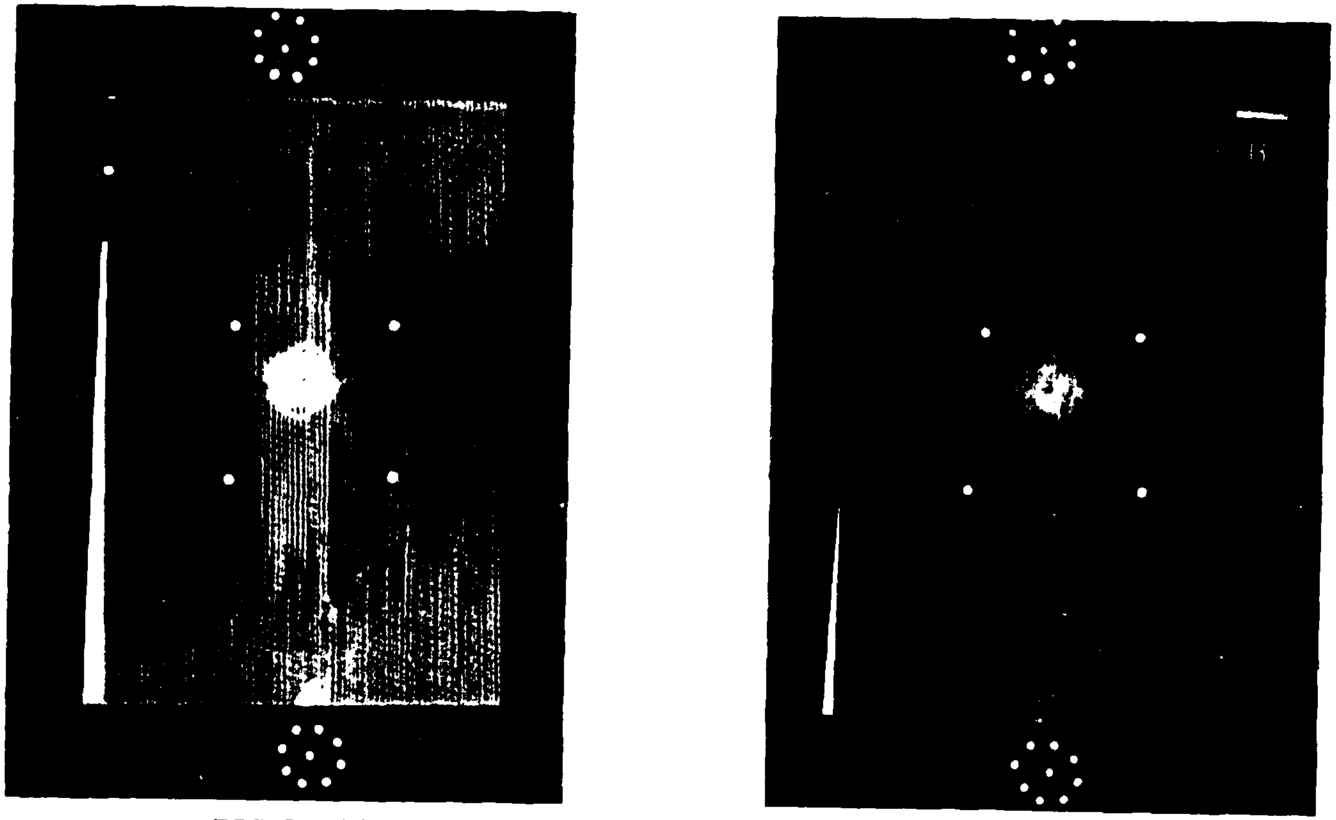

FIGURE 96 SPECIMEN 16B-1-2 AFTER FATIGUE SEQUENCE 6
(ZnI_2 ENHANCED)

g. Fatigue Sequence - No. 6

The specimen failed during fatigue test after an additional 250 cycles. The specimen received a total of 10,250 cycles.

Visual inspection after failure showed the failure occuring at the grip opposite from the specimen identification. The composite material pulled out from under the grip.

Figure 97 shows the location of failure for this specimen.

FIGURE 97 SPECIMEN 16B-1-2 AFTER FATIGUE FAILURE

6. Fagitue Test of Specimen 16B-3

a. Initial Condition

Radiography (stereo), after impact damage, with no penetrant, showed numerous voids (0°, $+45^\circ$, 90°). There was no evidence of cracks or delaminations.

ZnI_2 was applied to the damaged areas and allowed to dwell for 30 minutes. The specimen was radiographed (stereo) and showed cracks at 0°, $+45^\circ$, 90° and delaminations at Levels 1 and 2. There was good capillary movement of the penetrant into the damaged area. (Figure 98)

ZnI_2 was then applied to the edges of the panel and allowed to dwell for 30 minutes. The specimen was radiographically inspected and showed no cracks at the edges. (Figure 99)

Fatigue Test

The specimen was fatigued at 70% average tensile failure load (70% of 77.7 = 54.4 KSI)
(Area = 0.371) (54.4 KSI) = 20,179 lbs maximum load

b. Fatigue Sequence - No. 1

Cycles	KSI stress	Total
5	54.5	5

After cycling, visual inspection showed no evidence of cracks, delaminations or lifting of the grips.

ZnI_2 was applied to the edges and to the damaged areas and allowed to dwell for 30 minutes. The specimen was radiographed (stereo) and showed extensive cracking from the edges. Change in the damage area showed cracks extending up to level - 7 (0.084 in.) from the bottom. There was (1) large crack (0°) at level - 6 (0.060 in.) from the bottom. All cracks in the damaged area showed growth in length. (Figure 100)

c. Fatigue Sequence - No. 2

Cycles	KSI stress	Total
45	54.4	50

After cycling, visual inspection showed no change from the Sequence 1 condition.

The specimen was bagged with ZnI_2, sealed under vacuum and allowed to dwell for two days.

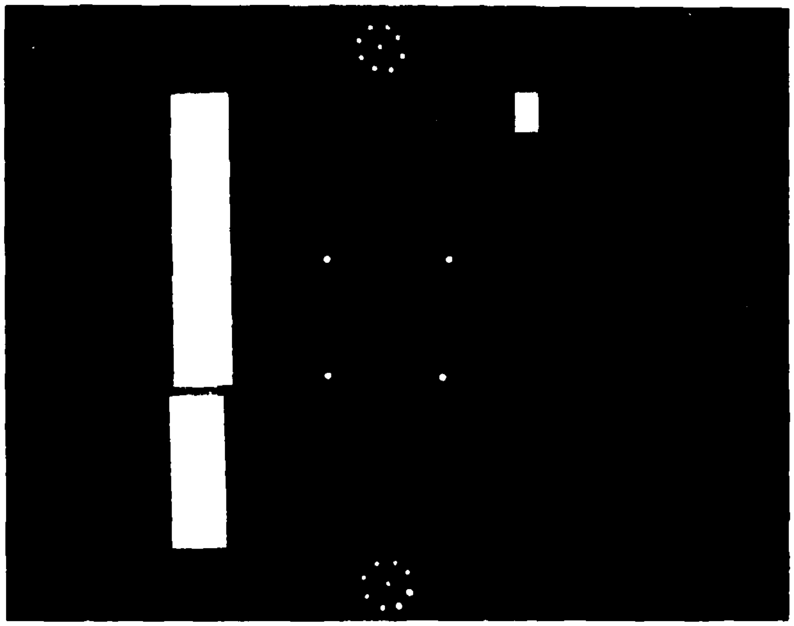

FIGURE 98 X-RADIOGRAPH OF SPECIMEN 16B-3 IN THE INITIAL CONDITION (ZnI_2 ENHANCED)

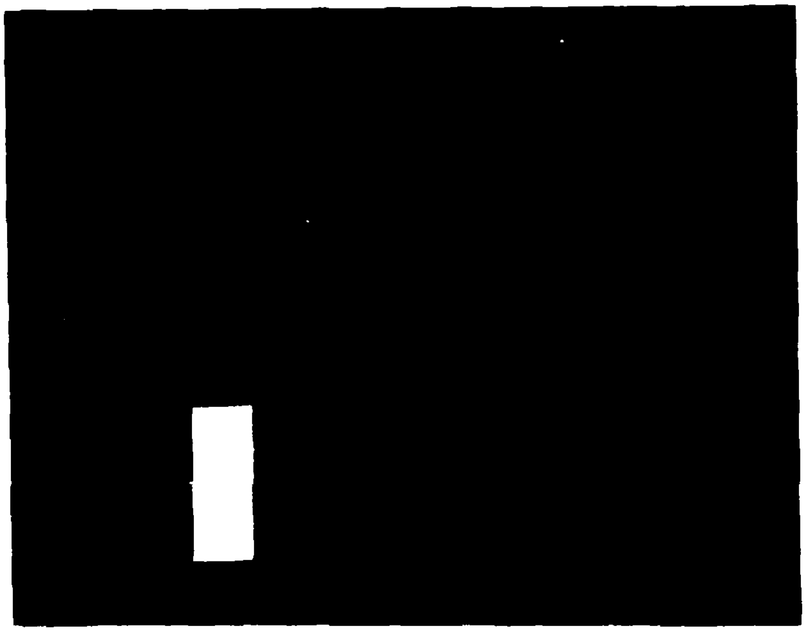

FIGURE 99 SPECIMEN 16B-3 AFTER ZnI_2 WAS APPLIED TO THE EDGES

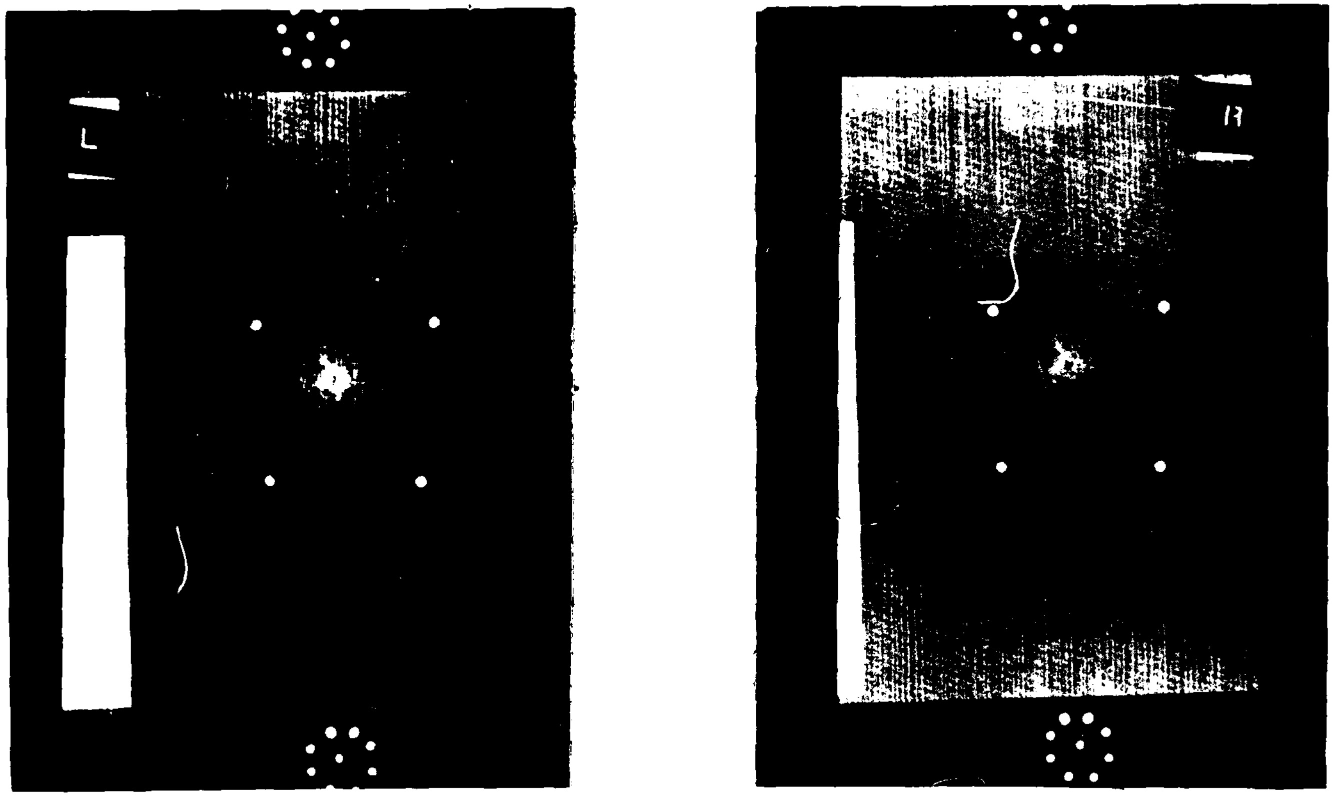

FIGURE 100 SPECIMEN 16B-3 AFTER FATIGUE SEQUENCE 1
(ZnI_2 ENHANCED)

After two days dwell, the specimen was radiographed (stereo) and showed extensive crack growth. The cracks through the impact damaged area now extended to the edges of the specimen. The cracks were at all levels. The impact damage area, cracks and delaminations, now extended up to level - 7 (0.084 in.) from bottom. (Figure 101).

d. Fatigue Sequence - No. 3

Cycles	KSI stress	Total
450	54.4	500

After cycling, visual inspection showed no change from Sequence 1.

ZnI_2 was applied to the damaged areas and allowed to dwell for 30 minutes. The specimen was radiographed (stereo) and showed no change from the Sequence 2 radiographs (Figure 102).

e. Fatigue Sequence - No. 4

Cycles	KSI stress	Total
500	54.4	1000

After Sequence 4, visual inspection showed no change from Sequence 1.

ZnI_2 was applied to the damaged areas and allowed to dwell for 30 minutes. The specimen was radiographed and showed no change from the Sequence 3 radiographic inspection. (Figure 103)

f. Fatigue Sequence - No. 5

Cycles	KSI stress	Total
2000	54.4	3000

After cycling, radiography (stereo) was performed in the Fatigue Testing machine with the specimen under 1000 pound static load. ZnI_2 was applied before the inspection and allowed to dwell for 1.0 hour. This inspection showed no change from the inspection performed in Sequence 4. (Figure 104)

Visual inspection after Sequence 5 showed lifting of the grip and cracks under the grip at the specimen identification end. There was also a lifting of the grip doubler at the end opposite and on the opposite side. There were also cracks and delaminations between the grips.

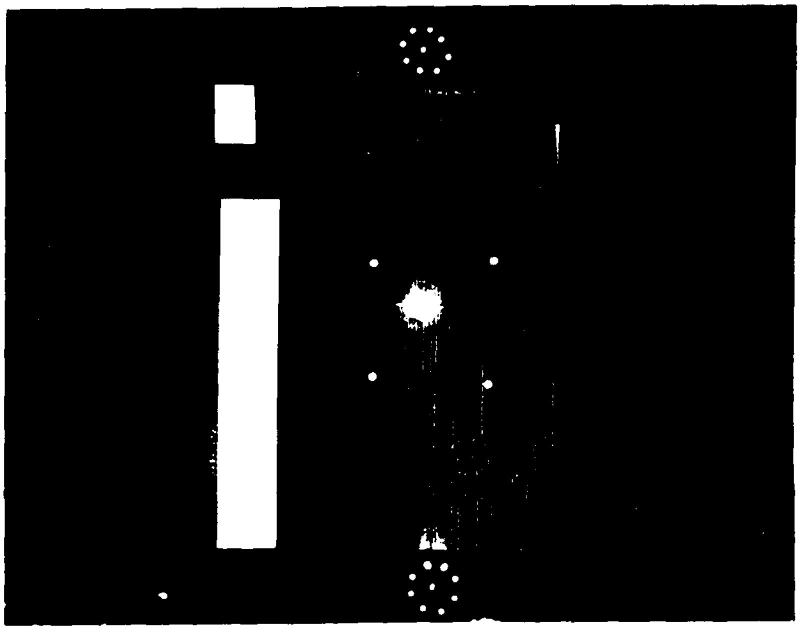

FIGURE 101 SPECIMEN 16B-3 AFTER FATIGUE SEQUENCE 2 (ZnI_2 ENHANCED)

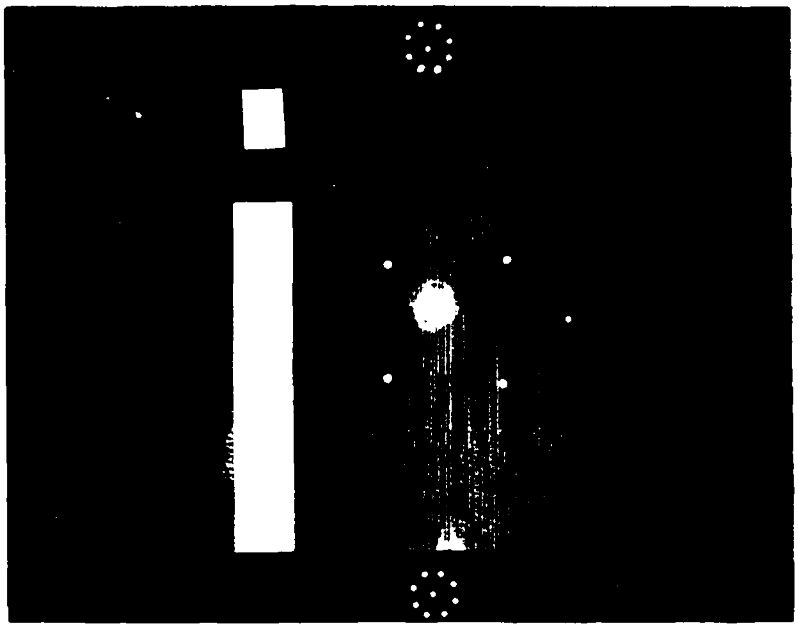

FIGURE 102 SPECIMEN 16B-3 AFTER FATIGUE SEQUENCE 3 (ZnI_2 ENHANCED)

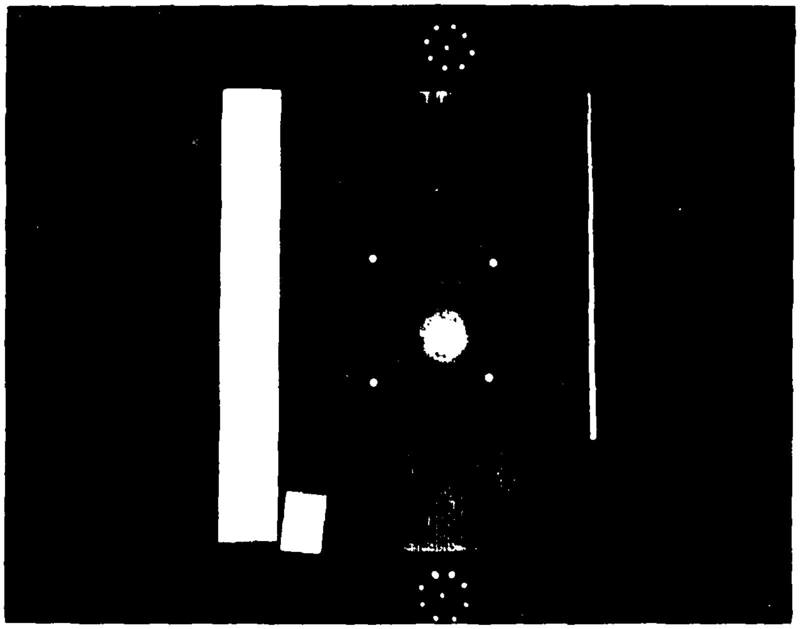

FIGURE 103 SPECIMEN 16B-3 AFTER FATIGUE SEQUENCE 4 (ZnI_2 ENHANCED)

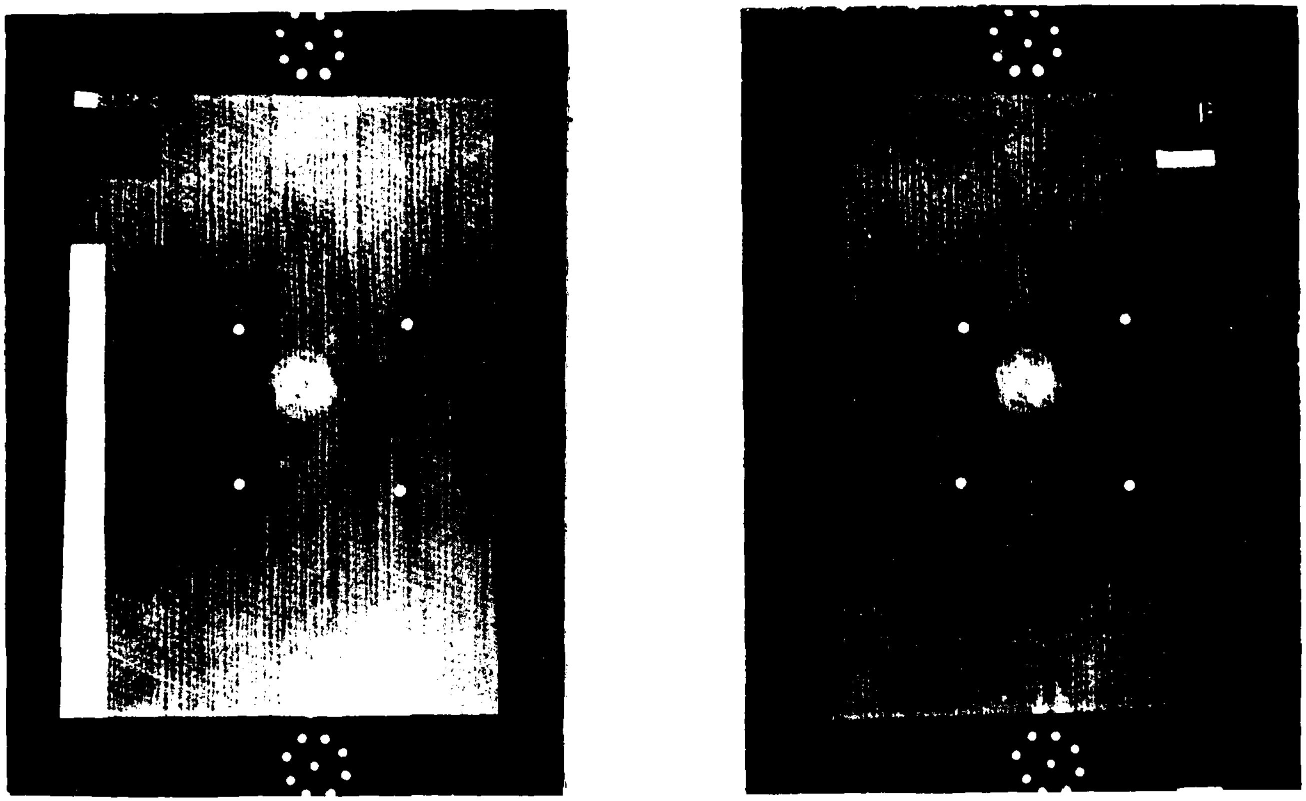

FIGURE 104 SPECIMEN 16B-3 AFTER FATIGUE SEQUENCE 5 (ZnI_2 ENHANCED)

g. Fatigue Sequence - No. 6

The specimen failed during fatigue test after an additional 820 cycles. The specimen received a total of 3,820 cycles. Visual inspection after failure showed the failure at the grip doubler on the identification end. The composite was starting to pull loose from under the grip. There was no evidence of failure in the impact damage area.

Figure 105 shows the location of failure for this specimen.

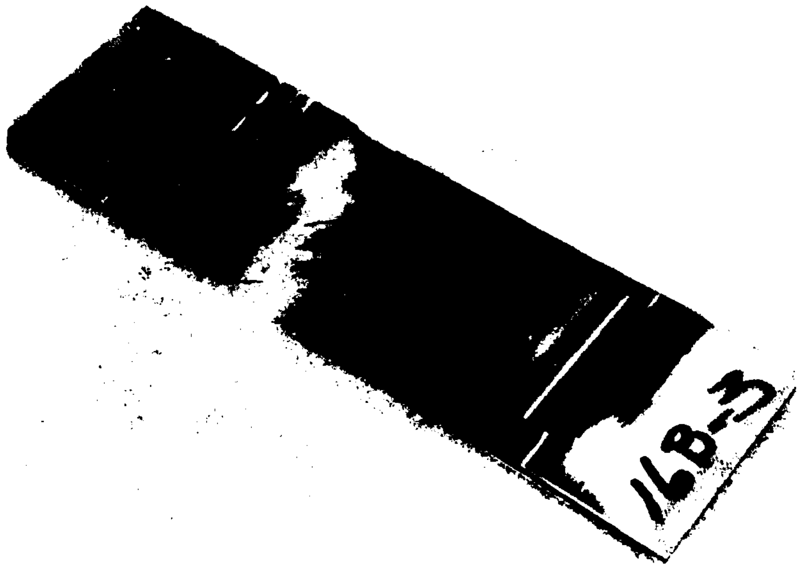

FIGURE 105 SPECIMEN 16B-3 AFTER FATIGUE FAILURE

7. <u>Fatigue Test of Specimen 16B-5</u>

a. <u>Initial Conditions</u>

Radiography after impact damage, with no penetrant, showed no evidence of cracks or delaminations.

ZnI_2 was applied to the damaged areas and allowed to dwell for 30 minutes. The specimen was radiographed (stereo) and showed cracks (0°, $+45^\circ$, 90°) and a delamination at level 1. (Figure 106)

<u>Fatigue Test</u>

The specimen was fatigued at 80% average tensile failure load. (80% of 77.7 = 62.0 KSI)
(Area = 0.350) (62.0 KSI) = 21,748 lbs maximum load

b. <u>Fatigue Sequence - No. 1</u>

The specimen failed during the 1st sequence of fatigue testing, after 990 cycles. The failure was at the grip doubler at opposite end from the specimen identification. There was no radiographic inspection performed after failure.

Figure 107 shows the location of failure for this specimen.

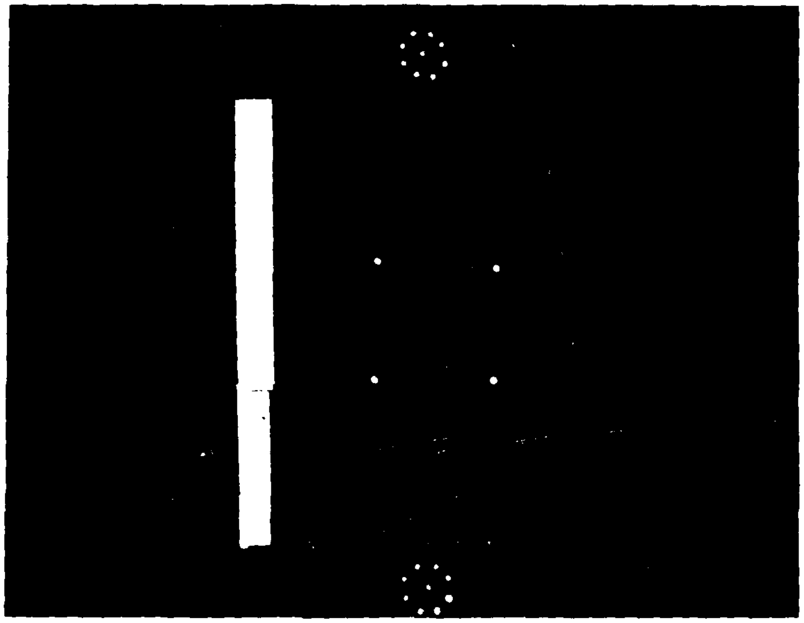

FIGURE 106 X-RADIOGRAPH OF SPECIMEN 16B-5 IN THE INITIAL CONDITION (ZnI_2 ENHANCED)

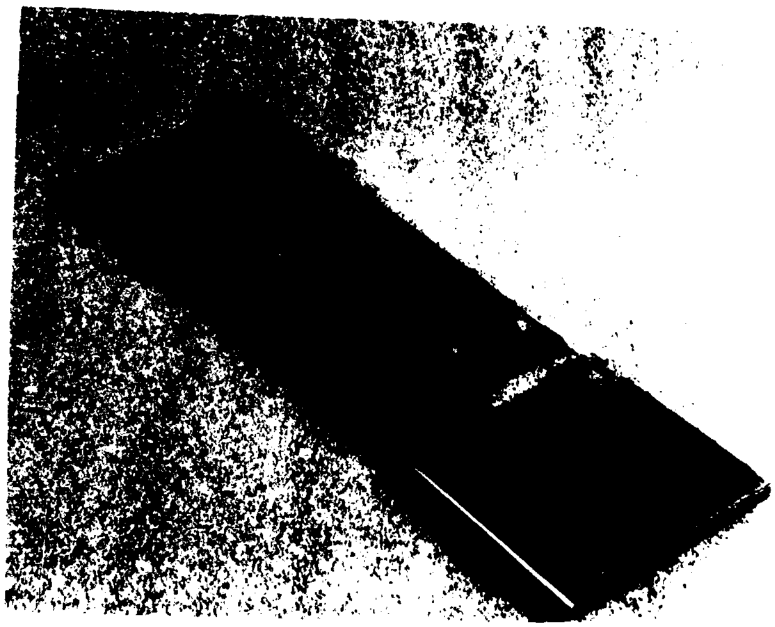

FIGURE 107 SPECIMEN 16B-5 AFTER FATIGUE FAILURE

8. Fatigue Test of Specimen 16B-6

a. Initial Conditions

Radiography after impact damage, with no penetrant, showed no evidence of cracks or delaminations.

ZnI_2 was applied to the impact areas and allowed to dwell for 30 minutes. The specimen was radiograph (stereo) and showed cracks (0°, $+45^\circ$, 90°) and delaminations at Levels 1 and 2. (Figure 108)

Fatigue Test

The specimen was fatigued at 80% average tensile failure load (80% of 77.7 = 62.0 KSI) (Area = 0.355) (62.0 KSI) = 22,059 lbs maximum load

b. Fatigue Sequence - No. 1

Cycles	KSI stress	Total
10,000	62.0	10,000

After cycling, visual inspection showed the grips lifted at both ends. There were delaminations on both edges propagating under the grips at both ends.

ZnI_2 was applied to the damaged areas and allowed to dwell for 30 minutes. The specimen was radiographed (stereo) and showed delaminations propagating to levels 5 and 6. There were numerous cracks in (0°) direction. (Figure 109).

ZnI_2 was applied to the edges of the specimen, and allowed to dwell for 2.0 hours. The panel was radiographed (stereo) and showed extensive cracking through-out the area between the grips at all levels. (Figure 110)

ZnI_2 was applied to the edges and allowed to dwell for 4.0 hours. The specimen was radiographed (stereo) and showed the cracks being considerably longer than was apparent after a 2.0 hour penetrant dwell. (Figure 111)

c. Fatigue Sequence - No. 2

The specimen failed during fatigue test after receiving an additional 4,350 cycles.

Visual inspection after failure, showed that failure occured at the grip doubler on the specimen identification end. There was no failure associated at the impact damage areas. The composite pulled from under the grip. There was a considerable amount of delamination and cracking along both edges in the

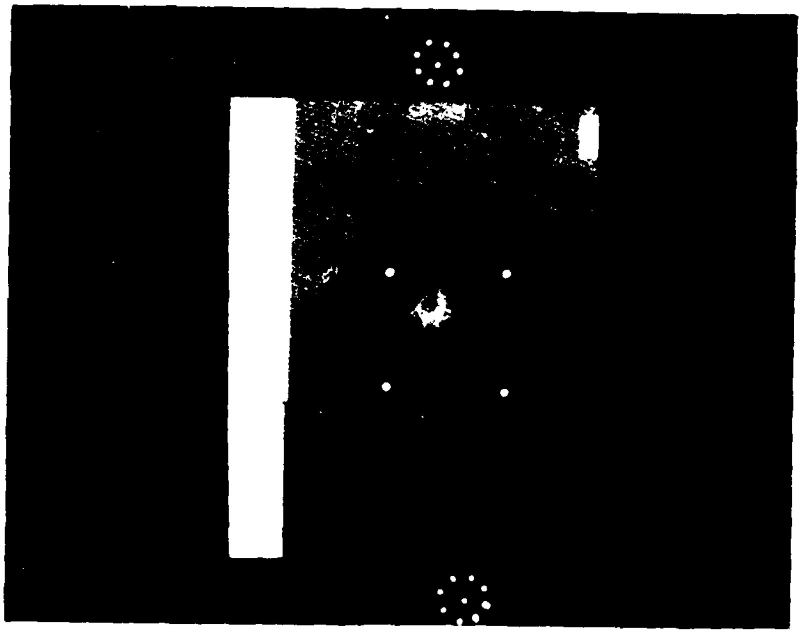

FIGURE 108 X-RADIOGRAPH OF SPECIMEN 16B-6 IN THE INITIAL CONDITION (ZnI_2 ENHANCED)

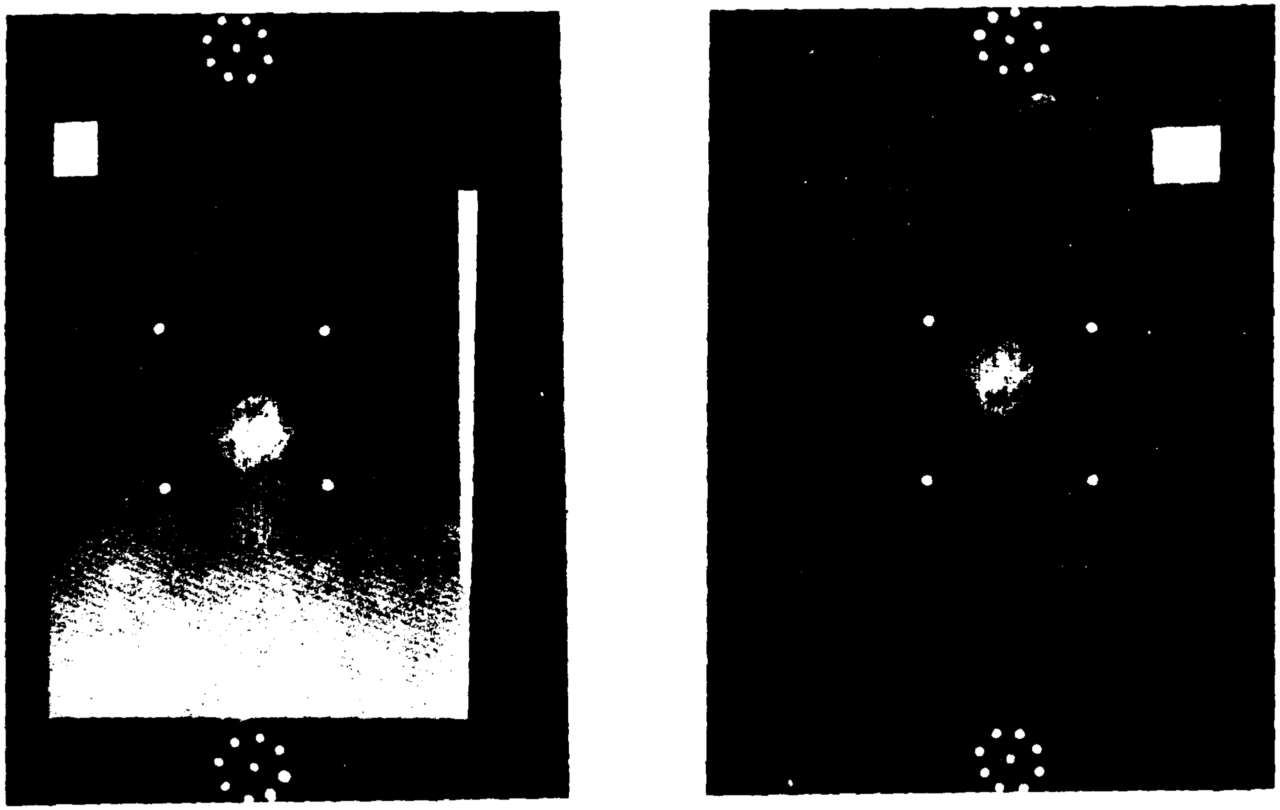

FIGURE 109 SPECIMEN 16B-6 AFTER FATIGUE SEQUENCE 1 (ZnI_2 ENHANCED)

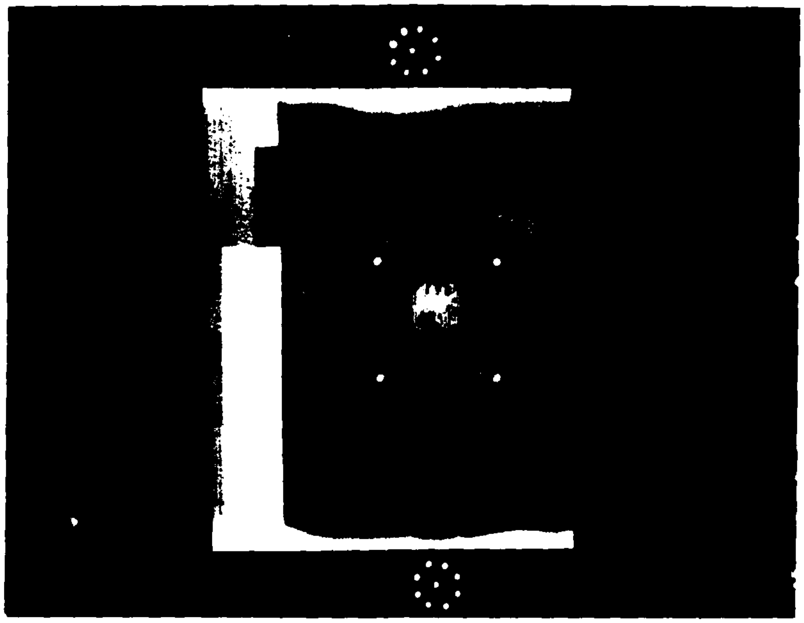

FIGURE 110 SPECIMEN 16B-6 AFTER FATIGUE SEQUENCE 1 WITH ZnI_2 APPLIED TO THE PANEL EDGES

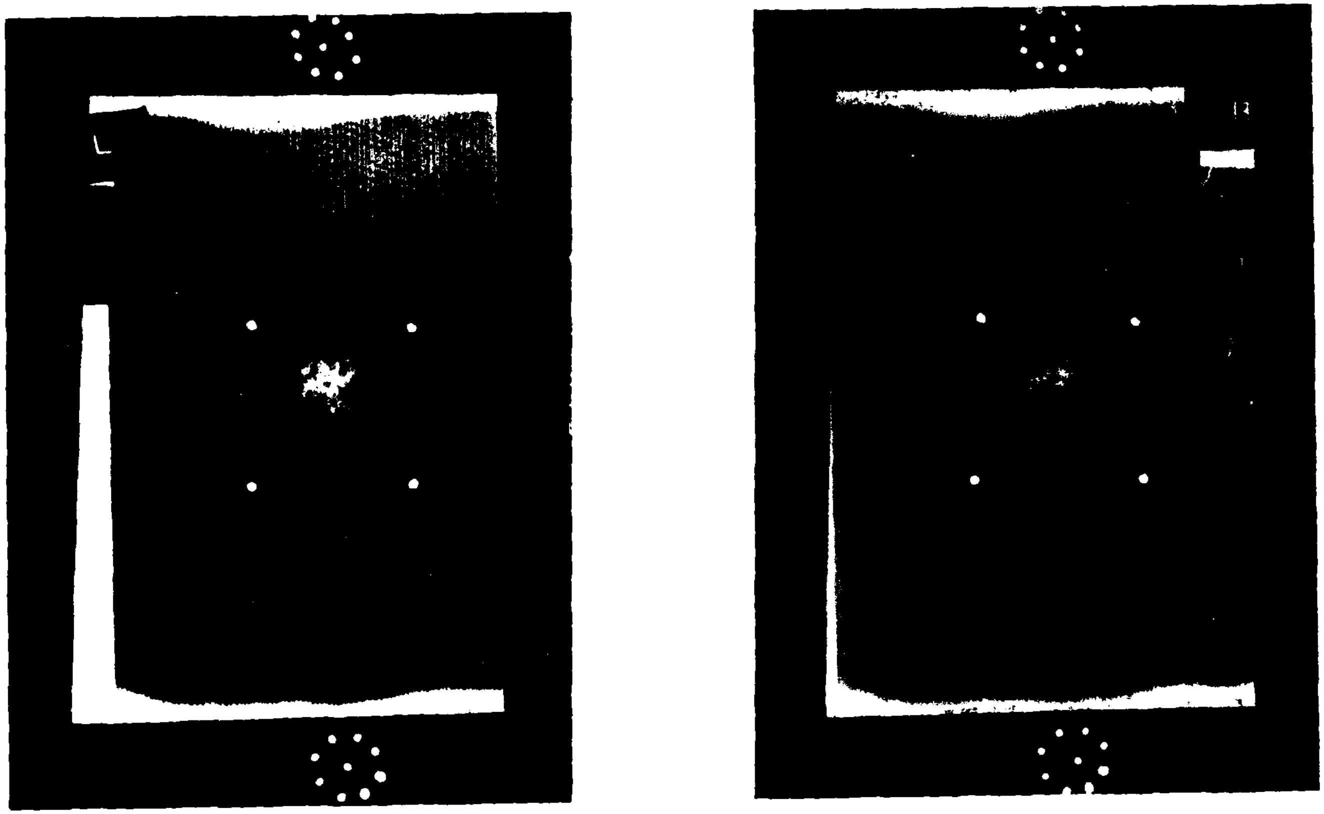

FIGURE 111 SPECIMEN 16B-6 AFTER SEQUENCE 1, ADDED DWELL TIME

area between the grips and under the grips. There was no radiographic inspection after failure.

Figure 112 shows the location of failure for this specimen.

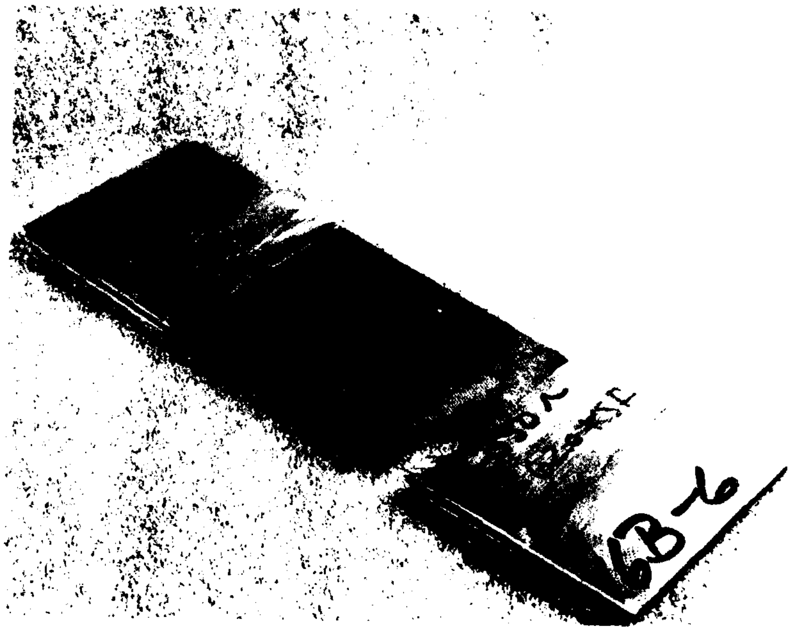

FIGURE 112 SPECIMEN 16B-6 AFTER FATIGUE FAILURE

9. Fatigue Test of Specimen 16B-8

a. Initial Conditions

Radiography after impact damage, with no penetrant, showed voids 0° $\pm 45^{\circ}$, 90°. There was no evidence of cracks or delaminations.

ZnI_2 was applied to the damaged areas and allowed to dwell for 30 minutes. The specimen was radiographed (stereo) and showed cracks at 0°, $\pm 45^{\circ}$, 90° and small delamination between level 0 and level 1. (Figure 113)

Fatigue Test

The specimen was fatigued at 70% average tensile failure load (70% of 77.7 = 54.4 KSI)
(Area = 0.366) (54.4 KSI) = 19,764 lbs maximum load

b. Fatigue Sequence - No. 1

This specimen failed after receiving 570 cycles. The failure was at the grip and opposite from the specimen identification. There was no evidence of failure through the impact damage area. Radiographic inspection was not performed after failure.

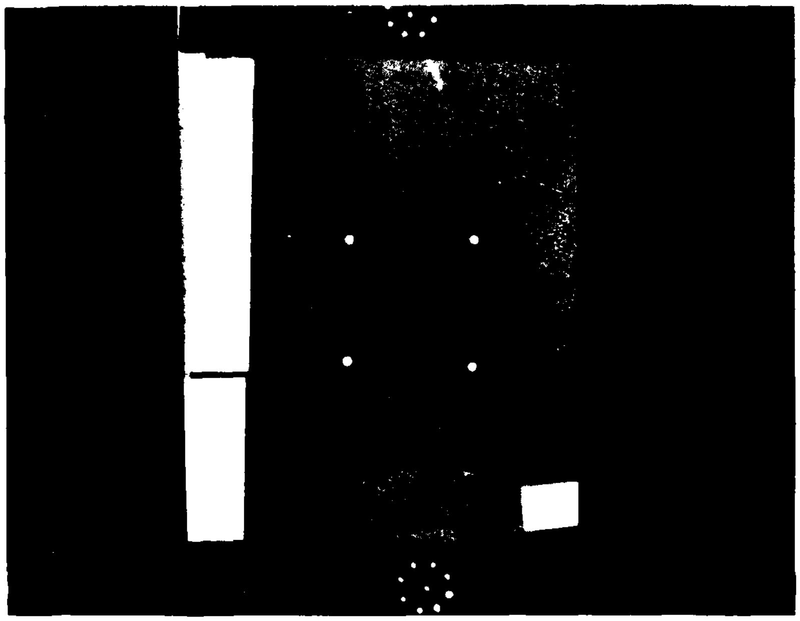

FIGURE 113 X-RADIOGRAPH OF SPECIMEN 16B-8 IN THE INITIAL CONDITION (ZnI_2 ENHANCED)

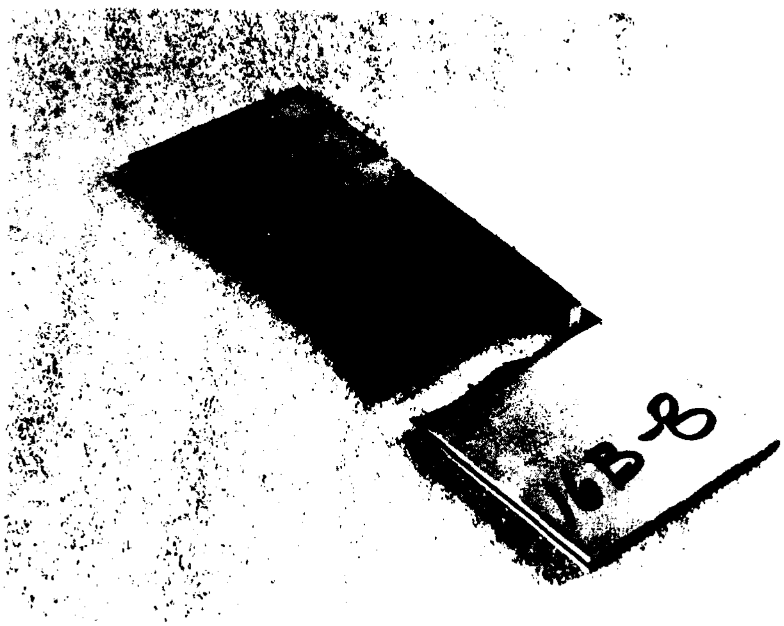

FIGURE 114 SPECIMEN 16B-8 AFTER FATIGUE FAILURE

10. Fatigue Test of Specimen 16B-9

a. Initial Conditions

Radiography after impact damage, showed voids (0°, $+45^\circ$, 90°). There was no evidence of cracks or delaminations.

ZnI_2 was applied to the impact damage areas and allowed to dwell for 30 minutes. The specimen was radiographed (stereo) and showed cracks (0°, $+45^\circ$, 90°) and delamination at Level 1 (Figure 115)

ZnI_2 was then applied to the edges of the specimen and allowed to dwell for 30 minutes. Radiographic inspection showed no cracks at the edges. (Figure 116)

Fatigue Test

The specimen was fatigued at 70% average tensile load (70% of 77.7 = 54.4 KSI)
(Area = 0.370) (54.4 KSI) = 20,135 lbs maximum load

b. Fatigue Sequence - No. 1

Cycles	KSI stress	Total
5	54.4	5

After cycling, visual inspection showed no evidence of cracks, delaminations or lifting of the grips.

ZnI_2 was applied to the edges and to the damaged areas and allowed to dwell for 30 minutes. The specimen was radiographed (stereo) and showed extensive cracking from the edges. There was no change in the impact damage area. (Figure 117)

c. Fatigue Sequence - No. 2

Cycles	KSI stress	Total
45	54.4	50

After cycling, visual inspection showed that some of the composite had fallen out from under the grip doubler at the opposite end from the specimen identification. No other changes were noted.

The specimen was bagged with ZnI_2, sealed under vacuum and allowed to dwell for two days. After two days the specimen was radiographed (stereo) and showed the cracks through the impact damage area propagating to the edges. The cracks were at all levels. The impact damaged area of cracks and delamination extended to level 7 (Figure 118)

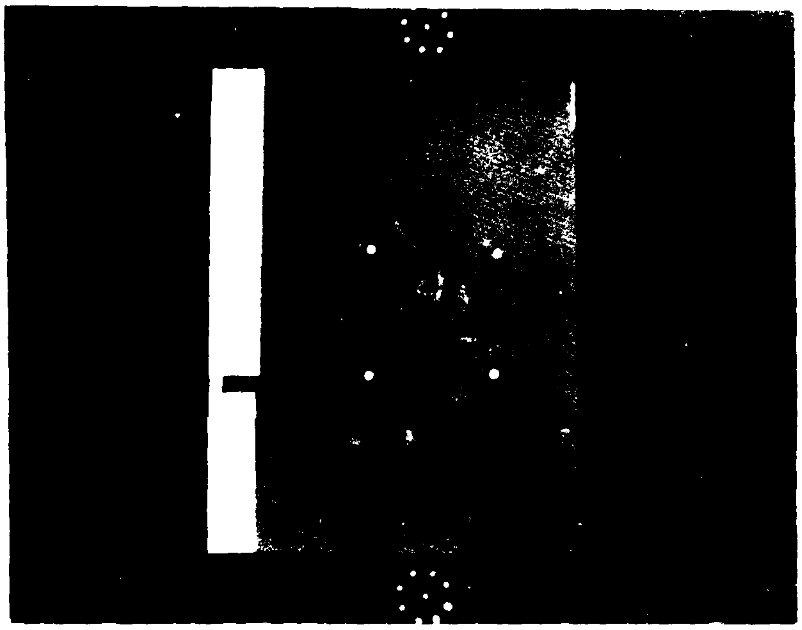

FIGURE 115 X-RADIOGRAPH OF SPECIMEN 16B-9 IN THE INITIAL CONDITION (ZnI_2 ENHANCED)

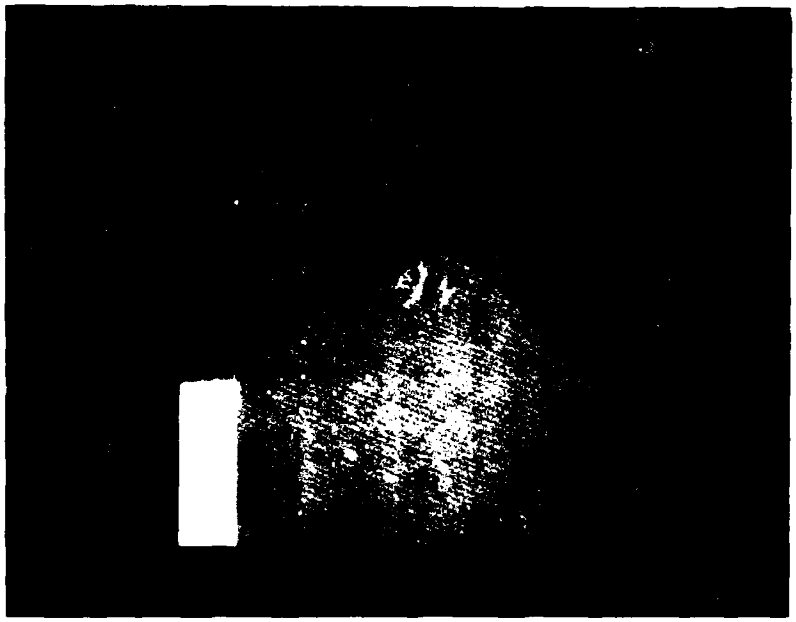

FIGURE 116 SPECIMEN 16B-9 WITH ZnI_2 APPLIED TO THE EDGES (INITIAL CONDITION)

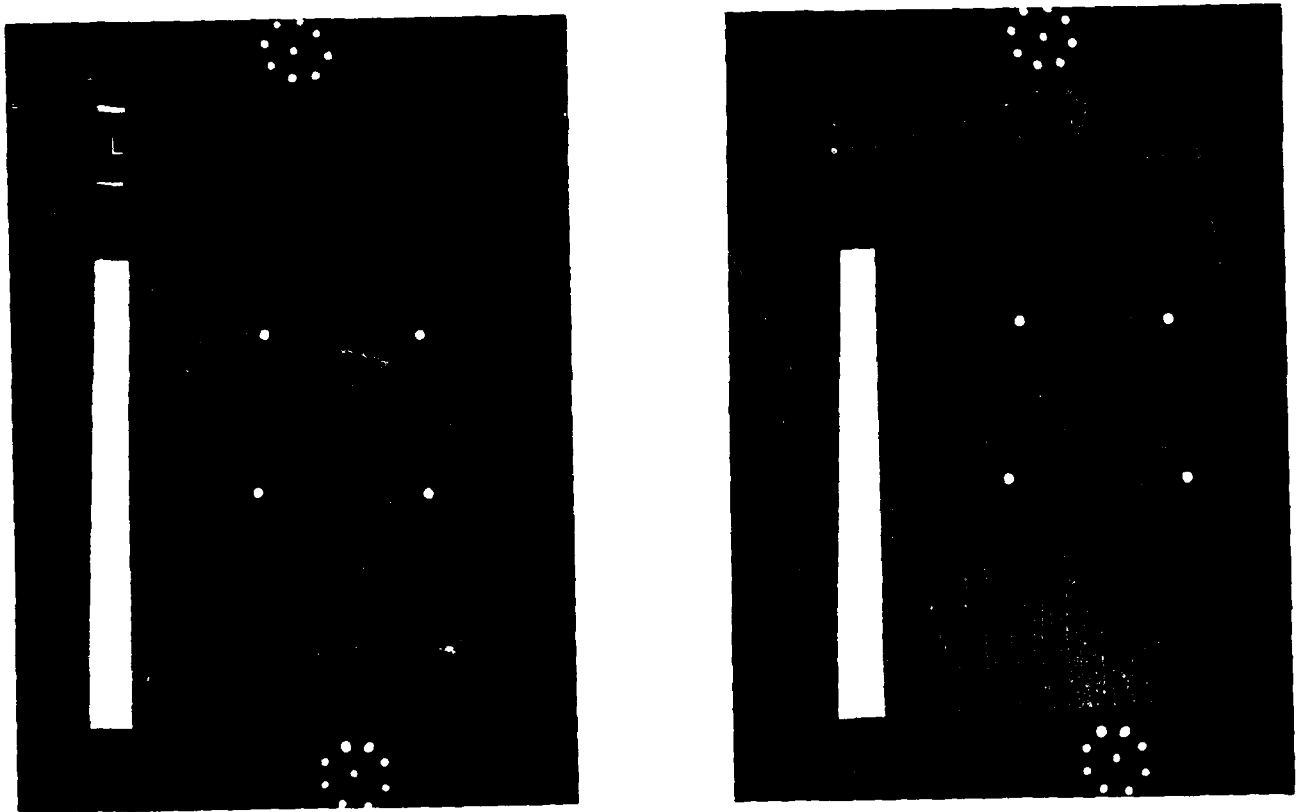

FIGURE 117 SPECIMEN 16B-9 AFTER FATIGUE SEQUENCE 1
(ZnI_2 ENHANCED)

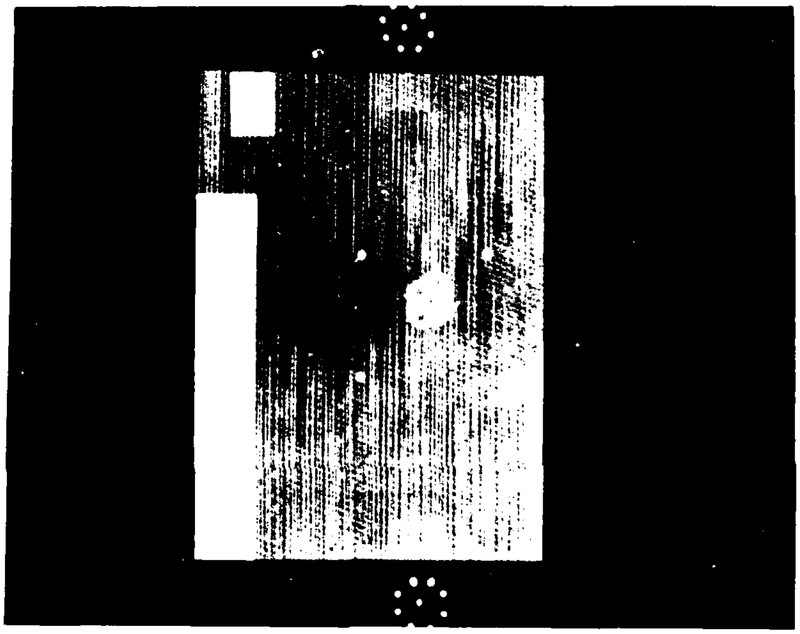

FIGURE 118 SPECIMEN 16B-9 AFTER FATIGUE SEQUENCE 2 (ZnI_2 ENHANCED)

d. <u>Fatigue Sequence - No. 3</u>

Cycles	KSI stress	Total
450	54.4	500

After cycling, visual inspection showed no change from Sequence 2.

ZnI_2 was applied to the damaged areas and allowed to dwell for 30 minutes. Radiographic (stereo) inspection showed no change from Sequence 2. (Figure 119)

e. <u>Fatigue Sequence - No. 4</u>

Cycles	KSI stress	Total
500	54.4	1000

After cycling, visual inspection showed no change from Sequence 2.

ZnI_2 was applied to the damaged areas and allowed to dwell for 30 minutes. Radiographic (stereo), inspection showed no change from Sequence 3. (Figure 120)

f. <u>Fatigue Sequence - No. 5</u>

The specimen failed during fatigue test after receiving an additional 1,227 cycles.
The specimen received a total of 2,227 cycles.
Visual inspection showed the failure to be at the edge of taper of the grip on opposite end from identification. There was no failure associated with the impact damage area.

Figure 121 shows the location of failure for this specimen.

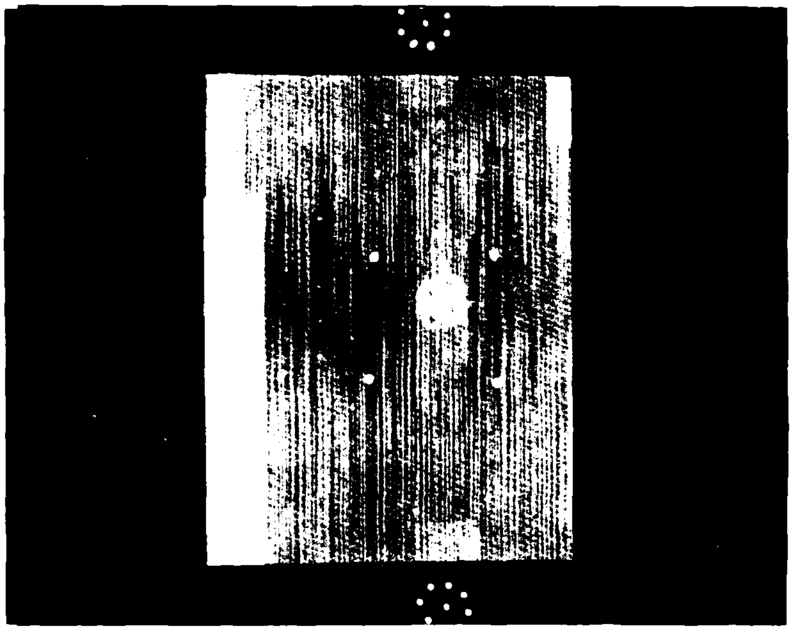

FIGURE 119 SPECIMEN 16B-9 AFTER FATIGUE SEQUENCE 3 (ZnI_2 ENHANCED)

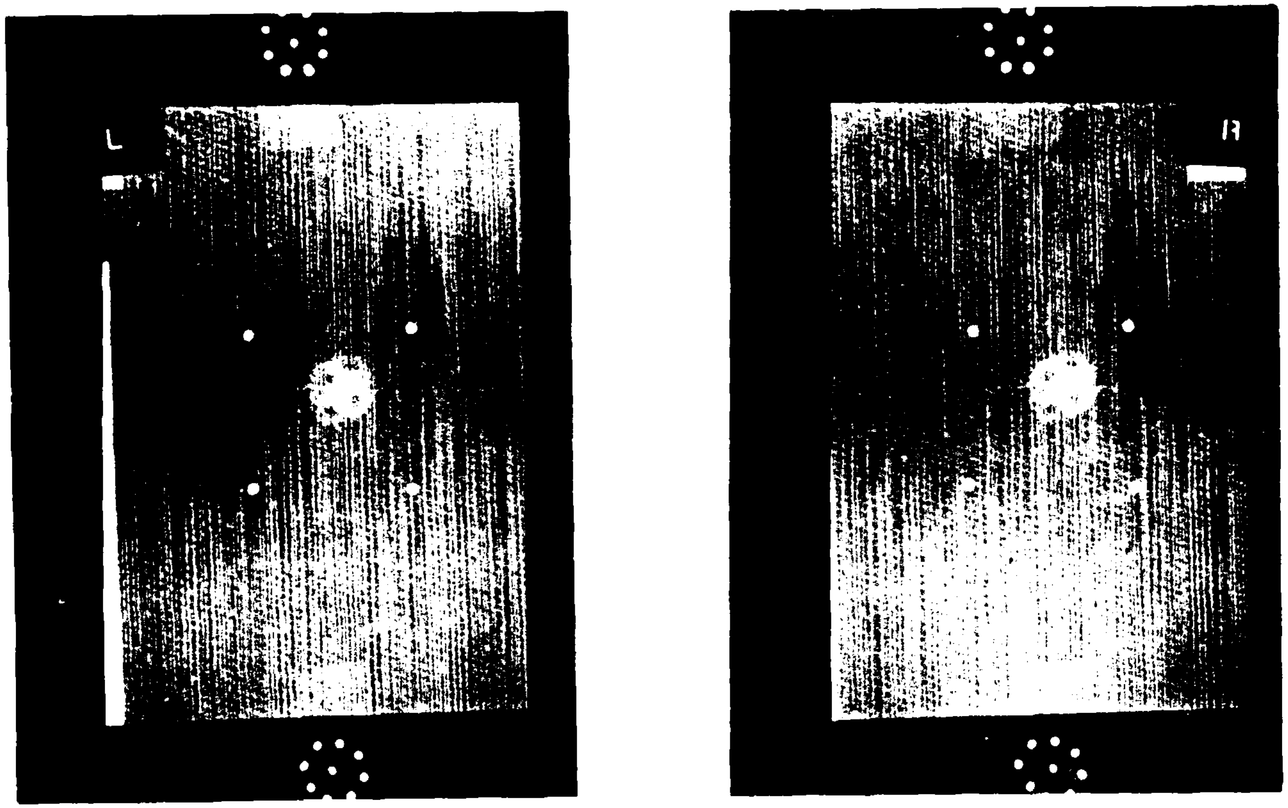

FIGURE 120 SPECIMEN 16B-9 AFTER FATIGUE SEQUENCE 4
(ZnI_2 ENHANCED)

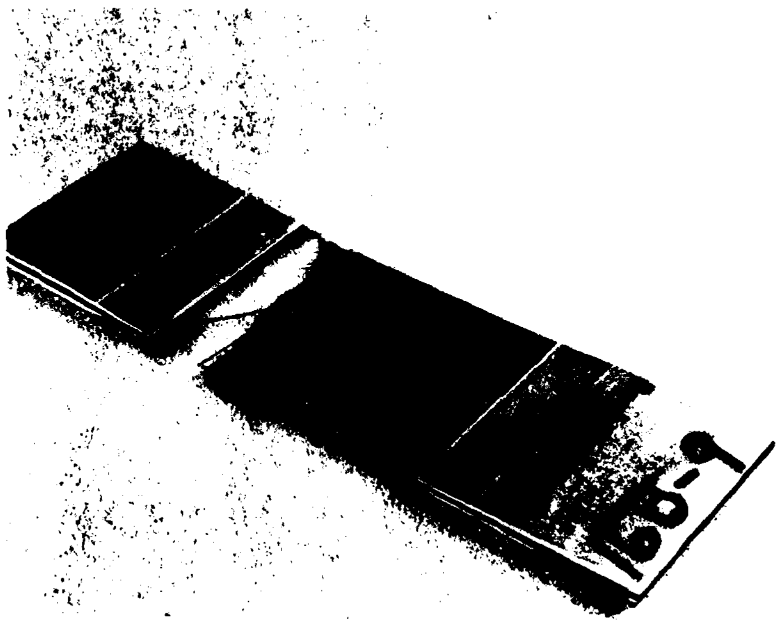

FIGURE 121 SPECIMEN 16B-9 AFTER FATIGUE FAILURE

11. Fatigue Test of Specimen 16B-10

a. Initial Conditions

Radiography after impact damage, with no penetrant, showed no evidence of cracks or delaminations.

ZnI_2 was applied to the damaged areas and allowed to dwell for 30 minutes. Radiographic (stereo) inspection showed cracks 0^o, $\pm 45^o$, 90^o and a delamination at Level 1. (Figure 122)

Fatigue Test

The specimen was fatigued at 60% average tensile failure load (60% of 77.7 = 46.6 KSI)
(Area = 0.350) (46.6 KSI) = 16,310 lbs maximum load

b. Fatigue Sequence - No. 1

Cycles	KSI stress	Total
2000	46.6	2000

After cycling, visual inspection showed no evidence of cracks, delaminations or lifting of the grips.

ZnI_2 was applied to the impact damaged areas and allowed to dwell for 30 minutes. The specimen was radiographed and showed no change from the radiograph taken before start of fatigue test. (Figure 123)

The specimen was bagged with ZnI_2, vacuum sealed, and allowed to dwell for 3 days. After 3 days the specimen was radiographed and showed extensive cracking from the edges at all levels. There was no change in the impact damage area. (Figure 124)

c. Fatigue Sequence - No. 2

Cycles	KSI stress	Total
2000	46.6	4000

After cycling, visual inspection showed no change from Sequence 1.

ZnI_2 was applied to the impact damaged areas and allowed to dwell for 30 minutes. Radiographic (stereo) inspection showed no change in the delamination. Some cracks were more pronounced due to more penetrant being trapped in them. There was no change in the cracks from the edges of the specimen. (Figure 125)

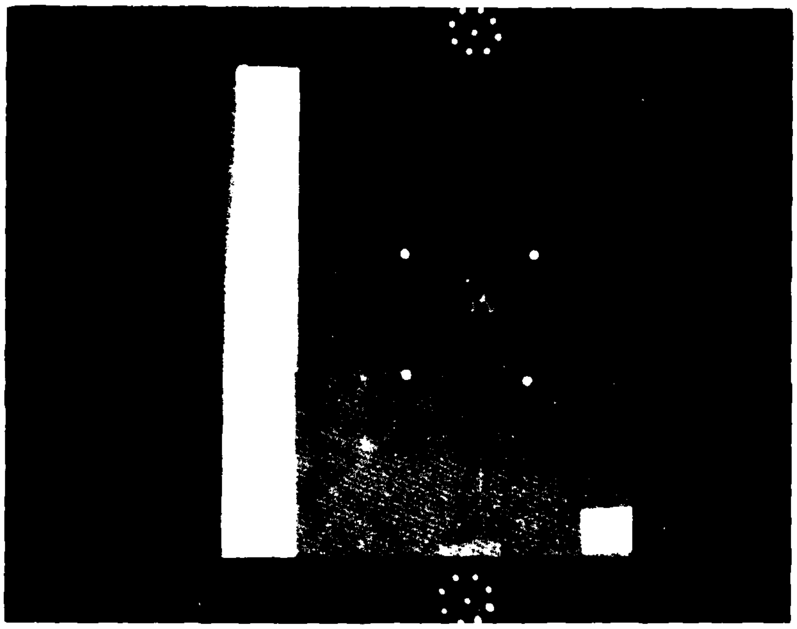

FIGURE 122 X-Radiograph of SPECIMEN 16B-10 IN THE INITIAL CONDITION (ZnI_2 ENHANCED

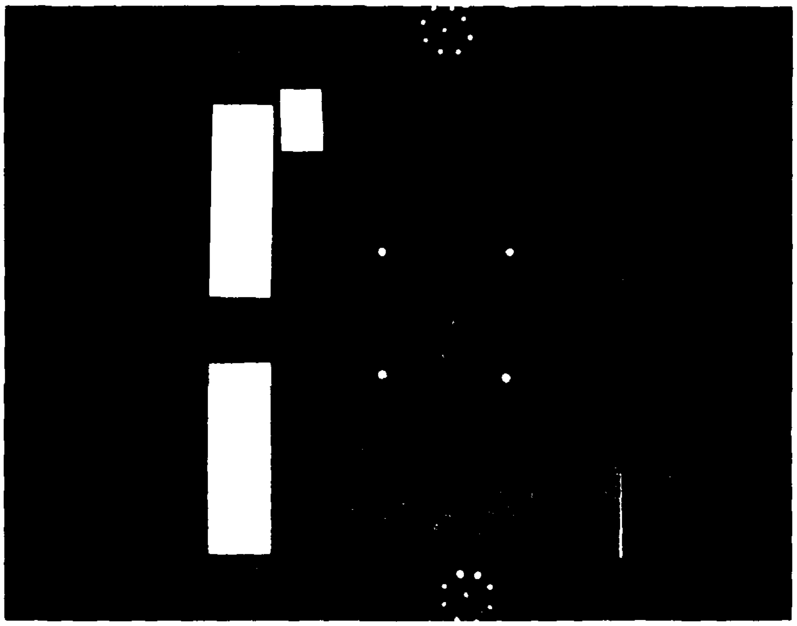

FIGURE 123 SPECIMEN 16B-10 AFTER FATIGUE SEQUENCE 4 (ZnI_2 ENHANCED

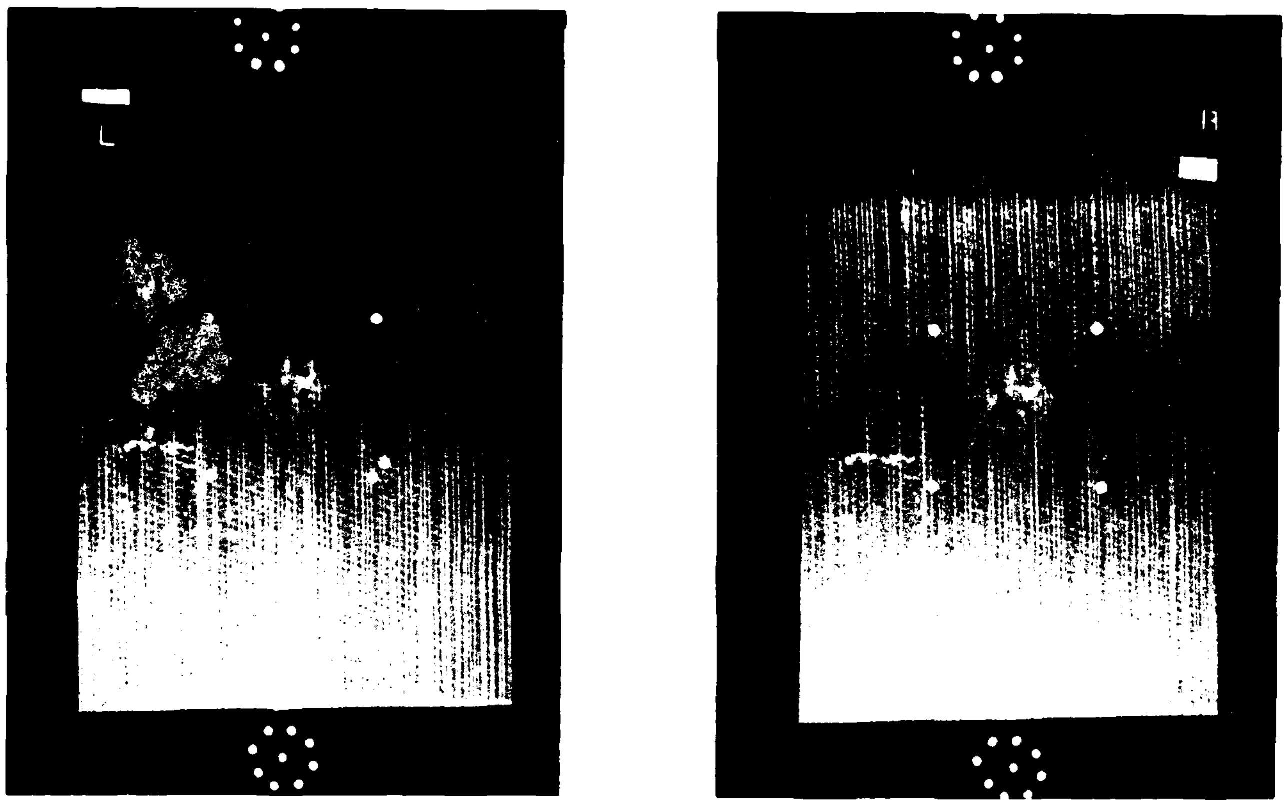

FIGURE 124 SPECIMEN 16B-10 AFTER FATIGUE SEQUENCE 1 AND 3 DAY DWELL TIME

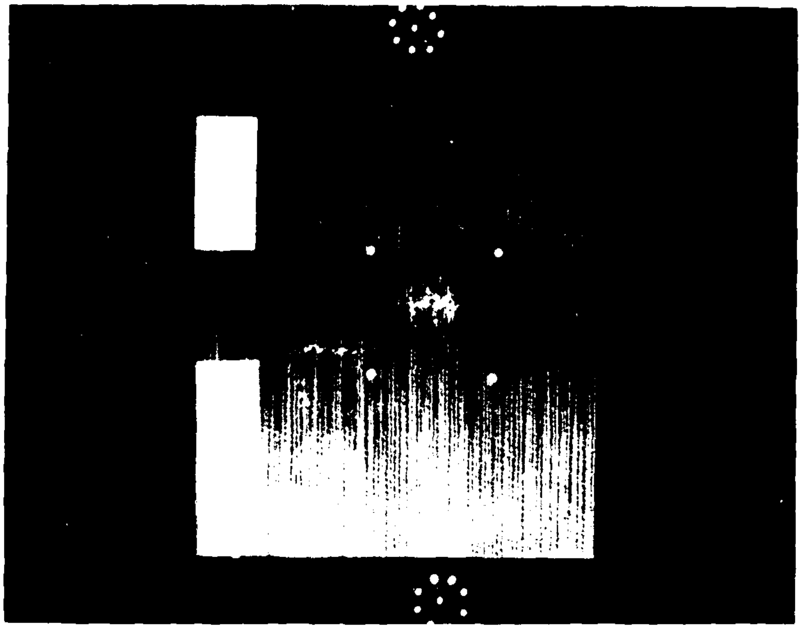

FIGURE 125 SPECIMEN 16B-10 AFTER FATIGUE SEQUENCE 2 (ZnI_2 ENHANCED)

d. Fatigue Sequence - No. 3

Cycles	KSI stress	Total
2000	46.6	6000

After cycling, visual inspection showed no change from Sequence 1.

ZnI_2 was applied to the damaged areas and allowed to dwell for 30 minutes. Radiographic (stereo) inspection showed no change from Sequence 2. (Figure 126)

e. Fatigue Sequence - No. 4

Cycles	KSI stress	Total
2000	46.6	8000

After cycling, visual inspection showed no change from Sequence 1.

ZnI_2 was applied to the damaged areas and allowed to dwell for 30 minutes. Radiographic (stereo) inspection showed no change from the Sequence 3. (Figure 127)

The specimen was bagged with ZnI_2, vacuum sealed, and allowed to dwell for 16 hours. After 16 hours, the panel was radiographed (stereo) and showed more cracks in the impact damage area. (Figure 128)

f. Fatigue Sequence - No. 5

Cycles	KSI stress	Total
2000	46.6	10,000

After visual inspection, it showed no change from Sequence 1.

ZnI_2 was applied to the damaged areas and allowed to dwell for 30 minutes. The panel was radiographed and showed no change from Sequence 4. (Figure 129)

g. Fatigue Sequence - No. 6

Cycles	KSI stress	Total
2000	46.6	12,000

Visual inspection after Sequence 6, showed cracks in the area between the grips on both sides. There was also a delamination under the grip doubler at the specimen identification end.

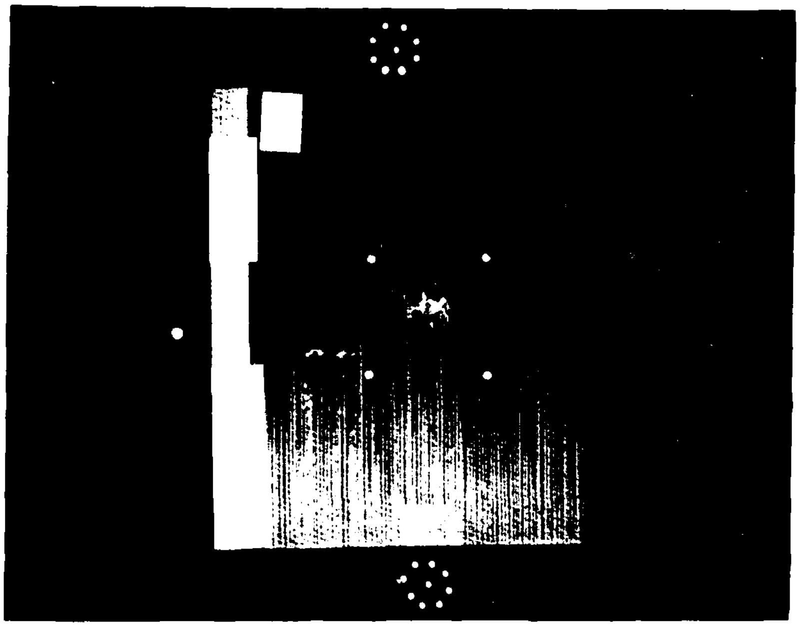

FIGURE 126 SPECIMEN 16B-10 AFTER FATIGUE SEQUENCE 3 (ZnI_2 ENHANCED)

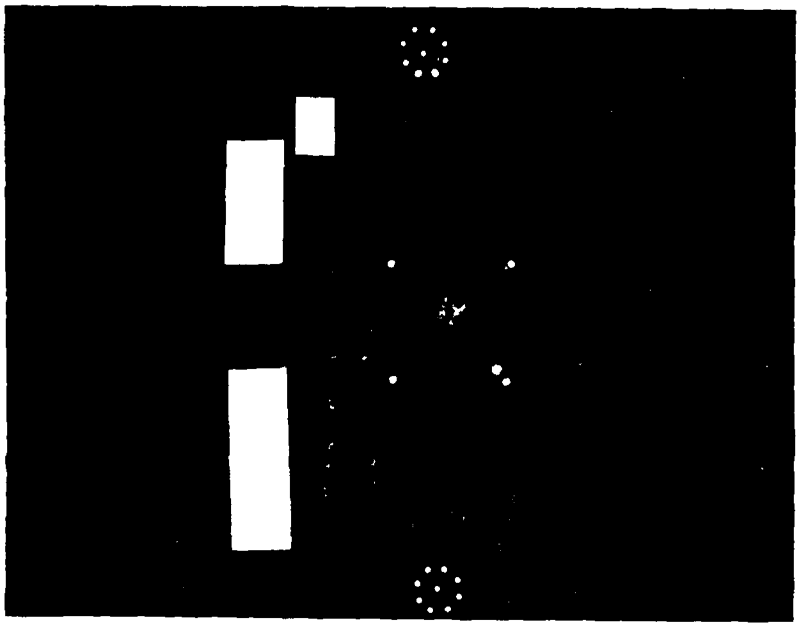

FIGURE 127 SPECIMEN 16B-10 AFTER FATIGUE SEQUENCE 4 (ZnI_2 ENHANCED)

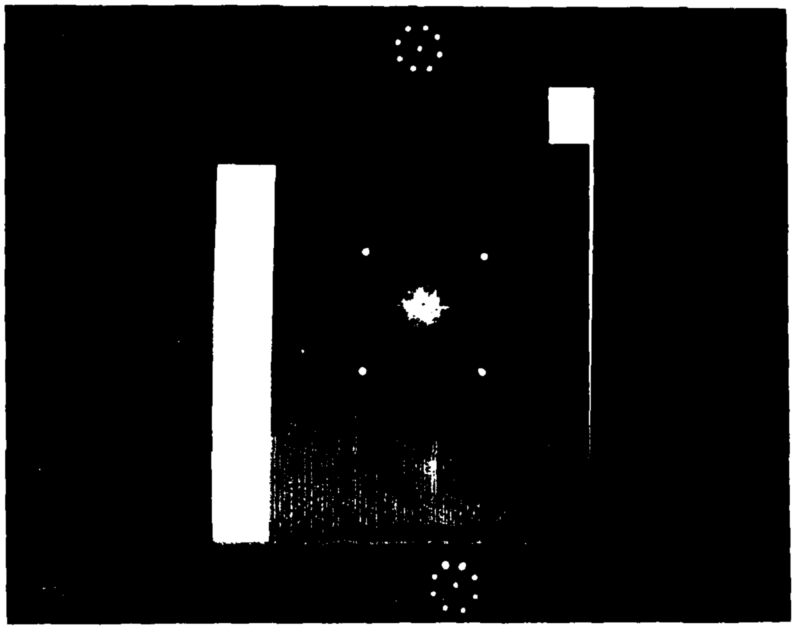

FIGURE 128 SPECIMEN 16B-10, 16 HOUR DWELL (SEQU[illegible]

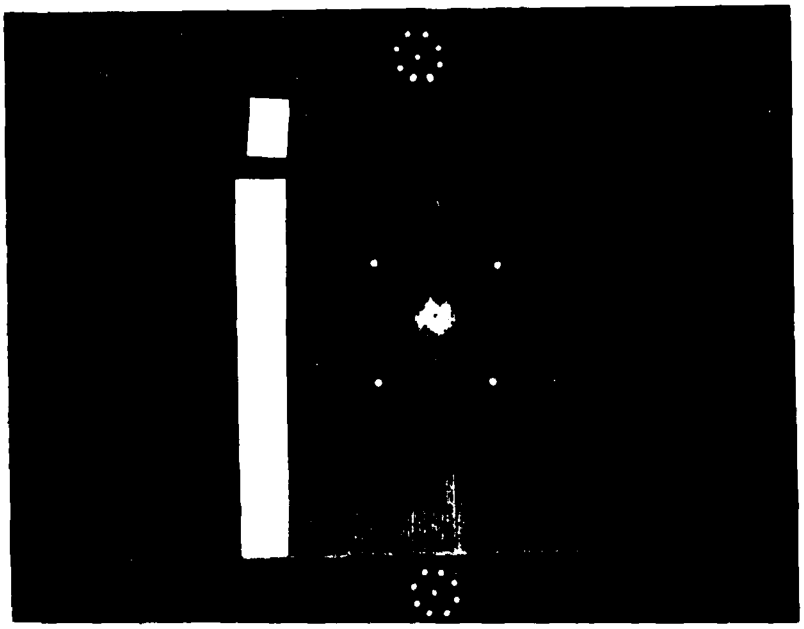

FIGURE 129 SPECIMEN 16B-10 AFTER FATIGUE SEQUENCE 5 (ZnI_2 ENHANCED)

The specimen was bagged with ZnI_2, vacuum sealed, and allowed to dwell for 16 hours. After 16 hours, the panel was radiographed (stereo) and showed no change from Sequence 5. (Figure 130)

h. Fatigue Sequence - No. 7

Cycles	KSI stress	Total
2000	46.6	14,000

After cycling, visual inspection showed that the grip doubler at panel identification end was delaminated on both sides.

ZnI_2 was applied to the damaged areas and allowed to dwell for 30 minutes. Radiographic inspection showed no change from Sequence 6. (Figure 131)

i. Fatigue Sequence - No. 8

The specimen was fatigued to failure. Failure occured after 198,500 total cycles. Visual inspection after failure showed the failure at the grip end opposite from the specimen identification. The composite pulled from under the grip. There was no failure associated with the impact damaged area. There were delamination and cracks on both edges between the grips and under the grips.

Figure 132 shows the location of failure for this specimen.

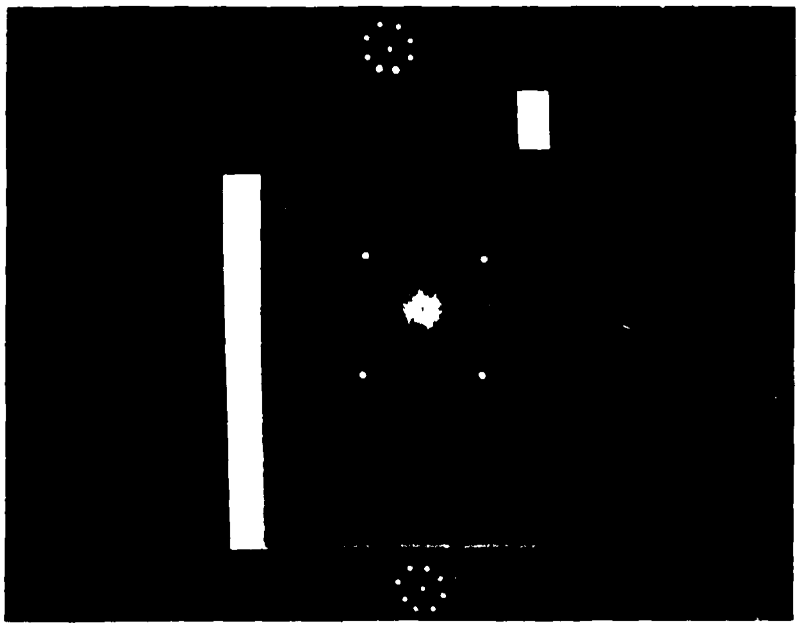

FIGURE 130 SPECIMEN 16B-10 WITH 16 HOUR DWELL TIME (ZnI_2) AFTER SEQUENCE 6

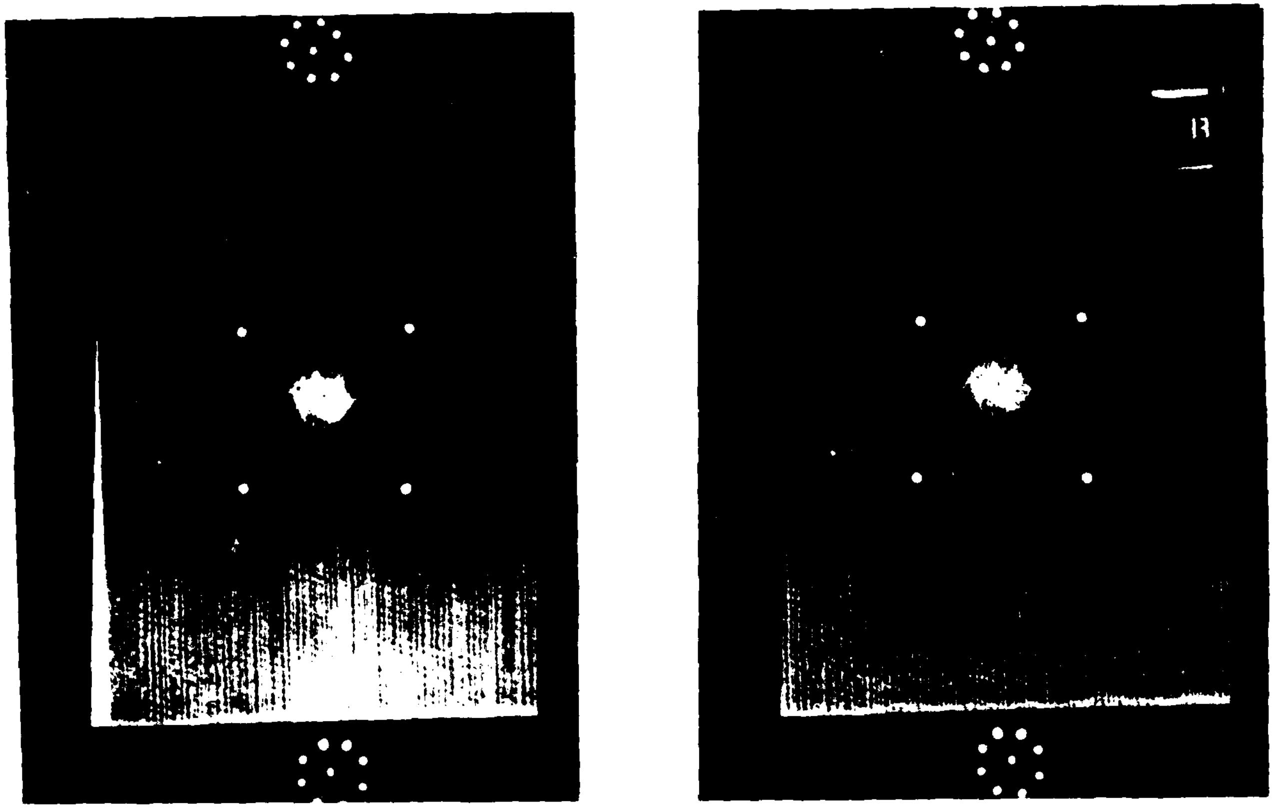

FIGURE 131 SPECIMEN 16B-10 AFTER FATIGUE SEQUENCE 7
(ZnI_2 ENHANCED)

FIGURE 132 SPECIMEN 16B-10 AFTER FATIGUE FAILURE

12. Fatigue Test of Specimen 16B-12

a. Initial Condition

Radiography after impact, with no penetrant, showed voids at 0°, $\pm 45^{\circ}$, 90°. There was no evidence of cracks or delaminations in the impact damage area.

ZnI_2 was applied to the damaged area and allowed to dwell for 30 minutes. Radiographic inspection showed cracks at 0°, $\pm 45^{\circ}$, 90° and a delamination at Level 1. Some of the voids, were in the damaged area. (Figure 133)

ZnI_2 was applied to the edges of the specimen and allowed to dwell for 30 minutes. Radiographic inspection showed no cracks. (Figure 134)

Fatigue Test

The specimen was fatigued at 80% average tensile failure load (80% of 77.7 = 62.2 KSI) (Area = 0.389) (62.2 KSI) = 24.180 lbs maximum load

b. Fatigue Sequence - No. 1

Cycles	KSI stress	Total
5	62.2	5

Frequence was 1 cycle per second.

After cycling, visual inspection showed no cracks or delaminations. There was evidence of grip separation from the composite at opposite end from the specimen identification and on the opposite side.

ZnI_2 was applied to the edges and to the damaged area and allowed to dwell for 30 minutes. Radiographic (stereo) inspection showed extensive cracking from the edges. There was crack growth in length in the damage area at same level as the delamination level 1. (Figure 135)

c. Fatigue Sequence - No. 2

Cycles	KSI stress	Total
45	62.2	50

Frequency was 10 cycles per second.

After cycling, visual inspection showed no change from Sequence 1.

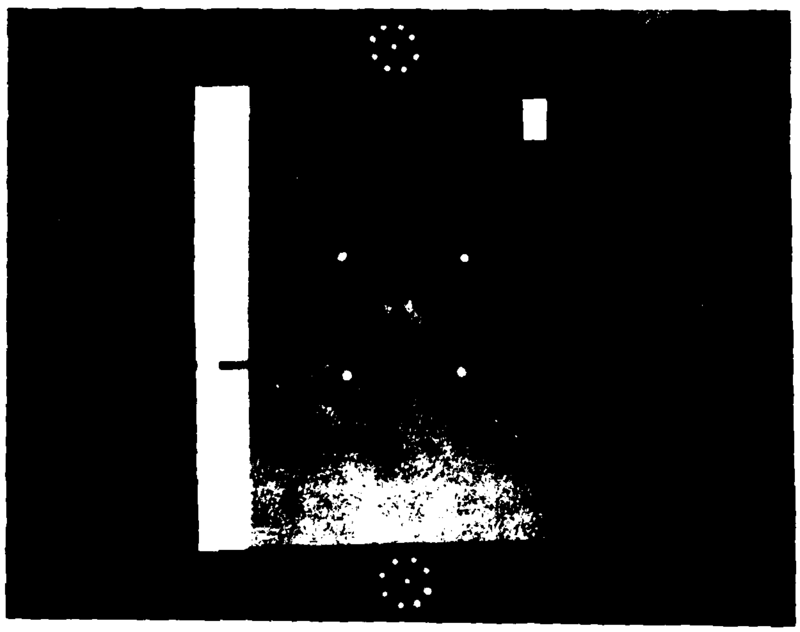

FIGURE 133 X-RADIOGRAPH OF SPECIMEN 16B-12 IN THE INITIAL CONDITION (ZnI_2 ENHANCED)

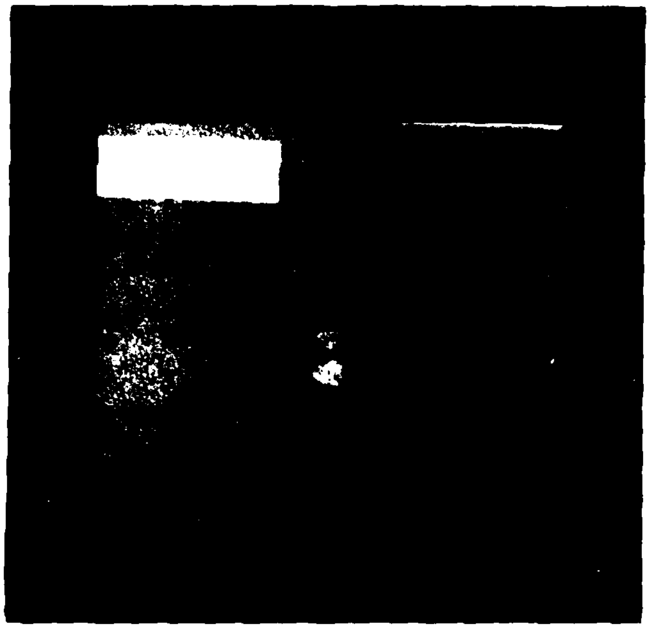

FIGURE 134 SPECIMEN 16B-12 IN THE INITIAL CONDITION AFTER APPLICATION OF ZnI_2 TO THE EDGES

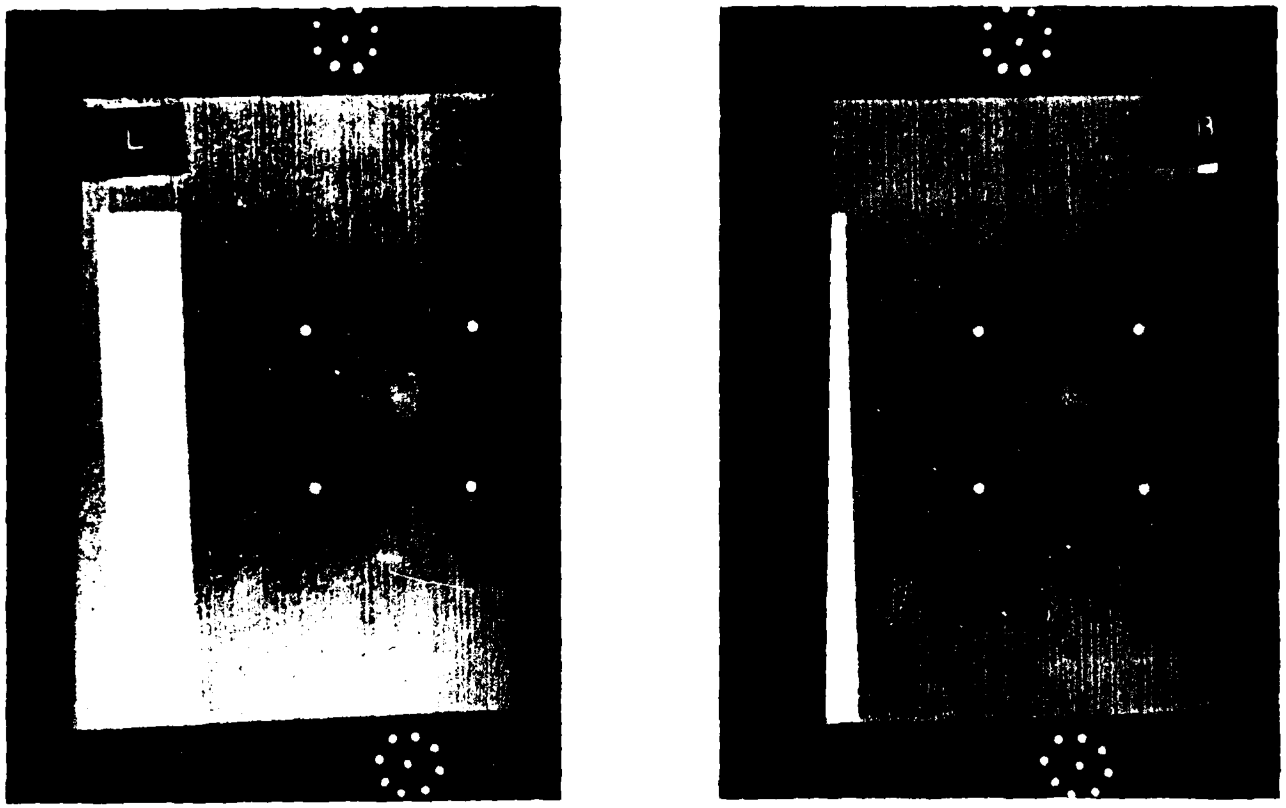

FIGURE 135 SPECIMEN 16B-12 AFTER FATIGUE SEQUENCE 1
(ZnI_2 ENHANCED)

The specimen was bagged with ZnI_2, vacuum sealed, and allowed to dwell for 2 days. After 2 days the specimen was radiographed and showed the cracks were at all levels. The impact damage, cracks and delaminations extended to level 7. (Figure 136)

d. Fatigue Sequence - No. 3

The specimen failed during fatigue test after receiving an additional 144 cycles. The specimen received a total of 194 cycles. Visual inspection after failure showed failure at grip doubler at opposite end from specimen identification. The failure was at the tapered edge. There was no failure associated with the impact damage area. There were cracks and delaminations under the grip doubler at the failed end. There was no damage of the grip doubler at the opposite end.

Figure 137 shows the location of failure for this specimen.

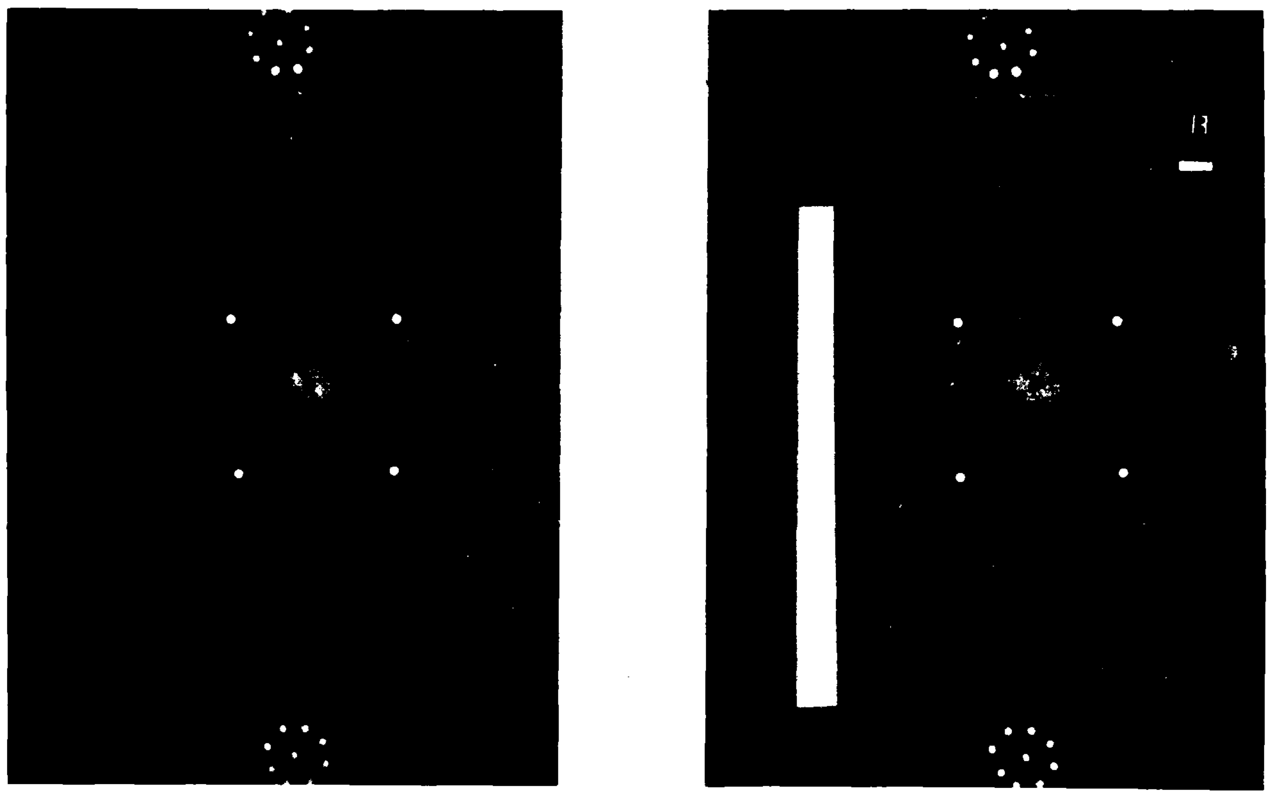

FIGURE 136 SPECIMEN 16B-12 AFTER FATIGUE SEQUENCE 2 (ZnI_2 ENHANCED)

FIGURE 137 SPECIMEN 16B-12 AFTER FATIGUE FAILURE

13. Conclusions:

Fatigue life tests for nine (9) specimens demonstrated the benefits of stereo-x-radiographic inspection in analyzing damage accumulation and interaction of damage accumulation sites. Practicality of the technique was demonstrated by application of a portable inspection set-up during one fatigue sequence.

The use of zinc iodide solution was demonstrated to be sensitive to material interactions during fatique for those cases affording a capillary path to the specimen surface.

Some difficulty in specimen design was encountered causing premature failure at the doubler joint. The joint was tapered to relieve this failure mode but did not totally eliminate the problem. A longer and narrower specimen design would help the failure problem. The wide specimens design was needed to assure containment of the impact fatigue damage, thus a longer specimen with longer tapers would be suggested for future work.

AD-A111 303 MARTIN MARIETTA AEROSPACE DENVER CO QUALITY ASSURANC--ETC F/G 11/4
ENHANCED X-RAY STEREOSCOPIC NDE OF COMPOSITE MATERIALS.(U)
JUN 80 W D RUMMEL, T TEDROW, H D BRINKERHOFF F33615-79-C-3220

UNCLASSIFIED AFWAL-TR-80-3053 NL

3 OF 3
AD
A111303

END
DATE
FILMED
3-82
DTIC

SECTION VI

RESULTS AND CONCLUSIONS

Stereo-X-Radiography was shown to be a significant aid in documenting, describing and in monitoring three dimensional interactions of matrix cracking, fiber fracture and delaminations induced in resin-matrix graphite composite material. Evaluation aids developed during this study improve the potential sensitivity and application of the technique in a variety of material characterization tasks with reduced concern for effect of the penetrant materials used on the performance of resin matrix materials or on the personnel involved in inspection applications.

The following items summarize the observations and conclusions from this study:

1. Results of work performed clearly demonstrated that conventional X-radiographic methods require use of an opaque additive in order to image impact damage in resin matrix graphite composite materials. Penetration into the specimen requires that the damage be connected to a surface by a capillary path.

2. The sensitivity of halogenated organics. used in previous work as opaque additives was reconfirmed. Zinc iodide base solution as an alternate opaque additive was compared and demonstrated to be capable of equaling the sensitivity of the halogenated organic materials.

3. The zinc iodide solution used as an opaque penetrant in this work was not a saturated solution, thus some additional increase in sensitivity may be affected by varying the concentration.

4. The desirability of using stereo-X-radiography to provide depth information in locating damage in a composite was demonstrated. Capability of the technique in locating a single ply within a lay-up was demonstrated.

5. A circular step-wedge was designed, fabricated and shown to be a useful aid (reference) in locating and describing depth features within a stereo image field.

6. Room temperature and elevated temperature exposure of graphite materials to tetrabromoethane, diiodobutane, ZLX-418B (methylene iodide) and a zinc iodide solution was shown to have no readily observable effects on graphite-epoxy material properties.

7. Stereo-X-radiography was demonstrated to be useful in documenting and quantifying impact damage and accumulated fatigue damage in quasi-isotropic graphite/epoxy composite material.

8. Application of the stereo-x-radiographic technique reconfirms the known tolerance of resin matrix composite materials to accumulated damage. Low energy impact damage sites were documented and were not shown to be failure sites in any of the specimens listed.

SECTION VII

RECOMMENDATIONS

As a result of performing this investigation, several areas were identified that merit more detailed analysis. They include:

A. Further analysis of the formulation of the opaque penetrant materials for application to composite structures is in order. The formulation used was satisfactory for laboratory use but tends to dry out. Alternative carriers and wetting agents would improve handling and reduce dwell time requirements.

B. The interaction and long term effect of exposure to the penetrant at elevated temperatures need to be evaluated for the penetrant material selected.

C. The step wedge should be further developed to increase its versatility and range of application. Incorporation of the step wedge and penetrameter into one unit would aid in the exposure process and in automated readout.

D. Automated film analysis techniques should be investigated to assess the location and extent of damage accumulation. Automation of image analysis offers capability to display (and analyze) a single layer within a stack as well as identification of specific predetermined anomalies. Development of the 3D penetrameter for internal calibration of the film image is a prerequisite to precise analysis. Methods in current use are available for image separation (a single layer or plane) and analysis.

E. The mechanics of the damage accumulation process should be further explored to resolve the observed reactions between the edge of the specimen and the pre-damaged center section (impact damaged) area. The 3D X-radiographic method should be considered for evaluation of damage accumulation in test specimens and structures on all future programs. Considerable work is required to identify and assess the mechanisms for the damage accumulation process. Various specimen designs should be used to resolve dominance and interactions between edge damage and impact damage mechanisms.

F. Doubler design appeared to be an operating variable in this program. Specimen design and doubler design should be evaluated to minimize the effects of specimen configuration on damage assessment analysis.

SECTION VIII

REFERENCES

1. McMasters, Robert C., NONDESTRUCTIVE TESTING HANDBOOK, Volume 1, Ronald Press, New York, 1959, pp. 20.46-20.49.

2. Anon., RADIOGRAPHY IN MODERN INDUSTRY, Eastman Kodak, Rochester, N.Y., 3rd, Edition, 1969, pp. 106-109.

3. Clark, George L., APPLIED X-RAYS, McGraw-Hill Book Co., New York, 4th. Edition, 1955, pp. 196-197, 255.

4. Maddux, G. E. and G. P. Sendeckyj, "Holographic Techniques to Defect Detection in Composite Materials", Special Technical Publication 696, American Society for Testing and Materials, Philadelphia, PA, 1979, pp. 26-44.

5. Sendeckyj, G. P., "The Effect of Tetrabromoethane-Enhanced X-Ray Inspection on Fatigue Life of Resin-Matrix Composites", COMPOSITES TECHNOLOGY REVIEW, Vol. 2, No. 1. Winter 1980, pp. 9-10.

6. Ratwani, M. N., "Influence of Penetrants Used in X-Ray Radiography on Compression Fatigue Life of Graphite/Epoxy Laminates", COMPOSITES TECHNOLOGY REVIEW, Vol. 2. No. 2, Winter 1980, pp. 10-12.

APPENDIX A

TIPS ON VIEWING STEREO X-RADIOGRAPHS

The stereo X-radiography presented in this report have been exposed for optimum viewing using suitable stereo viewing equipment. Stereo images have been mounted in pairs on the same page in this report and are distinguished by a small L or R near the upper left or right hand corner of the image. Images are mounted in the position exposed and can be viewed in this position.

Some observers will be able to view the images in three-dimensions by simply holding a 3 X 5 inch card on-edge between the eyes to "separate" the images for direct viewing. Distance from the observer to the images may be varied. To provide ease of viewing, separation of the images may be necessary for some observers.

Proper viewing of the image is attained by aligning the fiducial marks on the step wedges such that one image is observed by the both eyes. Once the images are merged, image detail on the radiographs may be observed in-depth. The depth of fiber distortion, fiber damage and matrix cracking may be observed by reference to the step wedge(s) exposed with the test object. Each step has been made to provide the equivalent spacing of one layer of composite material.

*U.S.Government Printing Office: 1982 — 559-005/4040

DA

FILM